The first 30 minutes of kidney transplantation

Strandberg, Gabriel

2026

Document Version:
Publisher's PDF, also known as Version of record

The first 30 minutes of kidney transplantation

GABRIEL STRANDBERG
DEPARTMENT OF CLINICAL SCIENCES, MALMÖ | FACULTY OF MEDICINE | LUND UNIVERSITY

The first 30 minutes of kidney transplantation

The first 30 minutes of kidney transplantation

Gabriel Strandberg

LUND
UNIVERSITY

DOCTORAL DISSERTATION

Doctoral dissertation for the degree of Doctor of Philosophy (PhD) at the Faculty of Medicine at Lund University to be publicly defended on 20th of February at 13.00 in “Lilla Aulan”, MFC, Jan Waldenströms gata 5, Skåne University Hospital, Malmö

Faculty opponent
Professor Gabriel Oniscu
Division of Transplantation Surgery, Department of Clinical Science, Intervention and Technology, Karolinska Institutet, Stockholm, Sweden.

Organization: LUND UNIVERSITY

Document name: Doctoral Dissertation **Date of issue:** 2026-01-30

Author(s): Gabriel Strandberg **Sponsoring organization:** -

Title and subtitle: The first 30 minutes of kidney transplantation

Abstract:
Background: Ischemia-reperfusion injury remains an unavoidable and early determinant of kidney transplant outcomes. However, characterization of this injurious process in the clinical kidney transplant setting remains limited – particularly concerning the earliest biological events following reperfusion.

Aims: To characterize early biological events occurring during clinical kidney transplantation, with specific focus on the first 30 minutes following reperfusion. The work aimed to delineate donor-type-specific patterns of tissue injury, inflammatory profiles, innate immune cascade activation, and immune-cell dynamics, and to relate these early responses to ischemic exposure and clinical outcomes.

Methods: The studies are based on large prospective cohorts of adult kidney transplant recipients at Skåne University Hospital, Malmö, Sweden, included from August 2018 to June 2021. Intraoperative samples were drawn from the recipient's external iliac vein pre-implantation, followed by samples from the allograft renal vein at 1, 10, and 30 minutes post-reperfusion. Paper I assessed activation components of the complement, coagulation, and kallikrein-kinin systems using Luminex and ELISA. Paper II profiled 92 inflammatory proteins through proteomics by proximity extension assay. Paper III measured nuclear and mitochondrial cell-free DNA using ddPCR, and markers for neutrophil extracellular traps formation using ELISA. A supportive in vitro necrosis model was incorporated to relate cfDNA release from necrosis to complement activation. Paper IV quantified circulating immune cell subsets using flow cytometry.

Results: Kidneys from deceased donors showed prompt and pronounced biological responses following reperfusion. Evidence of acute structural cell injury was detected within the first minute, reflected by release of nuclear cell-free DNA. This was accompanied by early upregulation of injury-associated and pro-inflammatory proteins, as well as a coordinated activation of the complement, coagulation, and kallikrein-kinin systems, indicating a thrombo-inflammatory response. The magnitude and persistence of these early responses were associated with delayed graft function and impaired long-term allograft function. In contrast, living-donor kidneys showed minimal early injury signals and instead demonstrated regulatory and reparative protein profiles. Early redistribution of specific immune-cell subsets, including non-classical monocytes, natural killer cells, and T cells was observed upon reperfusion. Across studies I-III, prolonged cold ischemic time, particularly beyond approximately 8 hours, emerged as a critical determinant of amplified early IRI-responses of injury and immune activation.

Conclusions: These findings establish the first 30 minutes of the reperfusion phase of clinical kidney transplantation as a critical interval in which early determinants of allograft injury are both measureable and interpretable.

Key words: Ischemia-reperfusion injury (IRI), Kidney transplantation (KT), Delayed graft function (DGF), Thromboinflammation, Cell-free DNA (cfDNA), Cold ischemic time (CIT), Immune cells, Inflammation

Classification system and/or index terms (if any) Supplementary bibliographical information

Language English **Number of pages**: 108

ISSN and key title: 1652-8220

ISBN: 978-91-8021-820-7

Recipient's notes Price - Security classification

Signature Date 2026-01-13

The first 30 minutes of kidney transplantation

Gabriel Strandberg

LUND
UNIVERSITY

Published by:

Department of Clinical Sciences, Malmö

Faculty of Medicine

Lund University

Lund 2026

ISBN 978-91-8021-820-7

ISSN 1652-8220

Series title Lund University, Faculty of Medicine Doctoral Dissertation Series 2026:22

Printed in Sweden by Media-Tryck, Lund University,
Lund, 2026

Media-Tryck is a Nordic Swan Ecolabel certified provider of printed material. Read more about our environmental work at www.mediatryck.lu.se

MADE IN SWEDEN

To my family

Table of Contents

List of included papers

This thesis is based on the following papers, referred to in the text by their Roman numerals (I-IV):

I. **Strandberg G**, Öberg C M, Blom A M, Slivca O, Berglund D, Segelmark M, Nilsson B, and Biglarnia AR.
Prompt Thrombo-Inflammatory Response to Ischemia-Reperfusion Injury and Kidney Transplant Outcomes. *Kidney International Reports*. 2023;8(12):2592-2602. doi:10.1016/j.ekir.2023.09.025

II. **Strandberg G**, Raihle C, Nilsson B, Öberg C M, Blom A M, Axman S, Slivca O, Paul C, Berglund D, Biglarnia AR.
Early Postreperfusion Proteomics Reveal Divergent Inflammatory Responses in Kidney Transplantation with Implications on Outcomes. *Transplantation*. 2025;():10.1097/TP.0000000000005561. doi: 10.1097/TP.0000000000005561

III. **Strandberg G**, Trattner R, Martin M, Öberg C M, Raihle C, Slivca O, Alam S, Segelmark M, Christensson A, Nilsson B, Paul C, Blom A M, Biglarnia AR.
Nuclear cell-free DNA on the Loose: An Early Warning Signal of Ischemia–Reperfusion Injury in Kidney Transplantation. *Frontiers in Immunology*. 2026;16. doi:10.3389/fimmu.2025.1704152

IV. **Strandberg G**, Sellberg F, Liedberg AS, Hult A, Berglund D, Biglarnia AR.
Leukocyte redistribution during early kidney allograft reperfusion: Evidence from intraoperative venous effluent analysis. *Manuscript.*

Abbreviations

4E-BP1	Eukaryotic translation initiation factor 4E-binding protein 1
ADA	Adenosine deaminase
ANOVA	Analysis of variance
ART	Aligned rank-transformed
ARTN	Artemin
AT	Antithrombin
AUC	Area under the curve
C1INH	C1-inhibitor
C4BP	C4b-binding protein
cfDNA	Cell-free DNA
DAMP	Damage-associated molecular pattern
DBD	Donation after brain death
DCD	Donation after circulatory death
DD	Deceased donor
DGF	Delayed graft function
eGFR	Estimated glomerular filtration rate
ELISA	Enzyme-linked immunosorbent assay
FGF-23	Fibroblast growth factor 23
HGF	Hepatocyte growth factor
HK	High-molecular-weight kininogen
HMP	Hypothermic machine perfusion
HNE	Human neutrophil elastase
IIIS	Intravascular innate immune system
IL-33	Interleukin-33

IL-6	Interleukin-6
IRI	Ischemia-reperfusion injury
KDPI	Kidney donor profile index
KDRI	Kidney donor risk index
KK	Kallikrein
KT	Kidney transplantation
LD	Living donor
LIF	Leukemia inhibitory factor
MAC	Membrane attack complex
MASP-1	Mannose-associated serine protease 1
MASP-2	Mannose-associated serine protease 2
MCP-4	Monocyte chemoattractant protein 4
NETs	Neutrophil extracellular traps
NHS	Normal human serum
NK	Natural killer (cell)
NPX	Normalized protein expression
OPG	Osteoprotegerin
PAMP	Pathogen-associated molecular pattern
RMSE	Root mean square error
ROC	Receiver operating characteristics
sC5b-9	Soluble C5b-9
TGF-α	Transforming growth factor alpha
TRANCE	Tumor necrosis factor-related activation-induced cytokine

Introduction

Kidney transplantation – overview

Kidney transplantation is the preferred treatment for patients with end-stage kidney disease, providing superior survival, improved quality of life, as well as cost-effectiveness compared with maintenance dialysis[1–4]. Since the first successful clinical kidney transplant in 1954 by Dr Joseph Murray, advances in surgical technique, donor management, organ preservation and immunosuppressive treatment have steadily improved outcomes, establishing kidney transplantation as a routine and durable form of renal replacement therapy[5–9]. In 2024, approximately 110 000 kidney transplants were performed worldwide, including 512 in Sweden[10,11].

A substantial proportion of these advances is attributable to the development of immunosuppressive therapy predominantly targeting the adaptive immune system, particularly the alloreactive T cell response. The introduction of the calcineurin inhibitor cyclosporine in the 1980s marked a major advance in immunosuppression, followed by subsequent adoption of new antimetabolite and calcineurin inhibitor drugs such as mycophenolate mofetil and tacrolimus, as well as poly- and monoclonal antibody induction therapies, leading to marked reduction of acute rejection rates and improved graft survival[9,12,13]. Subsequent refinement of dosing strategies and immunosuppressive drug combinations has further improved therapeutic safety and efficacy[14–16]. By effectively targeting adaptive immune responses, these advances have contributed to improved short-term outcomes, prolonged patient and graft survival, and have consolidated kidney transplantation as a safer and more predictable clinical intervention.

Despite these achievements, several challenges remain. Long-term functional decline continues to limit graft longevity, even in the era of modern immunosuppression. Chronic alloimmune injury, immunosuppressive drug-induced nephrotoxicity, as well as recurrent primary disease, all contribute to progressive graft dysfunction and late graft loss[16–18].

Notably, disparities in long-term outcome between living-donor and deceased-donor kidneys have not substantially changed throughout the years, with living-donor kidneys showing consistently superior survival in large registry data[19–21]. This persistent gap highlights long-lasting donor-related factors inherent to deceased-

donor kidneys that shape subsequent graft trajectory. Moreover, at a population level, access to kidney transplantation remains limited by the global shortage of donor organs, driving efforts to expand the utilization of deceased-donor kidneys traditionally considered higher risk in order to reduce organ discard and increase transplant activity[22,23].

A major unresolved challenge in kidney transplantation is the early injury imposed by the transplantation process itself. All kidneys are subjected to an unavoidable period of total oxygen deprivation – ischemia – during organ procurement and preservation, followed by the abrupt restoration of blood flow – reperfusion – upon implantation in the recipient. In deceased donors, ischemic stress may also precede organ procurement due to hemodynamic instability during intensive care. This sequence induces severe metabolic stress and structural cell damage, which culminate in exaggerated injurious responses at reperfusion, termed ischemia-reperfusion injury, and represents the principal early insult in kidney transplantation. Although more pronounced in deceased-donor kidneys, ischemia-reperfusion injury affects all allografts to varying degrees and is closely associated with early graft dysfunction and adverse long-term outcomes[24,25].

Despite its clear clinical relevance, ischemia-reperfusion injury remains largely unmitigated and insufficiently characterized in the clinical setting, particularly during the immediate reperfusion phase following the first contact between the allograft and recipient blood.

Donor categories

Kidney allografts are obtained from two principal sources: living and deceased donors. The degree of ischemic and physiological stress sustained before implantation differs by donor types. These differences shape the condition of the allograft at the time of implantation and influence its susceptibility to reperfusion injury.

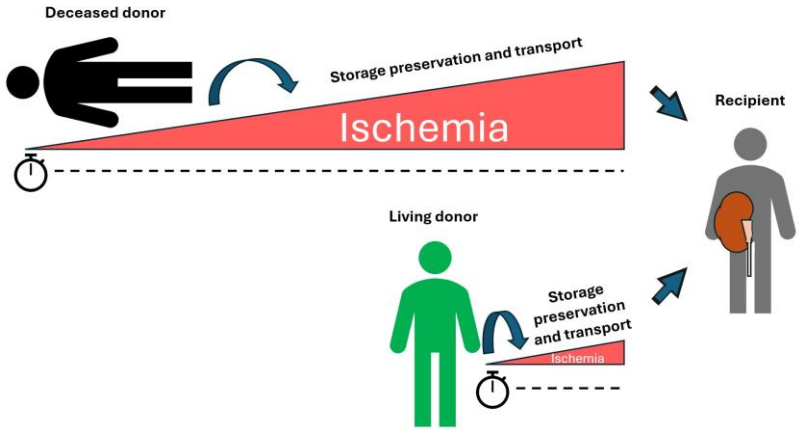

Figure 1. Living and deceased kidney donation. Schematic illustration depicting the difference in ischemic exposure to kidneys of different donor types until recipient implantation.

Living donation

Living donor nephrectomy is performed electively in healthy individuals under controlled surgical and hemodynamic conditions, typically using minimally invasive surgical techniques[26–28]. As recipient surgery is elective and routinely performed simultaneously with, or immediately after, donor nephrectomy, warm ischemia (ischemia at physiological temperature, from vascular clamping to initiated back-table cold perfusion) is minimal, cold ischemic time is short, and reperfusion occurs within a narrow and predictable timeframe. These conditions reduce the magnitude of tissue stress responses. As a result, living-donor kidneys provide a clinical reference point for minimal ischemic insults and are preset at lower risk of early injury and dysfunction after reperfusion, often resulting in superior early allograft function[29,30].

Deceased donation

Deceased donation involves two principal categories: donation after brain death and donation after circulatory death. Unlike the planned circumstances in living donation, deceased donors are individuals from the general population who have suffered acute or acute on chronic illness requiring intensive care, followed by multi-organ procurement shortly after death is declared. Moreover, these donation modalities involve distinct donor-physiological and procedural characteristics that differentially add to the ischemic stress and vulnerable state of the kidney.

Donation after brain death

Donation after brain death refers to organ procurement from donors in whom death has been determined by the irreversible cessation of all brain function, established according to standardized neurological criteria and, when required, confirmed by cerebral angiography or radionuclide perfusion imaging[31]. Following formal declaration of brain death, and acquired information on consent to organ donation, organ procurement is initiated – within 24 hours in Sweden – while donor circulation is maintained through ongoing mechanical ventilation and hemodynamic support[32]. This allows for surgery under conditions of preserved systemic perfusion until vascular cannulation and the start of *in situ* cold perfusion, at which point the blood is flushed out by preservation solutions. However, despite intact circulation during procurement, brain death itself can alter the donor's physiological state, as this process entails a surge of catecholamines and inflammatory mediators, leading to transient hypertension followed by hypotension, and systemic inflammation[33–36].

Donation after circulatory death

In contrast, donation after circulatory death involves organ procurement after death has been determined based on irreversible cessation of circulatory and respiratory function[37]. According to the Maastricht classification, donation after circulatory death is subdivided into controlled and uncontrolled categories[38,39]. In Sweden, controlled donation after circulatory death (Maastricht category III) was implemented into clinical practice following a national pilot project conducted between 2016 and 2019. Initial clinical cases were performed from 2018, and by 2019 donation after circulatory death had been formally implemented as a complement to donation after brain death within established ethical and legal frameworks[40,41].

Table 1. The original Maastricht classification of donation after circulatory death[38].

Category	Type	Circumstances
I	Uncontrolled	Dead on arrival
II	Uncontrolled	Circulatory arrest with unsuccessful resuscitation
III	Controlled	Circulatory arrest after planned withdrawal of life sustaining treatments
IV	Uncontrolled controlled	Circulatory arrest in a brain dead patient

In controlled donation after circulatory death, withdrawal of life-sustaining treatment is planned in an intensive care setting following a formal decision that continued treatment is no longer in the patient's best interest. This decision is made independently of, and prior to, any consideration of organ donation. After this breakpoint decision, and once consent to donation has been established, organ-preserving treatment is instituted to optimize organ function up until withdrawal of

life-sustaining treatment. The withdrawal of life support initiates an agonal phase, during which progressive hypoxia and circulatory deterioration occur, cumulating in circulatory arrest. Death is declared after a predefined no-touch observation period of 5 minutes (in Sweden), during which the persistent absence of circulation and respiration is confirmed[37,42]. Organ procurement must then be promptly initiated, as organs are no longer oxygenated.

Unlike donation after brain death, procurement in donation after circulatory death is initiated in the absence of ongoing circulation, resulting in unavoidable warm ischemia arising from hemodynamic instability during the agonal phase and throughout circulatory arrest until vascular cannulation[43].

Organ recovery may then proceed via one of two distinct strategies: (i) rapid cannulation with immediate initiation of *in situ* cold perfusion, resulting in prompt organ cooling and termination of warm ischemia; or (ii) establishment of normothermic regional perfusion (NRP), in which oxygenated circulation is first restored to the abdominal organs, while cerebral reperfusion is excluded, for approximately 120-180 minutes, allowing controlled reperfusion and metabolic stabilization prior to organ procurement[44].

Following cannulation and initiation of *in situ* cold perfusion, the subsequent procurement procedure largely parallels to that of donation after brain death, after which organs enter the preservation phase (outlined below).

Donor risk assessment

Heterogeneity in donor characteristics and comorbidities, together with procedure-related factors inherent to donation after brain death and donation after circulatory death and typically longer cold ischemic times increases the vulnerability of deceased-donor kidneys. Clinically, this is reflected in higher rates of early graft dysfunction and inferior long-term outcomes compared with living-donor kidneys[45,46].

These differences have driven the development of composite donor risk indices to support organ allocation and acceptance decisions. Among these, the Kidney Donor Risk Index (KDRI) and its derivative, Kidney Donor Profile Index (KDPI) are the most widely used. Originally developed in the United States, the KDRI estimates the relative risk of graft failure for a deceased-donor kidney compared to a reference donor (initially an otherwise healthy brain-dead 40-year-old male without a cerebrovascular cause of death, which was later changed to the median donor of the previous calendar year). The scores integrate donor age, weight, height, history of hypertension and diabetes, creatinine level, cause of death, procurement by donation after circulatory death, hepatitis C status, and, initially, ethnicity. KDPI is a percentile mapping based on KDRI, expressing the risk as a percentage relative to all kidneys recovered in the previous calendar year. The results can be applied to aid in kidney allocation and acceptance as well as longevity matching between

donors and recipients[47,48]. For example, the KDPI score may also serve as a more continuous measure of donor quality compared to binary categorizations such as standard versus expanded criteria donors (a classification based on donor age and selected comorbidities), although the implementation of KDPI has not resulted in decreased discard rates compared to binary assessments[49]. While higher KDRI/KDPI values are associated with reduced graft survival and early dysfunction reflected by delayed graft function (commonly defined clinically as the need for dialysis within the first post-operative week)[50,51], these population-based estimates only incorporate preretrieval factors and do not fully capture the biological heterogeneity underlying early graft vulnerability. Indeed, external validation efforts have reported variable precision in applying specific cutoffs of these scores to reflect actual clinical outcome trajectories[47,52–55].

Among modifiable factors, cold ischemic time remains a particularly influential determinant of kidney transplant outcomes, associated with higher rates of delayed graft function, acute rejection, and poorer long-term outcomes across donor types and characteristics[56–59]. Even in living-donor kidney transplantation, prolonged cold ischemic times have been associated with higher risk of early dysfunction, further underscoring the intrinsic vulnerability of the renal parenchyma to ischemic insults[59].

Preservation methods

Organ preservation constitutes an inherent component of clinical practice and aims to maintain cellular integrity and limit further metabolic deterioration during the interval between procurement and transplantation. Central to current standard preservation strategies is hypothermia, which reduces cellular metabolic demand, slows enzymatic reactions, and serves to maintain cellular homeostasis and tissue integrity until implantation[60,61]. In clinical kidney transplantation, preservation strategies can be broadly divided into static cold storage and hypothermic machine perfusion, which differ in complexity and logistical requirements.

Static cold storage

Static cold storage is the most widely used method for kidney preservation worldwide and constitutes the standard approach in many transplant settings, reflecting its simplicity and low logistical demands[62,63]. Following organ procurement and *in situ* cold perfusion, the kidney is rapidly cooled and stored in a static state at approximately 4°C in preservation solution.

Preservation solutions used for static cold storage aim to mitigate hypoxia-associated cellular injury by limiting osmotic cell swelling, stabilizing cellular

membranes, buffering acidosis, and reducing ionic imbalance[8]. Commonly used solutions include University of Wisconsin (UW) solution and histidine–tryptophan–ketoglutarate (HTK), which differ in electrolyte composition, buffering systems, antioxidative components, and inclusion of metabolic intermediates intended to support cellular energy homeostasis during cold storage[64].

Although hypothermia markedly slows cellular metabolism and lowers oxygen demand, static cold storage relies on passive distribution of preservation solutions without dynamic control.

Hypothermic machine perfusion

Hypothermic machine perfusion represents an alternative preservation strategy in which the kidney is placed in a device and continuously perfused with cold preservation solutions under controlled pressure and flow conditions. By providing ongoing low-temperature perfusate circulation, hypothermic machine perfusion allows dynamic regulation of perfusion conditions and real-time monitoring of parameters, such as flow and vascular resistance, which may provide supplementary information on graft condition prior to implantation[64].

Clinical studies have demonstrated that hypothermic machine perfusion, compared to static cold storage, is potentially associated with improved early graft outcomes, most consistently reflected in reduced rates of delayed graft function, particularly in kidneys from higher estimated risk profiles, including those retrieved after circulatory death[65–67]. Accordingly, hypothermic machine perfusion has been preferentially applied in these donor contexts to improve transplantability and reduce discard rates.

Oxygenated hypothermic machine perfusion is a modification of hypothermic machine perfusion in which controlled amounts of oxygen are added to the perfusion circuit. At hypothermic temperatures, in which cellular metabolism is reduced, supplementation of oxygen is intended to limit hypoxia-related metabolic stress without inducing normothermic metabolic demand[68,69]. Clinical studies indicate that oxygenated hypothermic machine perfusion is safe and may confer benefits in selected donor populations, particularly with respect to early complications and graft survival. However, consistent benefits have not been uniformly demonstrated[70]. Thus, while oxygen supplementation represents a biologically plausible refinement of hypothermic machine perfusion, its precise clinical role and benefit remain to be fully determined.

Innate immunity

To better understand how ischemic stress and reperfusion responses affect kidney allografts, it is essential to consider the innate arm of the immune system. Innate immunity is fundamental in the dynamic process of injury and repair, carrying the immediate mechanisms for recognizing and responding to tissue stress.

Unlike adaptive immunity, which relies on antigen specificity and clonal expansion, innate immune mechanisms are preconfigured, rapidly activated and operate without prior sensitization[71]. This immediate recognition is achieved through detection of structural and molecular patterns rather than individual highly specific antigens. These include so-called danger signals from pathogen-associated molecular patterns (PAMPs), derived from microbial structures, and damage-associated molecular patterns (DAMPs), which originate from stressed, injured, or dying host cells[72,73]. DAMPs encompass a broad range of intracellular and extracellular constituents, including nucleic acids such as DNA, histones, mitochondrial components, and extracellular matrix fragments that are normally concealed from the intravascular compartment but become exposed or released during tissue injury[74,75]. Through pattern-recognition receptors in both soluble form and expressed on immune and non-immune cells, these signals enable innate immunity to function as a rapid sensor of invasive pathogens and altered tissue integrity[76].

Main components

Intravascular innate immune responses are rapidly executed through coordinated actions of cellular and soluble components. Together, these elements allow immediate recognition of tissue infection or stress, triggering the initiation of both inflammatory and reparative programs.

Key immune effector cells include circulating leukocytes such as neutrophils, monocytes, dendritic cells, natural killer (NK) cells, and innate-like T cell subsets[71]. These cells are equipped with pattern-recognition receptors and respond rapidly to changes in tissue integrity through mechanisms ranging from phagocytosis, cytokine production, chemotaxis, antigen-presentation, direct cytotoxicity, to modulation of vascular permeability and endothelial activation[71,77,78]. Platelets also play an important effector role, acting as sensors of vascular injury, binding DAMPs and interacting with immune cells, releasing inflammatory mediators, and interacting with soluble innate inflammatory cascades[79,80].

Complementing cellular components, innate immunity also encompasses soluble plasma protein components. These include the complement, coagulation, and kallikrein-kinin/contact cascade systems, as well as natural antibodies and pattern recognition molecules such as pentraxins[81]. Together, these components interact

closely with immune cells, and amplify effector mechanisms, modulate vascular permeability, while shaping downstream inflammatory responses[82].

The complement system

The complement system represents one of the evolutionary oldest and most rapidly acting plasma-borne recognition mechanisms of host defense[83,84]. It can be activated through three principal pathways and serves an integrative role in inflammation and repair in injurious conditions. Each pathway converges on the cleavage of complement components C3 and C5, producing the anaphylatoxins C3a and C5a that attract and activate leukocytes, the opsonin C3b that facilitates phagocytosis, and the terminal end-activation complex C5b-9 that, when inserted into cell membranes as the membrane attack complex (MAC), promotes cell activation or lysis[85]. A soluble form of the terminal complex, soluble C5b-9 (sC5b-9), reflects terminal complement activation in the fluid phase (**Figure 2**).

The classical pathway

The classical pathway is initiated by C1q, a recognition protein mainly produced by mononuclear myeloid cells such as monocytes, macrophages and dendritic cells[86]. C1q binds to the Fc regions of aggregated, antigen-bound IgG or IgM antibodies or pentraxins, such as C-reactive protein, leading to subsequent activation of C1r and C1s[87]. C1q may also recognize negatively charged surfaces signaling injury or infection such as double-stranded DNA and PAMPs on bacteria[88,89]. Activated C1s cleaves C4 and C2, forming the C4b2a complex, which constitutes the classical pathway C3 convertase that cleaves C3 into C3a and C3b. This enables downstream amplification and progression toward C5 cleavage and subsequent formation of C5b-9[85].

The lectin pathway

The lectin pathway is activated when pattern-recognition molecules such as mannose-binding lectin, ficolins or collectins bind to DAMPs or PAMPs on damaged cells and pathogens[90,91]. Ligand binding activates the mannose-associated serine proteases 1 and 2 (MASP-1 and MASP-2), which cleave C4 and C2 to generate the C4b2a lectin pathway C3 convertase.

The alternative pathway

The alternative pathway is continuously active at a low level, by proposed mechanisms such as spontaneous hydrolysis of C3 as well as contact-activation of C3 to biological and artificial surfaces, forming C3(H_2O) that initiates the fluid-phase C3 convertase variant C3(H_2O)Bb upon binding factor B[92–94]. Additionally, any C3b deposited on a surface, regardless of pathway origin, may bind factor B and is subsequently cleaved by factor D to assemble the alternative pathway C3

convertase termed C3bBb[95]. This convertase is further stabilized into C3bBbP by properdin, a protein capable of recognizing damaged cells and itself stimulate alternative pathway activation[96,97].

In contrast to the C4b2a convertase of the classical and lectin pathways, C3bBb also serves as a positive feedback amplification loop, generating additional C3b that can bind factor B to form new convertase complexes and thereby propagate surface activation if complement regulation is insufficient.

Complement activation is tightly regulated by soluble fluid-phase inhibitors, including C1-inhibitor (C1INH), clusterin, factor H, factor I, and C4b-binding protein (C4BP), as well as membrane-bound regulators expressed on host cells such as membrane cofactor protein (MCP), decay-accelerating factor (DAF), and CD59[85,98]. Together, the presence of these regulators confines complement activation to appropriate surfaces by limiting pathway initiation, C3 and C5 convertase amplification, and C5b-9 formation.

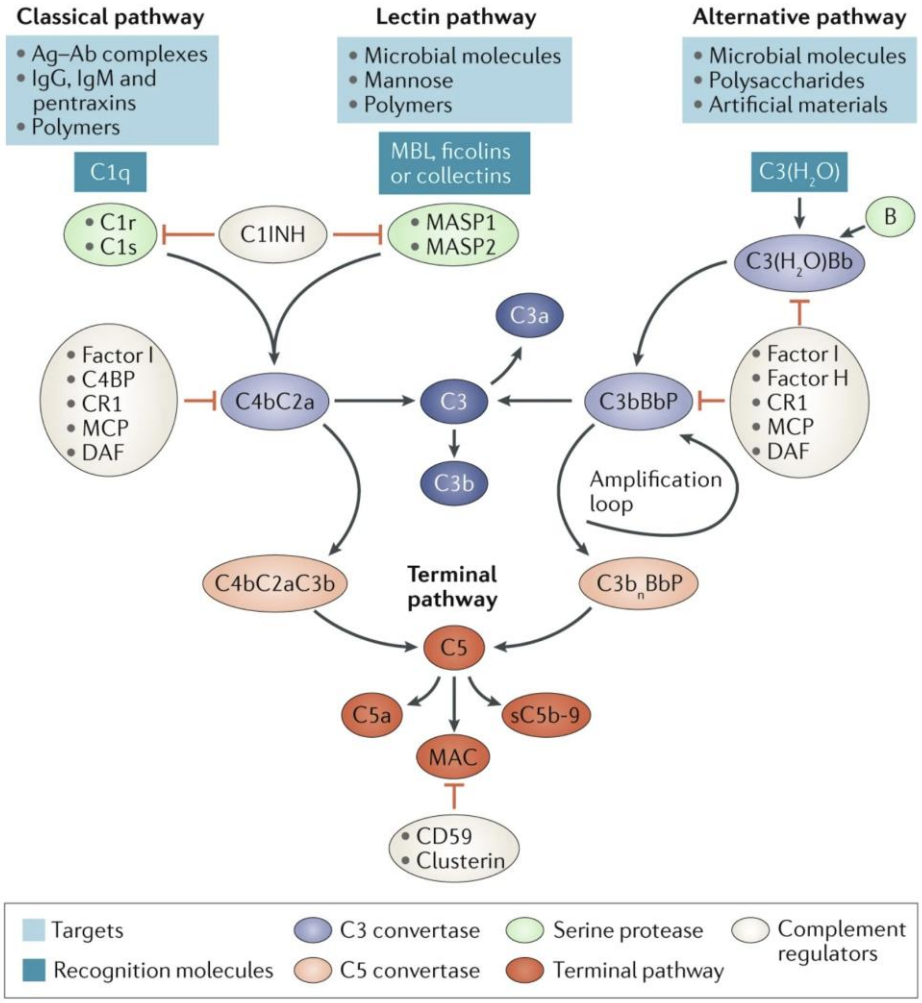

Figure 2. The complement system.
C1-INH = C1-inhibitor, MAC = membrane attack complex (C5b-9), sC5b-9 = soluble C5b-9. Source: Biglarnia, AR., Huber-Lang, M., Mohlin, C. et al. The multifaceted role of complement in kidney transplantation. Nat Rev Nephrol 14, 767–781 (2018). https://doi.org/10.1038/s41581-018-0071-x. *Image reproduced with permission from © Springer Nature*.

The coagulation system

The coagulation cascade maintains hemostasis through thrombin generation and fibrin formation. The activation of the coagulation cascade (like complement) is a surface-oriented event which normally takes place on the surface of aggregated platelets which have been activated during primary coagulation. The cascade can be initiated by two pathways: the tissue factor pathway (extrinsic) or contact system

pathway (intrinsic), both of which converge on activation of factor X (FX) to FXa and subsequent thrombin generation from prothrombin. Thrombin then converts soluble fibrinogen into fibrin and activates FXIII, which cross-links fibrin into net formations[99].

The extrinsic pathway is initiated when tissue factor is exposed on activated or damaged cells, such as endothelial cells or monocytes[100,101], and binds circulating FVII, forming the tissue factor-FVIIa complex that activates both FIX and FX. Furthermore, FIXa, FXa and subsequent thrombin generation are largely amplified by the intrinsic tenase (FIXa–FVIIIa) and prothrombinase (FXa–FVa) complexes on activated platelets[102].

The intrinsic pathway is triggered by contact system component FXIIa that activates FXI to FXIa, with downstream activation of FIX to FIXa and thereby initiating the common coagulation pathway by FXIa and its co-factor FVIIIa activating FX to FXa[99] (**Figure 3**).

Thrombin drives a powerful amplification loop by activating FV, FXI and FVIII, thereby accelerating factor Xa and thrombin generation. This is counterbalanced by endogenous inhibitors, including antithrombin (AT), which neutralizes thrombin and factor Xa, the protein C system, which inactivates FVa and FVIIIa, and tissue factor pathway inhibitor, which limits tissue factor–dependent initiation[103].

The kallikrein-kinin/contact system

The kallikrein-kinin and contact system is activated when FXII is converted to FXIIa upon contact with negatively charged or altered surfaces such as exposed basement membrane components and free DNA. FXIIa cleaves plasma prekallikrein to kallikrein (KK) and activates FXI, with high-molecular-weight kininogen (HK) acting as a co-factor. Kallikrein amplifies FXII activation, reinforcing the contact pathway, and cleaves HK to release bradykinin, a potent vasoactive peptide promoting vasodilation, endothelial permeability and leukocyte recruitment, as well as angiogenesis in the long term[99,104].

FXIIa and kallikrein are primarily inhibited by C1INH, with additional control by AT and α2-macroglobulin[105], while bradykinin is mainly inactivated by angiotensin-converting enzyme[106].

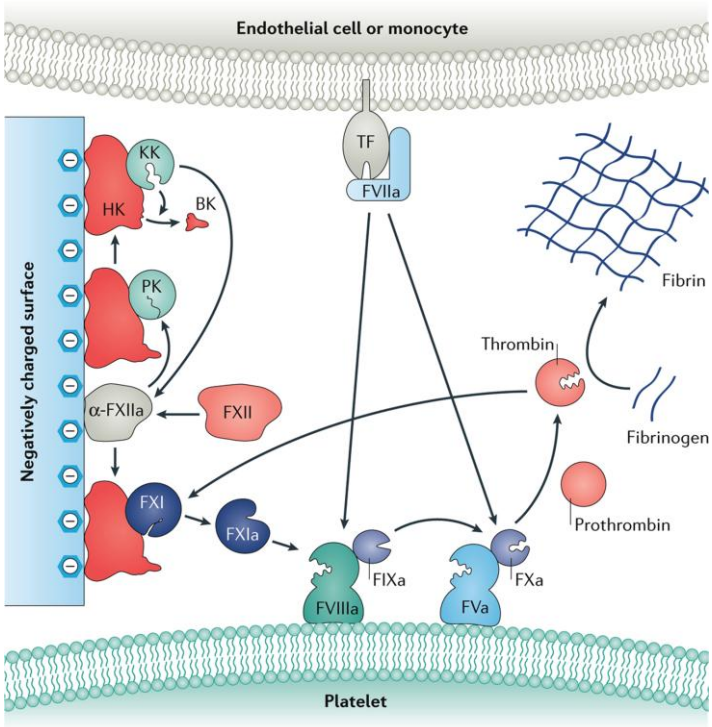

Figure 3. The coagulation and kallikrein-kinin/contact systems.
KK = kallikrein, PK = prekallikrein, TF = tissue factor. Source: Ekdahl, K., Soveri, I., Hilborn, J. *et al.* Cardiovascular disease in haemodialysis: role of the intravascular innate immune system. *Nat Rev Nephrol* **13**, 285–296 (2017). https://doi.org/10.1038/nrneph.2017.17. *Image reproduced with permission from © Springer Nature*.

Thromboinflammation

The intravascular innate immune system (IIIS), encompassing these soluble cascade components and circulating effector cells, shares many non-alloimmune triggers from danger signals such as PAMPs and DAMPs. As a result, danger signals may engage the IIIS components in a cross-talk response, linking pro-thrombotic and pro-inflammatory pathways into a unified thrombo-inflammatory response[107,108].

Although the cascade systems are classically described as distinct entities, experimental findings demonstrate that they are functionally interconnected. This integration is supported by several points of intersection. For example, contact activation via FXII can initiate both intrinsic coagulation and kallikrein–kinin system activation, while kallikrein itself can amplify FXII activation and cleave complement component C3. Furthermore, complement-derived anaphylatoxins such as C5a can promote tissue factor expression and leukocyte activation[104,109–111].

Thrombin, in turn, not only drives fibrin formation but also engages protease-activated receptors on endothelial cells, platelets, and leukocytes, further amplifying vascular inflammation[112]. While the precise hierarchy and relative contribution of individual pathways likely vary across biological contexts, their combined activation enables a unified and multifaceted response. This framework provides a basis supporting how IIIS activation can rapidly escalate in settings enriched by danger signals when regulatory control is insufficient.

Innate immunity in sterile injury

A defining feature of innate immunity is its ability to distinguish self from non-self at a species level, but not at the individual level. Consequently, innate immune activation inherently lacks dependency on alloantigen recognition and can be triggered by damaged- or altered-self stimuli in the absence of infection. While acting as a first responder to pathogens, innate immunity is equally essential in responding to sterile injury. This property underlies its central role in a wide range of non-infectious injurious conditions including trauma, myocardial infarction, stroke, and organ transplantation[113–116].

Importantly, innate immune activation to damaged-self provides an important maintenance function in tissue homeostasis through the clearance of damaged cells and debris, as well as initiation of tissue repair[117–119]. On the other hand, when activated excessively and in dysregulated conditions, innate immune responses can disproportionally amplify tissue injury rather than facilitate resolution. This duality is particularly relevant in the context of ischemia-reperfusion injury, where the response to injury leads to aggravated damage[120].

Ischemia-reperfusion injury

Upon implantation, the transplanted kidney is abruptly transitioned from ischemia to reperfusion of warm, oxygenated blood. While inevitable and essential for graft viability and recovery, this transition marks the point at which accumulated ischemic insults translate into acutely amplified damage, referred to as ischemia-reperfusion injury, a process that has been extensively investigated in experimental models[25,120,121].

Ischemia primes renal cells through metabolic stress and progressive disruption of structural integrity and cell-surface regulatory functions. Under ischemic conditions anaerobic metabolism, mitochondrial dysfunction, intracellular acidosis, and lost ionic gradient homeostasis develop[122–124]. Transcriptional programs shift toward stress responses, including induction of pro-inflammatory mediators and activation of regulated necrotic cell death pathways[120,124,125].

Importantly, ischemia induces phenotypic changes in both endothelial and parenchymal cells that are recognized by the innate immune system. Critically, ischemic injury extends beyond intracellular compartments to remodel the endothelial–blood interface. Under physiological conditions, the endothelial surface is inherently anti-inflammatory, largely due to the presence of the glycocalyx, a three-dimensional luminal structure, composed of proteoglycans, glycoproteins, and glycosaminoglycans such as heparan sulfate[126]. The glycocalyx serves as a physiological barrier that prevents direct interaction between circulating blood components and the endothelial cell surface, while simultaneously functioning as a regulatory platform that limits vascular permeability and leukocyte adhesion and anchors key local regulators of the innate immune system[126–128].

However, ischemic conditions drive enzymatic degradation and shedding of the glycocalyx through upregulation of metalloproteinases and heparanases. As a consequence, surface-bound regulators, such as factor H, antithrombin (AT), tissue factor pathway inhibitor (TFPI), C4b-binding protein (C4BP), and C1-inhibitor (C1INH) are lost from the endothelial surfaces[116,127] (**Figure 4**). In parallel, endothelial activation from ischemia increases the expression of pattern-recognition receptors and cell adhesion molecules, further altering the appearance of the cells[129–132].

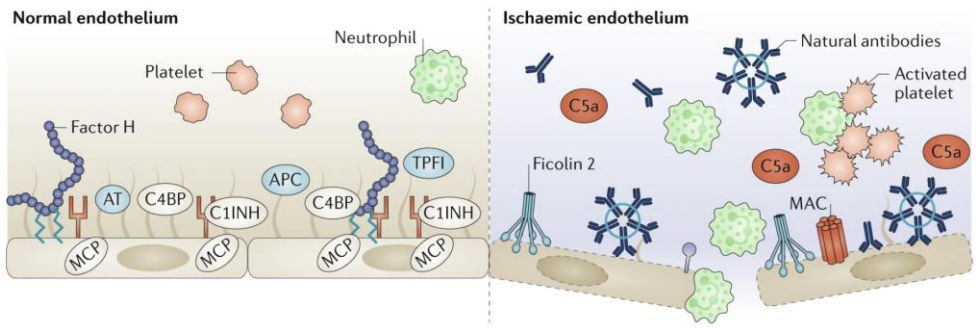

Figure 4. The glycocalyx layer under normoxic and ischemic conditions.
The normoxic endothelium is protected by the glycocalyx, which binds fluid-phase regulators of the complement system, including C1 inhibitor (C1INH), factor H and C4b-binding protein (C4BP) as well as the coagulation inhibitors antithrombin (AT), tissue factor pathway inhibitor (TFPI) and activated protein C (APC). In addition, endothelial expression of membrane cofactor protein (MCP; also known as CD46) inhibits C3 and C5 convertase activity, maintaining an anti-inflammatory and antithrombotic surface. During ischaemia and reperfusion, cytokine exposure and/or complement activation products such as the membrane attack complex (MAC) result in the breakdown of the glycocalyx and subsequent loss of regulators. In this setting complement activation can be driven by molecules such as ficolin 2 and natural antibodies, resulting in the formation of complexes between activated platelets and polymorphonuclear leukocytes (PMNs) such as neutrophils. Activated PMNs bind to the endothelial cells and migrate through the endothelium into the parenchyma, thereby aggravating the inflammatory response. Errata: TPFI should be TFPI. Source: Biglarnia, AR., Huber-Lang, M., Mohlin, C. et al. The multifaceted role of complement in kidney transplantation. Nat Rev Nephrol 14, 767–781 (2018). https://doi.org/10.1038/s41581-018-0071-x. *Image reproduced with permission from © Springer Nature*.

Upon reperfusion in the recipient, functional denudation of the cell surface combined with ischemia-induced phenotype changes exposes cell surfaces to direct interaction with circulating key components of the innate immune system[116,127,133]. Concurrently, injured cells release and expose DAMPs such as alarmins, histones and cell-free DNA fragments, which act as potent danger signals that amplify the initial inflammatory response[120,132,134,135].

Rather than restoring homeostasis, reperfusion thus initiates a coordinated response in which complement, coagulation, and contact systems, together with platelets and leukocytes are concurrently activated. This complex and interlinked activation of the intravascular innate immune system culminates in a prompt thrombo-inflammatory response that propagates inflammation and tissue injury beyond the damage imposed by ischemia alone[136]. This sequence of events captures the core pathophysiological mechanism of ischemia-reperfusion injury.

The fundamental mechanism by which ischemia alters the appearance of cell surfaces, thereby eliciting a comprehensive innate immune response upon reperfusion, is demonstrated by a recent experimental study employing *ex vivo* surface shielding of kidney allografts[137]. In this study, ischemia-exposed porcine kidney allografts were treated *ex vivo* by intra-arterial administration of an inert amphiphilic polymer, polyethylene glycol–conjugated lipid (PEG-LIPID), which spontaneously inserts into cell membranes to form a dense, biocompatible protective coating. This artificial surface layer physically masks denudated cell surfaces and replaces the lost barrier function of the glycocalyx, thereby preventing direct interaction between circulating innate immune components and ischemia-primed cell surfaces. As a result, the prompt thromboinflammation together with downstream inflammatory response to reperfusion was markedly attenuated. These recent findings provide direct evidence that loss of structural and regulatory surface protection is a central determinant of ischemia–reperfusion injury severity, and that restoration of a protective cell-surface barrier can broadly mitigate innate immune response at reperfusion.

It is important to recognize that ischemia-reperfusion injury is not confined to allogeneic organ transplantation but represents a shared pathophysiological mechanism across diverse clinical conditions involving transient interruption and restoration of blood flow, including myocardial infarction, stroke, and major trauma[123]. This broader relevance underscores ischemia-reperfusion injury as an evolutionarily conserved consequence of innate immune recognition of damaged- and non-self and positions kidney transplantation as a uniquely accessible clinical setting in which the earliest events of this process can be directly investigated in humans.

Clinical consequences of ischemia-reperfusion injury

The clinical relevance of ischemia-reperfusion injury is reflected in both early and long-term outcomes after kidney transplantation.

In the early post-transplant period, the severity of ischemia-reperfusion injury is most clearly reflected in early allograft dysfunction[121,138]. Delayed graft function, commonly defined as the need for dialysis within the first post-operative week, is a clinical consequence of initial allograft injury occurring almost exclusively in deceased-donor kidneys[139,140]. Importantly, delayed graft function is closely linked to donor- and preservation-related factors that determine ischemic exposure and modulate the allograft's vulnerability to ischemia-reperfusion injury. Prolonged cold ischemic time, donation after circulatory death, and higher KDPI score are strongly associated with the development of delayed graft function[51,141–144]. Moreover, delayed graft function is strongly associated with an increased risk of inferior long-term allograft function, higher incidence of rejections and graft failure[145–147], underscoring that the severity of ischemia-reperfusion injury exerts lasting effects on downstream allograft health.

At a population level, the consequences of ischemia-reperfusion injury extend beyond individual outcomes and carry substantial clinical and systemic implications. Chronic allograft dysfunction, premature graft loss, return to dialysis, increased patient morbidity and mortality, and the need for re-transplantation, collectively strain organ availability and healthcare resources[25,51,148]. In parallel, efforts to extend the donor pool have increased the reliance on donation-after-circulatory-death and expanded criteria donors with higher KDPI score, introducing a growing proportion of allografts with increased susceptibility to ischemia-reperfusion injury into contemporary practice[149]. Although these strategies have enabled broader transplant access with acceptable outcomes[53,150,151], they further reinforce ischemia-reperfusion injury as a central challenge in modern transplant care.

Rationale and knowledge gap

Despite substantial advances in kidney transplantation, ischemia-reperfusion injury remains a major unresolved determinant of early graft dysfunction and long-term outcomes. Current strategies primarily focus on limiting ischemic exposure through optimized donor management, improved organ allocation logistics to reduce cold ischemic times, promotion of living-donor kidney transplants, and advances in organ preservation technologies which have been shown to reduce the incidence of delayed graft function[152].

Nevertheless, the persistence of ischemia-reperfusion injury-related adverse outcomes across contemporary cohorts, despite modern immunosuppression, refined surgical techniques, and improved preservation strategies, indicates that current standard-of-care approaches do not sufficiently address this early, non-alloimmune component of allograft injury.

Although extensive mechanistic insight into ischemia-reperfusion injury has been generated from experimental models, translation into effective clinical interventions has been limited. To date, no pharmacologic therapy for renal ischemia-reperfusion injury has achieved clinical translation[153]. Pathway-specific interventions such as complement inhibition, have shown promise in preclinical settings but have yielded inconclusive results in clinical trials[154–156]. Collectively, these findings suggest that critical features of the early response to ischemia-reperfusion injury may not be adequately captured by single-pathway targeted approaches.

A central limitation is the lack of detailed *in vivo* characterization of the immediate biological events occurring at the moment of reperfusion in clinical kidney transplantation. The earliest phase of ischemia-reperfusion injury unfolds at the interface between the post-ischemic allograft and incoming recipient circulation, rendering the intravascular compartment the earliest, and repeatedly accessible, site allowing for assessing of both donor- and recipient-related mediators of injury and inflammation.

Despite this accessibility and biological relevance, the immediate intravascular response during the first minutes of reperfusion remains poorly defined in the clinical setting.

Aims

The overall aim of this thesis was to investigate soluble and cellular constituents in the allograft venous effluent in the immediate reperfusion phase of clinical kidney transplantation and to characterize their immediate temporal patterns during the first 30 minutes of reperfusion. By doing so, this work aimed to advance understanding of the earliest biological processes that shape ischemia-reperfusion injury under real-life clinical conditions.

Specific aims

Paper I: To investigate the intravascular innate immune response to ischemia-reperfusion injury in clinical kidney transplantation, with particular focus on the coordinated activation of the complement, coagulation, and kallikrein-kinin systems, and to evaluate associations of this activation with short-term and mid-term allograft function.

Paper II: To characterize early intravascular proteomic signatures in response to ischemia-reperfusion injury, stratified by donor modality, and evaluate their associations with short- and long-term transplant outcomes.

Paper III: To investigate whether early cell-free DNA release in allograft venous effluent reflects acute ischemia-reperfusion injury and to evaluate its associations with neutrophil extracellular trap-markers along with downstream thrombo-inflammatory activation and subsequent allograft dysfunction.

Paper IV: To define early changes in circulating immune cell subsets and determine whether selective declines occur following reperfusion, consistent with early retention of specific cell types within the kidney allograft.

Material and methods

Study design and cohort data

All four studies underpinning the foundation of this thesis were conducted using consecutive kidney transplant recipients from a large prospective cohort study (ACTIVMED) initiated 2018 and still ongoing at Skåne University Hospital, Malmö, Sweden. Patients at the Department of Transplantation were asked to participate upon admission in the immediate pre-operative period and written informed consent was obtained from all participants. Maintenance immunosuppression consisted of prednisolone, mycophenolate mofetil, and tacrolimus. Clinical data were retrieved from patient medical records, the local transplant registry (iSmaRT), and the Scandiatransplant (YASWA) database. Plasma-creatinine-based estimated glomerular filtration rate (eGFR, mL/min/1.73m^2) was calculated using the Lund-Malmö-revised formula[157,158]. Delayed graft function was defined as dialysis within the first postoperative week. Cold ischemic time was defined as the duration between *in situ* (in deceased-donor [DD] kidneys) or *ex situ* (in living-donor [LD] kidneys) cold perfusion and established allograft reperfusion in recipients.

Paper I and II included 63 kidney transplant recipients (LD n = 26, DD n = 37) between August 2018 and June 2019.

Paper III included 127 kidney transplant recipients (LD n = 41, DD n = 86) from August 2018 to August 2020.

Paper IV included 29 kidney transplant recipients (LD n = 8, DD n = 21) between September 2020 to June 2021.

Sampling

The intraoperative sampling followed a standard operative procedure across all studies. A systemic baseline blood sample was drawn from the recipient's external iliac vein before allograft implantation. Following reperfusion, venous blood was sampled directly from the allograft vein at 1, 10, and 30 minutes. Samples were drawn using 21G BD Vacutainer UltraTouch butterfly needles (BD Biosciences) into 6ml EDTA tubes (K2E BD Vacutainer, BD Biosciences).

Sample handling and processing

Variations of sample handling were necessitated by analytic platform. **Papers I-III** used plasma samples for analyses involving the intravascular innate immune cascade activation, proteomic profiling, and cfDNA/NETs quantification. EDTA tubes were immediately stored in ice sludge after whole-blood sampling and then centrifuged at 1900 x *g* for 10 minutes at 4 °C, with the plasma supernatant extracted, aliquoted, and stored at -80 °C until analysis. For **Paper IV**, the obtained EDTA tubes of venous whole blood were stored in room temperature and processed for flow cytometric staining within 24 hours, except for samples from one patient processed within 48 hours after methodological validation experiments confirmed that cell viability and subset quantification remained adequately preserved during this interval.

All samples were assigned to a numeric study code at collection, and aliquots from the same patient and time point were processed as a single batch to minimize freeze-thaw cycles and technical drift.

Ethical considerations

The sampling strategy was designed to minimize risk and interference with routine transplant surgery. Venipuncture using a small-gauge needle was chosen as it entails minimal bleeding that is self-limiting and requires no additional surgical preparation. Although simultaneous arterial inflow sampling could provide trans-graft comparisons, this would require catheterization of the transplant or iliac artery, introducing an invasive procedure with non-negligible risks, including dissection, thrombosis, and compromising graft perfusion. Given these risks and the potential of this method to prolong surgery, arterial sampling was considered ethically unjustifiable.

The sampling methodology and specified investigations of **Paper I-IV** were approved by the Swedish Ethical Review Authority (2017/798, 2018/712). An additional permit was obtained for the use of normal human serum (NHS) in **Paper III** (2023/05543).

All procedures involving human participants were conducted in accordance with the ethical standards of the institutional and national research committees and with the Declaration of Helsinki. The studies also adhered to the principles of the Declaration of Istanbul on Organ Trafficking and Transplant Tourism.

Transplant candidates may be considered a potentially vulnerable population due to the acute clinical context and dependency on the healthcare system at the time of admission. To mitigate undue influence, participation was strictly voluntary, written

informed consent was obtained prior to inclusion, and patients were explicitly informed that providing, declining or withdrawing consent would not affect their clinical care.

Laboratory analyses

Innate cascade system activation (Paper I)

Assessments on innate cascade markers were performed in samples from 63 kidney transplant recipients (26 LD, 37 DD). The proteolytic cascade systems consist of proteases whose zymogens are activated by an upstream protease. Many of their inhibitors are serpins, such as C1INH and AT, which form complexes with the protease. This allows analyses of the activation of individual zymogens if the protease-serpin complex is quantified in blood plasma[159]. Activation markers of the complement, coagulation, and kallikrein-kinin systems were quantified by measuring protease-serpin complexes including FXIIa, KK, FXIa, thrombin, MASP-1, and MASP-2 with either C1INH or AT by in-house analyses based on previously described methods[159,160] using Luminex xMAP Technology (Merck Millipore) and read on a clinical diagnostics instrument (MAGPIX, Luminex Corporation). Terminal complement activation marker sC5b-9 and complement protein C3a were quantified using in-house enzyme-linked immunosorbent assays (ELISAs)[161,162].

Proteomic profiling (Paper II)

Protein profiling was performed by Olink Proteomics using the Olink Proteomics Inflammation panel, which targets 92 cytokines, chemokines, growth factors, and immune mediators by proximity extension assay technology. The study population was the same as in **Paper I**. Output was generated as Normalized Protein eXpression (NPX) units. All samples were analyzed in a randomized order, and laboratory personnel were kept unaware of the study design and of the characteristics associated with each sample. Validation data for the assay specificity, sensitivity, dynamic range, as well as reproducibility are available from the manufacturer: (Olink Proteomics, Validation methods and results: https://olink.com/knowledge/documents).

Cell-free DNA and NETs markers (Paper III)

Mitochondrial and nuclear cell-free DNA were quantified in 127 kidney transplant recipients (41 LD and 86 DD) by droplet digital polymerase chain reaction (ddPCR) on the Biorad QX200 platform. DNA was extracted using QIAamp DNA blood minikits (QIAGEN). Droplets were generated using a BioRad QX200 droplet generator, with specific primers for mitochondrial (#10031253; BioRad) and nuclear DNA (#10031244; BioRad) as well as restriction enzyme digestion using Hind III to optimize template accessibility. Samples were thermocycled with the following steps: activation at 95°C for 10 minutes, denaturation at 94°C for 30 seconds, 40 times 1-minute cycles of annealing/extension at 60°C, held at 98°C for 10 minutes and then cooled to 4°C. Plates were stored overnight at 4°C before readout. Results were expressed as copies/mL of plasma, normalized to plasma input volume. Reference ranges for mitochondrial and nuclear DNA have not been established.

NETs markers were assessed in a subset of 56 kidney transplant recipients (20 LD and 36 DD). Citrullinated histone H3 was measured using a commercially available ELISA (Cayman Chemical). Human neutrophil elastase (HNE-) DNA complexes were assessed using an in-house ELISA in which NETs generated ex vivo were used as standards. For this purpose, neutrophils were isolated from peripheral blood of healthy donors by cell separation using Histopaque-11191 (Sigma) and isolated by Percoll gradient. Neutrophils were stimulated with phorbol myristate acetate (Sigma) for 4 hours at 37°C and 5% CO_2 to induce NETosis and subsequently treated with MNase for 15 minutes at 37°C to release chromatin-protein complexes. The plates were coated with anti-neutrophil elastase antibody (Anti-DNA-POD, Roche), and captured NET material or study plasma sample HNE-DNA using anti-DNA-POD conjugate and developed with TMB substrate.

To support the interpretation of cell-free DNA and complement activation, human proximal tubular epithelial cells (HK-2 cell line, #CRL-2190; ATCC) were induced into necrosis by incubation at 56°C for 30 minutes and incubated with NHS at 37°C to evaluate C5b-9 deposition. Deposition was quantified by flow cytometry using C9 neoepitope-specific antibodies and also visualized by confocal microscopy. Flow cytometry data was assessed using FlowJo (Becton Dickinson & Company). Live HK-2 cells and secondary-antibody-only conditions served as controls.

Leukocyte immunophenotyping and gating strategy (Paper IV)

Flow cytometry was performed on samples from 29 kidney transplant recipients (8 LD and 21 DD) at an SS-EN ISO 15189-2022-accredited laboratory. White blood cell (WBC) count was measured on a Sysmex cell counter (Sysmex Corporation). For flow cytometry, red blood cells were lysed with Pharmalyse per manufacturer protocol and leukocytes were washed, counted and resuspended in staining buffer.

Two antibody panels were used. Panel A included markers identifying myeloid lineages, natural killer (NK) cells, T and B cells (CD45, CD16, CD14, HLA-DR, CD3, CD19, CD56). Panel B assessed T cell subsets phenotypes (CD2, CD3, CD4, CD8, CD25, CD45RA, CD45RO). Samples were run on a FACSCanto II (Becton Dickinson) instrument and pre-processed in FACSDiva (Becton Dickinson) before gating and quantification in FCS Express 7 (De Novo Software).

Gating strategy (Paper IV)

Debris was excluded by FSC/SSC, singlets were gated by FSC-A versus FSC-H, and viable cells identified by 7-AAD negativity. CD45 defined leukocytes. Granulocyte, monocyte and lymphocyte populations were first identified using FSC/SSC characteristics. In panel A, T cells and B cells were detected by CD3 and CD19, respectively. NK cells were defined within $CD3^-$ $CD19^-$ non-myeloid compartment and stratified into $CD56^{dim}$, $CD56^{bright}$, and $CD56^{lo/-}$ based on CD56 and CD16 expression. Monocyte subsets were classified as classical ($CD14^{++}$ $CD16^{dim/-}$), non-classical ($CD14^{dim}$ $CD16^{++}$), and intermediate ($CD14^{++}$ $CD16^{+}$). In Panel B, T cell subsets were identified within the $CD2^+$ $CD3^+$ population as $CD4^+$ or $CD8^+$, with naïve and memory phenotypes determined by CD45RA/CD45RO expression and activation phenotypes by CD25. HLA-DR^+ T cells were assessed from Panel A. Graphics on gating strategies are presented in **Supplementary Figure S2**.

Statistical analysis

Across all included studies, continuous variables were summarized as medians with 1^{st}-3^{rd} quartiles or means with standard deviations, as appropriate, and categorical variables as frequencies with percentages. Pairwise comparisons used Mann–Whitney U tests on continuous data and Chi-square or Fisher's exact tests on categorical data. A $P < 0.05$ was considered significant unless otherwise specified.

Paper I

Differences in continuous data across three subgroups were compared using Kruskal–Wallis tests. Temporal and donor-type-associated variation in innate cascade activation products was assessed using analysis of variance on aligned rank-transformed data (ART-ANOVA) with Geisser Greenhose correction, including interaction terms. Receiver operating characteristics (ROC) evaluated associations of area under the curve (AUC)-summarized marker levels with delayed graft function and was also applied to assess relationships with cold ischemic time. Linear regression assessed slopes of eGFR from 1, 3, 6, 12, and 24 months post-transplantation. Spearman correlation analyses quantified relationships among

intravascular innate immune cascade system activation products. Statistical analyses used GraphPad Prism 9.2.0 (GraphPad Software, San Diego, CA), IBM SPSS Statistics 28 (IBM Corp., Armonk, NY), and R 4.1.1 for Mac (R Foundation for Statistical Computing, Vienna, Austria).

Paper II

Baseline-subtracted values were used for all analyses of post-reperfusion measurements. Initial screening of all 92 proteins between LD and DD used repeated Mann–Whitney U tests with Holm–Šídák correction for multiple comparisons. As a tiered approach, proteins upregulated at $P < 0.01$ were selected for further analyses. ART-ANOVA with Geisser-Greenhouse correction assessed variation in these protein levels by timepoint post-reperfusion and donor type of kidney allografts, including interactions. Individual post-reperfusion protein levels were summarized as a single continuous parameter by AUC calculations (trapezoid method) for each patient for outcome analyses. For short-term outcome, associations between protein AUCs and delayed graft function used ROC analyses with Bonferroni correction and Mann-Whitney U tests. Long term graft function was represented by the 4-year AUC of eGFR (mL/min/1.73m² × months) derived from eGFR measurements at 1, 3, 6, 12, 24, 36, and 48 months post-transplantation. Multiple linear regression assessed associations between protein AUCs and long-term graft function, applying log10-transformations on individual protein AUCs to meet normality assumptions and improve model fit. K means clustering (k=2) was used to identify clusters in 1-minute protein levels and elapsed cold ischemic time, followed by ROC analysis and Youden's J Statistic to estimate the cold ischemic time threshold associated with increased protein release. Statistical analyses were performed using GraphPad Prism 10.3.1 (GraphPad Software, San Diego, CA) and IBM SPSS Statistics 28 (IBM Corp., Armonk, NY).

Paper III

Baseline subtraction was applied for post-reperfusion measurements of cell-free DNA, NETs markers, and sC5b-9. Pairwise comparisons of these markers between LD and DD kidney-transplant subgroups used Mann–Whitney U tests. Correlations were assessed by Spearman correlation analyses. Differences in C5b-9 intensity, from flow cytometry, between necrotic and two HK-2 cell control groups were assessed using one-way ANOVA. Plasma markers were summarized as individual AUC values from 1-, 10-, and 30-minute levels for outcome analyses. Associations with delayed graft function used logistic regression, ROC analyses, and Mann–Whitney U tests. Longitudinal graft function throughout 4-years follow-up was either summarized as time-weighted eGFR AUC (eGFR from 1, 3, 6, 12, 24, 36, 48 months post-transplantation divided by 48) or modelled using a linear mixed-effects

model with a random intercept and autoregressive AR(1) covariance structure. K means clustering (k=2) together with ROC analyses and Youden's J Statistic defined thresholds for elapsed cold ischemic time and 1-minute cell-free DNA or sC5b-9 release. Statistical analyses used GraphPad Prism 10.4.1 (GraphPad Software, San Diego, CA) and IBM SPSS Statistics 28 (IBM Corp., Armonk, NY).

Paper IV

Absolute leukocyte concentrations (cell/mL) were obtained by multiplying total white blood cell (WBC) count by the proportion of viable leukocytes and subsequently by the percentage of each gated subset within its parent population, preserving data linearity. ART-ANOVA with Geisser-Greenhouse correction assessed variation in cell counts by sampling timepoint and kidney allograft donor type (LD or DD), including interactions. To evaluate relative dynamics in this analysis, individual values from sampling timepoints were divided by the corresponding baseline value, while also accounting for the generally higher baseline levels and addressing inter-individual pre-implantation variability. Linear regression assessed slopes of cells/mL/min on linear data relative to the time elapsed since methylprednisolone induction. Leave-one-out cross-validation was used to compare monophasic and biphasic linear regression models for each cell subset to assess temporal absolute changes in cell-count trajectories around the reperfusion event. Three linear models from the study participants were fitted in the training set (n=28): 1) slope from baseline to 1 minute, 2) slope throughout 1, 10 to 30 minutes, and 3) single slope across, and including, all timepoints (baseline–30 minutes). The prediction error was quantified as root mean square error (RMSE) and computed for both the biphasic (model 1+2) and monophasic (model 3) models for the left out patient (n=1) in each fold. For each patient, the log-RMSE ratio was computed, where log-(biphasic RMSE/monophasic RMSE) values < 0 indicated better performance of the biphasic model consistent with a change in cell-count trajectory around reperfusion, whereas values > 0 indicated better performance of the monophasic model with no change in cell count trajectories at reperfusion. A Wilcoxon signed-rank test assessed whether the study population median log-RMSE ratio differed from zero, indicating consistent superiority of one model over the other across patients. Statistical analyses used GraphPad Prism 10.4.1 (GraphPad Software, San Diego, CA), IBM SPSS Statistics 28 (IBM Corp., Armonk, NY), and R 4.3.2 for Windows (R Foundation for Statistical Computing, Vienna, Austria).

Results

Paper I – main findings

Characteristics and general outcomes

Paper I included 63 kidney transplant recipients (26 LD and 37 DD) prospectively from August 2018 to June 2019. **Table 2** summarizes patient and donor characteristics. Overall, LD kidney recipients were younger, had younger donors, higher frequencies of predialytic patients, fewer patients on pre-transplant hemodialysis and lower median duration of pre-transplant dialysis compared to recipients of DD kidneys. Glomerulonephritis was more common as a cause of kidney failure in LD kidney recipients. The median cold ischemic time was higher in recipients of DD kidneys compared to LD kidneys (692 minutes [IQR 548-902] vs. 116.5 [95.0–154.8], P<0.001). No statistically significant difference in cold ischemic times was observed between non-oxygenated hypothermic machine-perfused and static cold-stored DD kidneys. Additionally, KDRI was comparable between DD kidney transplant cases of these preservation methods. Remaining characteristics parameters were similar.

One patient death with a functioning graft occurred in a static cold-stored DD kidney recipient (day 64, cytomegalovirus disease). Three graft failures were observed: two in DD kidney transplant recipients (one in a static cold-stored DD kidney recipient due to acute antibody-mediated rejection at day 151; one in a non-oxygenated hypothermic machine perfused DD kidney recipient due to recurrent thrombotic microangiopathy at day 396) and one in an LD kidney recipient (recurrent focal segmental glomerulosclerosis at day 469).

At 24-months follow-up, no differences were observed between kidney-transplant cases of the LD and DD subgroups in overall transplant function, the incidence of biopsy-proven acute rejections, and both graft and patient survival. Six cases of delayed graft function occurred among DD kidneys (**Table 3**).

Table 2. Baseline characteristics of the study population (Paper I) separated by kidney transplant subgroups LD, static cold stored DD (DD_{CS}), and hypothermic machine perfused DD (DD_{HMP}).

Baseline characteristics Median (1st-3rd quartile) or n (%)	Transplant modality (63)			P value for differences
		DD (37)		
	LD (26)	DD_{CS} (22)	DD_{HMP} (15)	
Donor age	51.0 (46.0–59.0)	56.5 (49.8–67.8)	62.0 (46.0–68.0)	0.036[a]
Donor BMI	26.4 (23.5–29.3)	24.8 (22.2–29.5)	23.6 (22.2–29.7)	ns
Donor anoxic brain injury (prior cardiac arrest)	-	6 (27.2)	7 (46.7)	ns
Kidney donor risk index	-	1.56 (1.28–1.97)	1.50 (1.28-1.97)	ns
Cold ischemic time in minutes	116.5 (95.0–154.8)	684.0 (546.8–858.0)	781.0 (504.0–1029.0)	<0.001[a,b,c]
Recipient sex–male	18 (69.2)	14 (63.6)	12 (80.0)	ns
Recipient age	45.5 (35.8–54.3)	53.5 (46.0–60.5)	60.0 (45.0–66.0)	0.011[a], 0.037[c]
Recipient BMI	25.9 (22.5–28.0)	26.0 (23.8–28.5)	24.9 (23.1–26.9)	ns
Preformed DSA	4 (15.4)	4 (18.2)	2 (13.3)	ns
Induction treatment				
Basiliximab	26 (100.0)	20 (90.9)	14 (93,3)	ns
Basiliximab + Rituximab	0 (0.0)	0 (0.0)	1 (6.7)	ns
Thymoglobulin	0 (0.0)	2 (9.1)	0 (0.0)	ns
Pretransplant dialysis modality				
Predialytic	11 (42.3)	3 (13.6)	1 (6.7)	0.006[a], 0.03[c]
Hemodialysis	9 (34.6)	15 (68.2)	9 (60.0)	0.023[a], 0.04[b]
Peritoneal dialysis	6 (23.1)	4 (18.2)	5 (33.3)	ns
Days of pretransplant dialysis	392 (182–730)	1529 (683–1924)	785 (539–1354)	<0.001[a], 0.001[b]
Cause of kidney failure				
Glomerulonephritis	14 (53.8)	5 (22.7)	6 (40.0)	0.027[b]
Diabetic nephropathy	3 (11.5)	5 (22.7)	1 (6.7)	ns
Polycystic kidney disease	3 (11.5)	3 (13.6)	1 (6.7)	ns
Hypertensive nephrosclerosis	3 (11.5)	2 (9.1)	3 (20.0)	ns
Alport syndrome	1 (3.8)	3 (13.6)	0 (0.0)	ns
Unknown	0 (0.0)	1 (4.5)	3 (20.0)	0.043[c]
Other	2 (7.7)	3 (13.6)	1 (6.7)	ns

a LD vs DD
b LD vs DD_{CS}
c DD_{CS} vs DD_{HMP}

Table 3. Outcome parameters of the study population (Paper I) separated by kidney transplant subgroups LD, static cold stored DD (DD_{CS}), and hypothermic machine perfused DD (DD_{HMP})

Outcome at 24 months median (1st–3rd quartile) or n (%)	Transplant modality (63)			P value for differences
		DD (37)		
	LD (26)	DD_{CS} (22)	DD_{HMP} (15)	
s-Creatinine µmol/l	103.0 (93.8–138.5)	117.5 (96.3–149.0)	130.0 (103.0–155.0)	ns
eGFR ml/min per 1.73 m2	62.0 (49.0–69.8)	56.5 (34.3–68.0)	45.5 (34.8–64.8)	ns
Graft failure	1 (3.8%)	2 (9.1%)	1 (6.7%)	ns
Delayed graft function	0 (0.0%)	4 (18.2%)	2 (13.3%)	0.038[a,b]
Patient death	0 (0.0%)	1 (4.5%)	0 (0.0%)	ns
Biopsy-proven acute rejection	7 (26.9%)	6 (27.3%)	5 (33.3%)	ns
De novo DSA	3 (11.5%)	3 (13.6%)	0 (0.0%)	ns
a LD vs DD **b LD vs DD_{CS}**				

Generation of key innate immune cascade activation markers

Activation markers of complement, coagulation, and the kallikrein-kinin systems were profiled in the serial venous effluent samples at baseline and 1, 10, and 30 minutes post-reperfusion. ART-ANOVA showed that key markers of the complement (sC5b-9), coagulation (FXIa-AT/C1INH), and kallikrein-kinin (KK-AT/C1INH and FXIIa-C1INH) systems varied significantly by sampling time or transplant modality (including preservation methods for DD kidneys), with significant interaction terms indicating that temporal activation patterns differed between transplant modalities (**Figure 5**). Furthermore, downstream coagulation activation marked by Thrombin-AT and Thrombin-C1INH demonstrated variation by sampling time points, with significant interaction between sampling time and modality for Thrombin-C1INH.

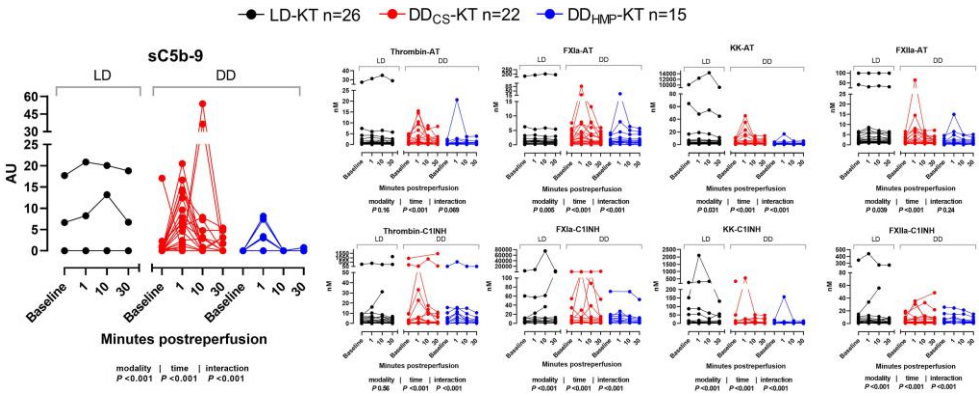

Figure 5. Levels of activation markers of the IIIS stratified by modality and time for the study population (n = 63).
Markers with significant interactions in either or both of their respective protease-serpin complexes are shown. Connected scatter plots are color-coded for the specified modalities; black = LD-KT, red = DD_{CS}-KT and blue = DD_{HMP}-KT. P-values for differences from analysis of variance on aligned rank-transformed data by modality (LD-KT [n = 26], DD_{CS}-KT [n = 22] and DD_{HMP}-KT [n = 15]), time (baseline, 1, 10, and 30 minutes postreperfusion), and the interaction (between time and modality) are presented below each graph (ns = not significant). DD_{CS} = deceased-donor kidney preserved with static cold storage; DD_{HMP} = deceased-donor kidney preserved with hypothermic machine perfusion; LD = living donor; IIIS = intravascular innate immune system.

Correlations of markers within and between the innate immune cascades

Generation of sC5b-9, the terminal complement activation fragment, was absent in 24 out of 26 LD kidneys throughout the pre- and post-reperfusion sampling. In contrast, static cold-stored DD kidneys (n=22) generally exhibited undetectable sC5b-9 at baseline, while reperfusion was associated with a marked release (**Figure 6**). Spearman correlation analyses demonstrated that the sC5b-9 release at 1 minute correlated with upstream complement marker MASP-2, coagulation products FXIa and thrombin, and kallikrein-kinin markers FXIIa and KK. Cross-cascade correlations persisted through 30 minutes, indicating prompt coactivation of the complement, coagulation, and kallikrein-kinin systems and, by extension, retained thrombo-inflammatory response throughout sampling. In non-oxygenated hypothermic machine-perfused DD kidneys (n=15), 1-minute sC5b-9 generation correlated with the activation of FXIa and MASP-1; however, these correlations were not retained throughout the sampling time (**Figure 6**).

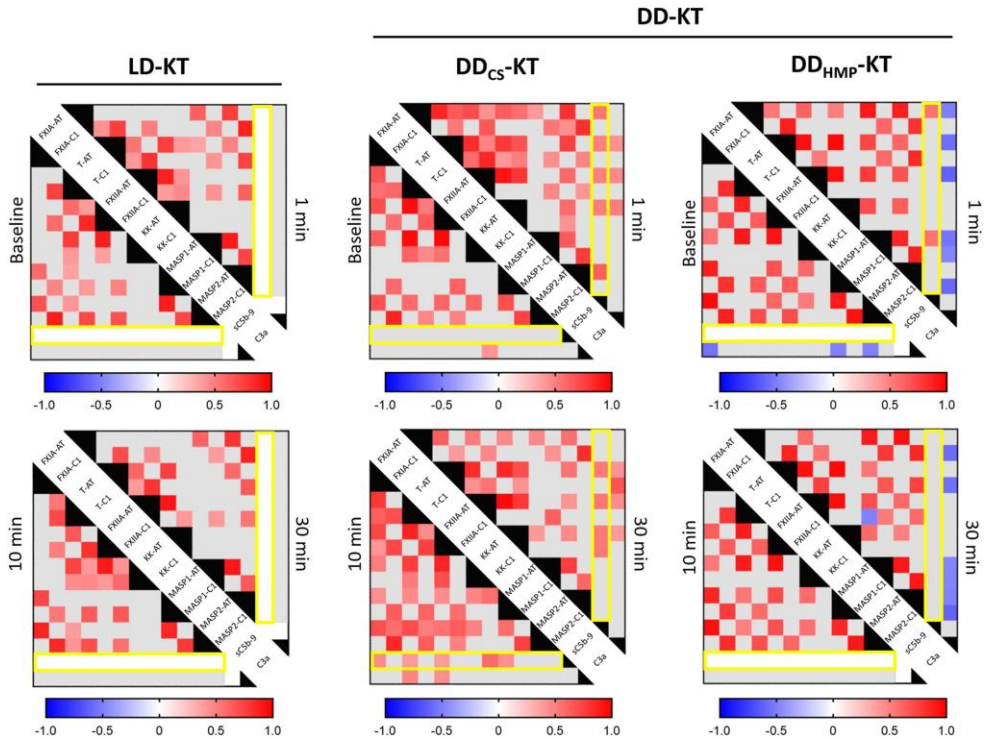

Figure 6. Spearman correlation matrices by modality (DD separated by preservation method) from baseline to 30 minutes postreperfusion. The red gradient denotes significant positive ρ coefficients, and blue denotes significant negative ρ coefficients. Gray squares denote nonsignificant correlations. White squares indicate incomputable correlations due to non or insufficient generation of sC5b-9. A yellow outline highlights sC5b-9. DD_{CS} = deceased-donor kidney preserved with static cold storage; DD_{HMP} = deceased-donor kidney preserved with hypothermic machine perfusion; LD = living donor, KT = kidney transplantation.

Associations with delayed graft function and mid-term allograft function

Soluble C5b-9 was considered as a response marker of IIIS cascade activation, reflecting its concurrent generation with other IIIS activation products during ischemia-reperfusion injury and its reduction in non-oxygenated hypothermic machine-perfused DD kidneys corresponding with attenuated IIIS activation. The cumulative early IIIS cascade response, quantified as sC5b-9 AUC from baseline to 30 minutes ($AUC_{b–30}$), was associated with delayed graft function (ROC AUC 0.81, 95% CI 0.61–1.00; P = 0.012).

Stratification by retained IIIS cascade activation, defined as detectable sC5b-9 generation at 30 minutes post-reperfusion, identified a small subgroup (LD kidneys 2/26, static cold-stored DD kidneys 6/22, and non-oxygenated hypothermic machine-perfused DD kidneys 1/15) with persistently impaired allograft function.

These patients exhibited significantly lower eGFR throughout the 24-month follow-up compared with those without retained sC5b-9 activity. (**Figure 7a**). In addition, the eGFR slope over 24 months was significantly lower in patients with retained sC5b-9 generation than in those without (median −0.31, [IQR −0.56 to −0.20] and 0.19 [IQR −0.13 to 0.39), P = 0.007), indicating progressive functional decline.

Among DD kidneys, eGFR slopes from 1 to 24 months differed significantly between static cold-stored DD kidney-transplant recipients with versus without retained sC5b-9 (−0.48 [IQR −0.56 to −0.31] versus 0.13 [IQR −0.09 to 0.51], P = 0.014). In contrast, eGFR slopes did not differ between recipients of non-oxygenated hypothermic machine-perfused DD kidneys and recipients of static cold-stored DD kidneys either with retained or without retained sC5b-9 generation (**Figure 7b**).

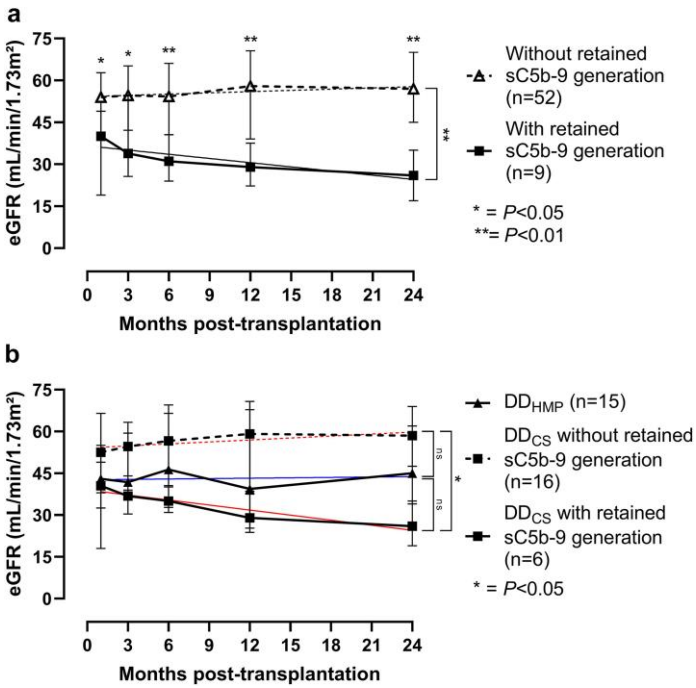

Figure 7. Progression of median eGFR (ml/min per 1.73 m2) with interquartile range from 1 to 24 months post-transplantation stratified (a) for retained sC5b-9 generation (defined as sC5b-9 generation at 30 minutes following reperfusion) within the study cohort and (b) for modalities DD_{HMP} and DD_{CS} with and without retained sC5b-9 generation. The eGFR slopes, calculated between 1 and 24 months, are represented by filled and dashed lines in the figures. The lines are color-coded in red for DD_{CS} and blue for DD_{HMP}. Two LD-KT patients with missing data on 30-minute sC5b-9 are excluded from the analyses. In addition, 2 patients (DD_{CS}-KT and LD-KT) are excluded from the slope analyses due to patient death on day 64 and loss to follow-up on day 69, respectively. DD_{CS} = deceased-donor kidney preserved with static cold storage; DD_{HMP} = deceased-donor kidney preserved with hypothermic machine perfusion; eGFR = estimated glomerular filtration rate, KT = kidney transplantation.

Immediate sC5b-9 expression in relation to cold ischemic time

The relationship between elapsed cold ischemic time and immediate sC5b-9 expression post-reperfusion was evaluated within all subgroups of transplant modalities and preservation methods. A ROC analysis was performed to determine the threshold of elapsed cold ischemic time for immediate sC5b-9 release (> 0 AU/mL) at 1-minute (**Figure 8**). Here, Youden's J Statistic indicated that a cutoff at 522.4 minutes was associated with immediate sC5b-9 release (73% specificity, 83% sensitivity).

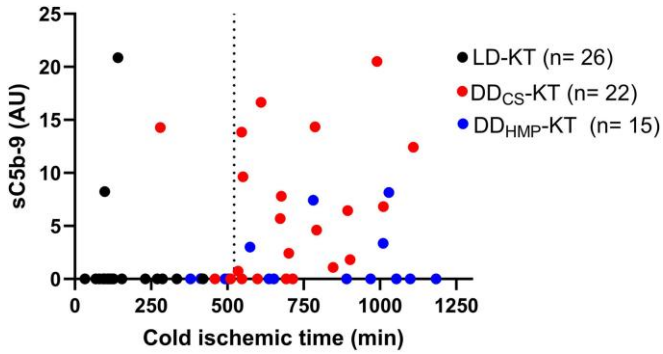

Figure 8. Scatterplot presenting levels of sC5b-9 by cold ischemic time.
A dashed line denotes 522.4 minutes on the x-axis. DD_{CS}, deceased donor kidney preserved with static cold storage; DD_{HMP} = deceased-donor kidney preserved with hypothermic machine perfusion; LD = living donor, KT = kidney transplantation.

Paper II – main findings

Characteristics and general outcomes

Paper II used the same cohort as **Paper I**. Baseline donor and patient characteristics are summarized in **Table 2**. At 4 years of follow-up, 6 cases of delayed graft function occurred among recipients of DD kidneys. In the DD group, two patients died with functioning grafts (days 64 and 939), one patient died with concurrent graft failure (day 774), and three additional graft failures occurred due to acute antibody-mediated rejection, recurrent thrombotic microangiopathy, and unknown cause (days 151, 396, and 1397). In the LD group, one graft failure occurred due to recurrent focal segmental glomerulosclerosis (day 469). One patient in each of the LD and DD groups was lost to follow-up due to emigration (days 69 and 1100, respectively).

Overall, there were no differences between the LD and DD groups in transplant function, graft or patient survival, or biopsy-proven acute rejection at 4 years (**Table 4**).

Table 4. Outcome parameters of the study population separated by LD- and DD kidney transplant recipients

Outcomes by 48 months post-transplantation	Donor type (n = 63)		P value
	LD (n = 26)	DD (n = 37)	
P-Creatinine, µmol/L	111.5 (91.5–132.0)	121.0 (92.0–147.0)	0.41
eGFR, mL/min/1.73 m^2	58.0 (42.0–69.0)	51.0 (36.0–64.0)	0.29
Non-death-censored graft failure	1 (3.8)	6 (16.2)	0.22
Delayed graft function	0 (0.0)	6 (16.2)	0.038
Patient death	0 (0.0)	3 (8.1)	0.26
Biopsy-proven acute rejection	8 (30.8)	10 (27.0)	0.78
De novo DSA	3 (11.5)	4 (10.8)	1.00

Data are presented as frequencies (column percentages) and medians (first–third quartile). P values are expressed for comparisons of the 2 groups.
DD = deceased-donor; DSA = donor-specific antibody; eGFR = estimated glomerular filtration rate; LD = living-donor.

Protein release profiles between kidneys by donor type

Across the cohort, all 92 markers were initially screened using a P value threshold of <0.05 to identify proteins increased during the post-reperfusion phase between donor types. From this initial screening, only markers showing a distinct upregulation at $P < 0.01$ were subsequently evaluated for associations with clinical outcomes.

At 1 minute post-reperfusion, DD kidneys showed increased release of hepatocyte growth factor (HGF), osteoprotegerin (OPG), artemin (ARTN), and eukaryotic translation initiation factor 4E-binding protein 1 (4E-BP1) compared with LD kidneys. HGF release in DD kidneys persisted at 1, 10, and 30 minutes. In addition, transforming growth factor-α (TGF-α) and interleukin-33 (IL-33) increased in DD kidneys from 10 to 30 minutes post-reperfusion.

In the LD group, tumor necrosis factor–related activation-induced cytokine (TRANCE) increased at 1 min postreperfusion, while IL-6, leukemia inhibitory factor (LIF), fibroblast growth factor-23 (FGF-23), adenosine deaminase (ADA), and monocyte chemoattractant protein-4 (MCP-4) were elevated at 30 minutes (**Figure 9**).

In a complementary analysis within the DD group, non-oxygenated hypothermic machine perfusion was associated with higher 30-minute release of CXCL1, ADA,

and IL-7 compared with static cold storage, whereas no differences were observed at 1 or 10 minutes.

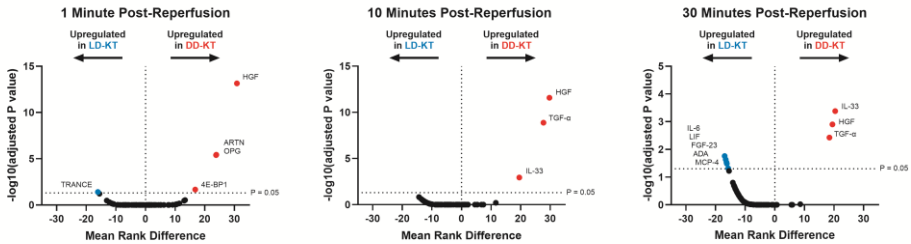

Figure 9. Post-reperfusion inflammatory protein expression profiles by kidney-transplant cases of different donor type. Volcano plots presenting the –log10 adjusted P values and mean rank differences from Mann-Whitney U tests on all 92 proteins between donor types of transplant cases at 1, 10, and 30 min postreperfusion. Mean rank differences are presented as DD kidneys minus LD kidneys. Red and blue dots indicate upregulated proteins in DD and LD kidneys, respectively. A horizontal dotted line indicates the –log10 adjusted P value for P = 0.05. Proteins above the significance threshold are labeled. DD-KT = deceased-donor kidney transplantation; LD-KT = living-donor kidney transplantation.

Temporal protein release dynamics between kidneys by donor type

The five proteins upregulated at $P < 0.01$ assessed for temporal release patterns by donor type. Levels of HGF, ARTN, OPG, TGF-α, and IL-33 all varied significantly by donor type, time post-reperfusion, and showed protein release dependent on the combined effect of donor type and elapsed time post-reperfusion (**Figure 10**).

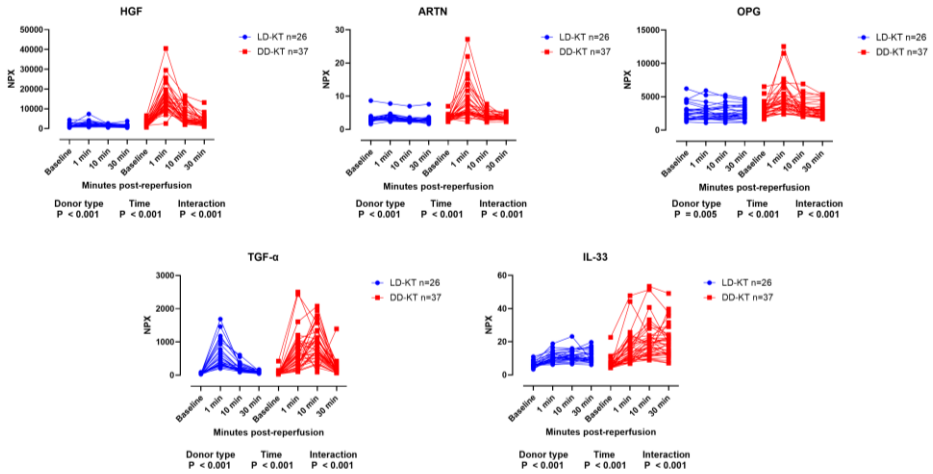

Figure 10. Protein levels by donor type and sampling time. Connected scatter plots of protein levels by sampling time and donor type. Protein levels are presented as nonbaseline adjusted to allow for visualization of preimplantation levels. Blue and red denote LD-KT and DD-KT, respectively. Proteins below the alpha limit of 0.01 from the multiple comparisons by transplant modality are presented. P values from aligned rank-transformed ANOVA are presented for differences in protein levels by donor type, sampling time, and their interaction. DD = deceased-donor; LD = living-donor; KT = kidney transplantation; NPX = normalized protein expression.

Post-reperfusion protein release and associations with delayed graft function and long-term allograft dysfunction

Proteins upregulated at $P < 0.01$ in the initial screening were summarized as individual post-reperfusion AUCs based on baseline-subtracted data to enable standardized comparisons across release patterns (**Figure 10**). In the full cohort, post-reperfusion IL-33 and HGF AUCs were associated with delayed graft function, whereas no associations were observed for the remaining proteins (**Table 5**). IL-33 levels were significantly higher in patients with delayed graft function than in those without delayed graft function, while HGF showed a non-significant trend toward higher levels in delayed graft function (**Table 6**).

TABLE 5. Baseline-adjusted protein levels from 1, 10, and 30 min post-reperfusion summarized into AUC and associations with delayed graft function

Protein	ROC AUC	Adjusted P value	95% CI
IL-33	**0.77**	**0.0012**	**0.63-0.91**
HGF	**0.73**	**0.0055**	**0.59-0.87**
TGF-α	0.66	0.29	0.49-0.83
ARTN	0.59	1.00	0.37-0.81
OPG	0.54	1.00	0.28-0.79

ARTN = artemin; AUC = area under the curve; CI = confidence interval; HGF = hepatocyte growth factor; IL-33 = interleukin 33; OPG = osteoprotegerin; ROC = receiver operating characteristic; TGF-α = transforming growth factor α.

TABLE 6. Mann-Whitney U tests by delayed graft function status on the AUC of protein levels from baseline-subtracted data at 1, 10, and 30 min post-reperfusion

Protein	DGF (n = 6)	No DGF (n = 57)	P value
IL-33	**391.55 (286.50-527.30)**	**204.80 (128.20-375.60)**	**0.030**
HGF	110 373.00 (91 281.00-150 703.00)	54 471.00 7906.00-110 608)	0.065
TGF-α	12 087.00 (10 867.00–20 392.00)	10224.00 (4428.00–17 966.00)	0.20
ARTN	23.42 (5.51–32.05)	13.43 (2.83–31.34)	0.47
OPG	3085.50 (943.40–30 639.00)	6593.00 (497.40–12 987.00)	0.78

Protein levels are presented as NPX × minutes in median (first–third quartile). ARTN = artemin; AUC = area under the curve; DGF = delayed graft function; HGF = hepatocyte growth factor; IL-33 = interleukin-33; NPX = normalized protein expression; OPG = osteoprotegerin; TGF-α = transforming growth factor α.

Increased post-reperfusion HGF release was associated with decreased allograft function over 4 years, indicated by the significant negative association between HGF release and the AUC of eGFR. Conversely, elevated post-reperfusion ARTN release was positively associated with the AUC of eGFR (**Table 7**).

TABLE 7. Log-transformed AUC baseline-adjusted protein levels from 1, 10, and 30 min post-reperfusion and associations long-term graft function (AUC of eGFR from 1-, 3-, 6-, 12-, 24-, 36- to 48-months post-transplantation)

Protein	Unstandardized coefficient B	Standardized coefficient β	t value	P	95% CI
Constant	4331.74	–	2.43	0.019	735.72 to 7927.77
HGF	**–768.20**	**–0.58**	**–2.62**	**0.012**	**–1359.03 to –177.37**
ARTN	**418.96**	**0.44**	**2.28**	**0.028**	**48.04 to 789.87**
TGF-α	418.39	0.16	0.76	0.45	–694.99 to 1531.77
IL-33	–90.67	–0.04	–0.24	0.81	–842.76 to 661.41
OPG	–64.85	–0.05	–0.31	0.76	–488.20 to 358.49

Bold text highlights significant associations. ARTN = artemin; AUC = area under the curve; CI = confidence interval; eGFR = estimated glomerular filtration rate; HGF = hepatocyte growth factor; IL-33 = interleukin 33; OPG = osteoprotegerin; TGF-α = transforming growth factor α.

Immediate HGF release in relation to cold ischemic time

To limit multiple comparisons, analyses of protein–cold ischemic time associations were restricted to the most robustly upregulated marker HGF. K-means clustering (k = 2) identified two distinct clusters defined by HGF release at 1 min post-reperfusion and elapsed cold ischemic time, with cluster centers of 1943.0 versus 14 580.2 NPX for HGF and 244.4 versus 743.5 min for cold ischemic time. Dichotomization by cluster membership followed by ROC analysis on patients in the high-cold ischemic time cluster and elapsed cold ischemic time. Youden's J statistic identified an approximate cold ischemic time cutoff of 475.5 min, yielding 97% sensitivity and 91% specificity for elevated HGF levels at 1 min post-reperfusion (**Figure 11**).

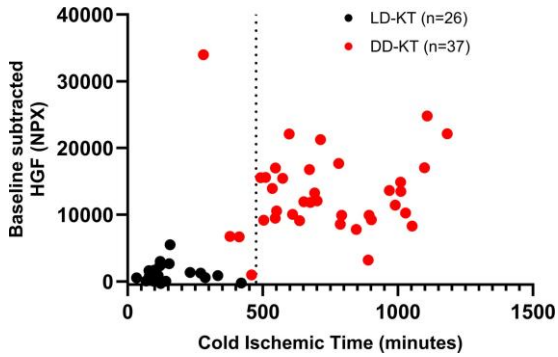

FIGURE 11. Cold ischemic time and immediate post-reperfusion HGF release.
Scatter plot of HGF levels by cold ischemic time at 1 min post-reperfusion. A vertical dotted line indicates 475.5 min of cold ischemic time. DD = deceased-donor; HGF = hepatocyte growth factor; KT = kidney transplantation; LD = living-donor; NPX = normalized protein expression.

Paper III – main findings

Baseline characteristics and general outcomes

Paper III included 127 kidney transplant recipients (41 LD and 86 DD) from August 2018 to August 2020. All LD and 54 DD kidneys were preserved by static cold storage, and 32 DD kidneys underwent non-oxygenated hypothermic machine perfusion. Characteristics are summarized in **Table 9**. Recipient and donor ages, as well as cold ischemic times were lower in LD kidney-transplant recipients than DD kidney-transplant recipients. Preemptive transplantations and glomerulonephritis were more frequent in the LD group. Three LD kidney transplant recipients received methylprednisolone-induction only. Apart from preservation methods, remaining baseline characteristics were similar. Within the DD group, cold ischemic times and KDPI were comparable between static cold-stored and non-oxygenated hypothermic machine-perfused kidneys (cold ischemic times: 668.0 min [544.0-767.0] versus 662.0 min [498.0-869.0], P = 0.939; KDPI 52.0% [20.0-78.0] versus 64.0% [55.0-78.0], P = 0.101, respectively).

In the DD group, 12 patients developed delayed graft function. Four patients died with functioning grafts (day 64, tissue-invasive cytomegalovirus; days 939, 1089, and 1144, undocumented causes), and one patient died with concurrent graft failure on day 774 due to COVID-19. One case of early allograft artery thrombosis required transplantectomy on day 1 and was not classified as graft failure. Three graft failures occurred in the DD group due to acute antibody-mediated rejection, recurrent thrombotic microangiopathy, and unknown cause (days 151, 396, and 1397). In the LD group, one graft failure occurred due to recurrent focal segmental glomerulosclerosis on day 469. Three LD kidney transplant recipients and one DD

kidney-transplant recipient were lost to follow-up due to emigration on days 63, 69, 232 and 1100, respectively.

At 4 years, eGFR, allograft and patient survival, rejection rates, and de novo donor-specific antibody frequencies were comparable between recipients of LD and DD kidneys (**Table 8**).

Table 8. General outcome parameters by 4 years post-transplantation

General outcomes			
Outcomes by 4-year follow-up (median [1st-3rd quartile] and n [percent])	LD-KT	DD-KT	*P* value
Delayed graft function	**0 (0.0)**	**12 (14.0)**	**0.009**
Non-death-censored graft failure	1 (2.4)	8 (9.3)	0.27
eGFR (ml/min/1.73m^2)	52.5 (40.5-69.0)	51.0 (37.1-66.5)	0.69
Biopsy-proven acute rejection	7 (17.1)	18 (20.9)	0.81
Patient death	0 (0.0)	5 (5.8)	0.32
De novo donor-specific antibodies	3 (7.3)	8 (19.5)	1.00

P values for differences between LD and DD are presented. Bold text indicates P values less than 0.05. LD-KT = living-donor kidney transplantation, DD-KT = deceased-donor kidney transplantation, eGFR = estimated glomerular filtration rate.

Table 9. Baseline characteristics (Paper III) of KT subgroups by donor type (LD versus DD).

Baseline characteristics				
Median (1st-3rd quartile) or n (percent)		**LD-KT (n=41)**	**DD-KT (n=86)**	***P* value**
Sex – male		31 (75.6)	58 (67.4)	0.347
Recipient	Age	44.0 (35.0-54.0)	53.0 (45.0-61.0)	0.002
	BMI	26.3 (22.9-29.1)	25.4 (23.3-27.7)	0.728
Donor	Age	52.0 (47.0-56.0)	60.0 (47.0-68.0)	0.015
	BMI	26.5 (23.4-28.4)	25.7 (23.1-29.3)	0.898
Deceased donor type	DBD		82 (95.3)	N/A
	DCD		4 (4.7)	N/A
Cold ischemic time (minutes)		111.0 (78.0-127.0)	668.0 (535.0-792.0)	< 0.001
Pre-formed donor-specific antibodies		6 (14.6)	6 (7.0)	0.200
Preservation method	SCS	41 (100.0)	54 (62.8)	< 0.001
	Non-oxygenated HMP	0 (0.0)	32 (37.2)	< 0.001
Kidney donor profile index			59.5 (34.5-78.0)	N/A
Induction therapy (methylprednisolone + additional)	Basiliximab	37 (90.2)	74 (86.0)	0.505
	Thymoglobulin	1 (2.4)	12 (14.0)	0.060
	Basiliximab + Rituximab	4 (9.8)	4 (4.7)	0.271
	Methylprednisolone only	3 (7.3)	0 (0.0)	0.032
Pre-transplant dialysis	Preemptive	17 (41.1)	11 (12.8)	< 0.001
	Hemodialysis	15 (36.6)	47 (54.7)	0.057
	Peritoneal dialysis	9 (22.0)	28 (32.6)	0.219
Cause of kidney failure	Glomerulonephritis	23 (56.1)	25 (29.1)	0.003
	Polycystic kidney disease	7 (17.1)	13 (15.1)	0.777
	Diabetic nephropathy	2 (4.9)	12 (14.0)	0.224
	Hypertensive nephrosclerosis	1 (2.4)	12 (14.0)	0.060
	Alport syndrome	1 (2.4)	3 (3.5)	1.000
	Unknown	1 (2.4)	6 (7.0)	0.427
	Other	6 (14.6)	15 (17.4)	0.690

Continuous variables are expressed as median (1st to 3rd quartile) and categorical variables as n (percent). P values for differences between LD and DD kidney transplant cases are presented. Bold text indicates P values less than 0.05. LD-KT = living-donor kidney transplantation, DD-KT = deceased-donor kidney transplantation, BMI = body mass index, DBD = donation after brain death, DCD = donation after circulatory death, non-oxygenated HMP = hypothermic machine perfusion, SCS = static cold storage.

Post-reperfusion releases of cell-free DNA and NETs markers between modalities

After reperfusion, DD kidneys exhibited higher nuclear cell-free DNA levels than LD kidneys at 1, 10, and 30 minutes (**Figure 12A**). Mitochondrial cell-free DNA levels were higher in DD kidneys at 1 minute, with no differences at 10 or 30 minutes (**Figure 12B**).

In the 56-patient subset analyzed for NETs markers, HNE–DNA levels were higher in DD kidneys at 10 and 30 minutes, but not at 1 minute (**Figure 12C**), whereas citrullinated histone H3 did not differ between donor types at any timepoint (**Figure 12D**).

HNE–DNA correlated with nuclear cell-free DNA at 10 and 30 minutes and with mitochondrial cell-free DNA at 1 minute. Citrullinated histone H3 correlated with mitochondrial cell-free DNA at 30 minutes, but not with nuclear cell-free DNA. No correlations were observed between HNE–DNA and citrullinated histone H3. Correlation matrices are provided in **Supplementary Tables S1** and **S2**.

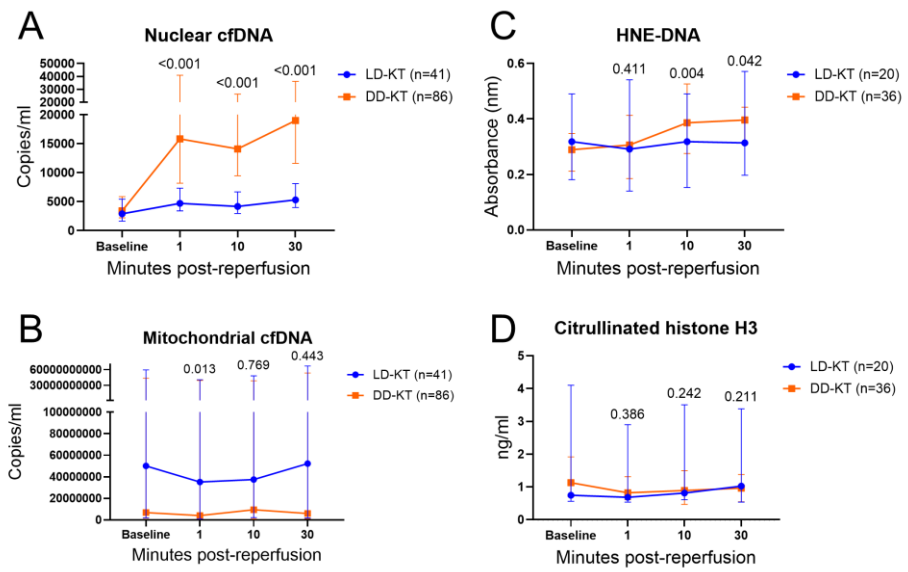

Figure 12. Pre- and post-reperfusion cell-free DNA and NETs marker levels. Connected scatter plots depicting median (interquartile range) of cfDNA (LD-KT n=41, DD-KT n=86) and NETs markers (LD-KT n=20, DD-KT n=36) by sampling time for LD (blue) and DD (orange) KT cases. To allow for visualization of baseline, plots present non-baseline-adjusted values for nuclear cfDNA (A), mitochondrial cfDNA (B), HNE-DNA (C), and citrullinated histone H3 (D). P values are presented for differences in baseline-subtracted levels between modalities. LD-KT = living-donor kidney transplantation, DD-KT = deceased-donor kidney transplantation, cfDNA = cell-free DNA, HNE-DNA = human neutrophil elastase-DNA.

Associations of cell-free DNA release and delayed graft function

Cumulative cell-free DNA levels ($AUC_{1\text{-}30min}$) were analyzed in the full cohort after exclusion of the day-1 transplantectomy case. Nuclear cell-free DNA levels were higher in patients with delayed graft function (n = 12) compared with those without delayed graft function (n = 114) (**Figure 13A**), whereas mitochondrial cell-free DNA levels did not differ by delayed graft function status (**Figure 13B**).

Nuclear cell-free DNA was significantly associated with delayed graft function (OR 8.65 per 10-fold increase) while no association was observed for mitochondrial cell-free DNA (**Figure 13C**). Consistently, nuclear cell-free DNA discriminated delayed graft function cases from non-delayed graft function cases, whereas mitochondrial cell-free DNA did not (**Figure 13D**).

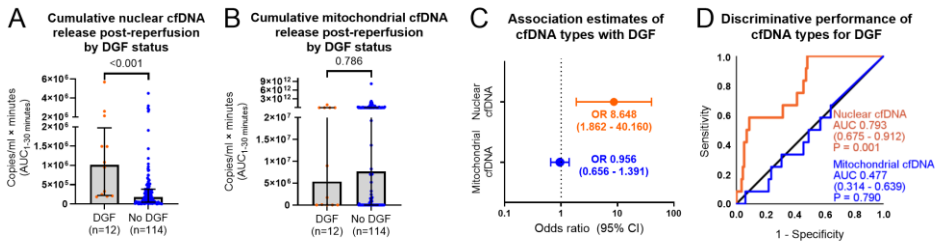

Figure 13. Nuclear and mitochondrial cell-free DNA and associations with delayed graft function. Plots presenting differences in cumulative cfDNA release post-reperfusion (AUC1-30 minutes) stratified by DGF status (DGF n=114, no DGF n=12) by Mann–Whitney U tests (A-B), association estimates of cumulative cfDNA release with DGF by binary logistic regression (C) and discriminative performance of cumulative cfDNA release for DGF by receiver operating characteristic curves (D). Cumulative post-reperfusion release of nuclear- and mitochondrial cfDNA are represented by individual AUCs from 1-, 10-, and 30-minutes post-reperfusion levels after baseline subtraction. For binary logistics regression, AUCs of cfDNA types were log10-transformed. Bar charts present median with scatter distribution and error bars of interquartile range, the dot plot presents OR with 95% confidence interval. P values are presented for the specified analyses. cfDNA = cell-free DNA, OR = odds-ratio, DGF = delayed graft function, AUC = area under the curve.

Association of cell-free DNA release and allograft function over the long-term follow-up

Longitudinal 4-year allograft function was assessed by cell-free DNA types. Neither nuclear nor mitochondrial cell-free DNA release was associated with eGFR over time (**Table 10**).

Table 10. Longitudinal allograft function and cell-free DNA release

Long-term impact of cfDNA on allograft function (eGFR) over 4 years follow-up			
Parameter	Estimate	*P* value	95% CI
Nuclear cfDNA (log10 AUC)	1.074	0.722	-4.925 – 7.074
Mitochondrial cfDNA (log10 AUC)	-1.071	0.276	-3.016 – 0.874

Linear mixed-effects model on the long-term association between baseline-subtracted AUC cfDNA types (log10 transformed) and eGFR levels over a 4-year follow-up (repeated eGFR values from 1-, 3-, 6-, 12-, 24-, 36-, and 48-months post-transplantation). A random intercept per patient accounts for individual variability. cfDNA = cell-free DNA, eGFR = estimated glomerular filtration rate, AUC = area under the curve.

Assessments on sC5b-9 associations with cell-free DNA and allograft function over the long-term follow-up

In **Paper I**, persistent thrombo-inflammatory activation, defined as detectable sC5b-9 levels at 30 minutes post-reperfusion and predominantly observed in DD kidneys, was associated with impaired allograft function at 2 years. Of the 63 recipients included in that cohort, 58 were also part of the present cohort. To examine the relationship between early post-reperfusion cell-free DNA release and thromboinflammation, corresponding cell-free DNA and sC5b-9 levels were analyzed in this subset, comparing recipients with persistent sC5b-9 generation (n = 8) to those without (n = 49). One LD kidney-transplant recipient lacking 30-minute sC5b-9 data was excluded from these analyses.

Nuclear cell-free DNA correlated with sC5b-9 levels at 1 minute and 10 minutes, whereas mitochondrial cell-free DNA correlated with sC5b-9 at 10 minutes only (**Supplementary Table S3**).

Recipients with persistent sC5b-9 generation exhibited a significantly lower 4-year time-weighted average eGFR, compared with recipients without persistent sC5b-9 (**Figure 14A**).

Cumulative nuclear cell-free DNA release was higher in recipients with persistent sC5b-9 generation than in those without (**Figure 14B**), whereas cumulative mitochondrial cell-free DNA levels did not differ according to 30-minute sC5b-9 status (**Figure 14C**).

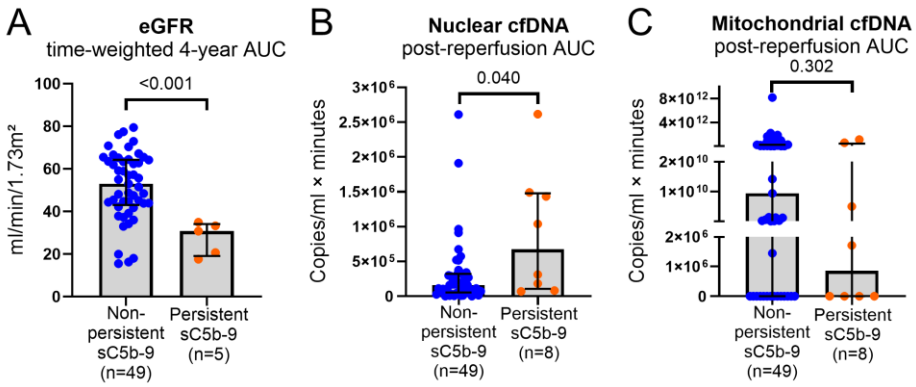

Figure 14. Soluble C5b-9 generation in relation to allograft function over 4 years and cell-free DNA release. Bar charts with scatter presenting distributions of time-weighted average of 4-year eGFR (AUC of 1-, 3-, 6-, 12-, 24-, 36-, to 48-months post-transplantation, divided by 48 months) (A), post-reperfusion AUCs of nuclear (B) and mitochondrial (C) cfDNA (from baseline-subtracted 1-, 10- and 30-minutes levels) stratified by persistent sC5b-9 status (denoted in blue and orange). Persistent sC5b-9 was defined as detectable sC5b-9 generation at 30 minutes post-reperfusion. Sample sizes were n=49 for and n=5 for non-persistent and persistent sC5b-9 in (A), and n=49 and n=8, respectively, in (B) and (C). Bars depict the median and error bars the interquartile range. P values are presented for differences by Mann–Whitney U tests. eGFR = estimated glomerular filtration rate, cfDNA = cell-free DNA, sC5b-9 = soluble C5b-9, AUC = area under the curve.

Comparison of nuclear cell-free DNA and sC5b-9 in deceased-donor kidneys by preservation method

To assess whether preservation strategy influenced early intragraft injury and thrombo-inflammatory activation, nuclear cell-free DNA and sC5b-9 were compared between non-oxygenated hypothermic machine-perfused and static cold-stored DD kidneys.

Nuclear cell-free DNA levels did not differ between machine-perfused (n = 32) and static cold-stored kidneys (n = 54) at 1, 10, or 30 minutes post-reperfusion (**Figure 15**).

Among recipients with available sC5b-9 data (machine-perfused kidneys n = 15; static cold-stored n = 20), baseline-subtracted sC5b-9 levels were lower after non-oxygenated hypothermic machine perfusion at 1 minute post-reperfusion (P = 0.033). Soluble C5b-9 generation at 10 and 30 minutes was rare in machine-perfused kidneys (0 and 1 cases, respectively) compared with static cold-stored kidneys (9 and 5 cases, respectively), precluding meaningful statistical comparisons. Nonetheless, cumulative sC5b-9 release ($AUC_{1\text{-}30min}$) was markedly lower after non-oxygenated hypothermic machine perfusion than static cold storage (P < 0.001).

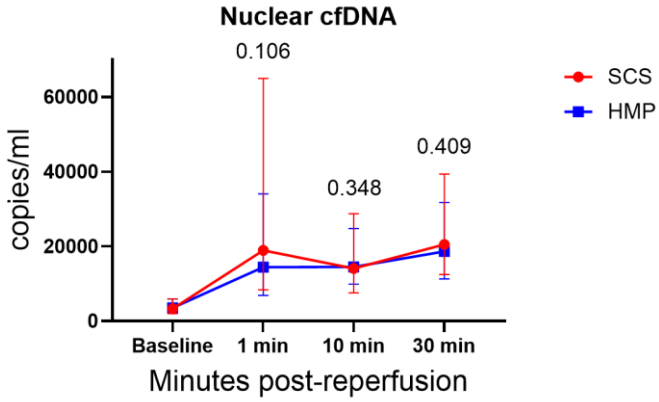

Figure 15. Nuclear cell-free DNA release by deceased-donor kidney preservation method. Connected scatter plots depicting median (interquartile range) of nuclear cfDNA levels (copies/mL) by sampling time for recipients of DD kidneys, stratified by preservation method: non-oxygenated HMP (n=32) and SCS (n=54). To allow for visualization of baseline, plots present non-baseline-adjusted values for nuclear cfDNA. P values are presented for differences in baseline-subtracted levels between preservation methods by Mann–Whitney U tests. cfDNA = cell-free DNA, DD = deceased-donor, HMP = hypothermic machine perfusion, SCS = static cold storage.

Immediate release of cell-free DNA and sC5b-9 by cold ischemic time

To assess the impact of ischemia on immediate cell-free DNA and sC5b-9 release, cold ischemic time was related to 1-minute post-reperfusion levels.

K-means clustering (k = 2) identified two distinct clusters of 1-minute nuclear cell-free DNA release with corresponding differences in cold ischemic times, defining a high cell-free DNA/high cold ischemic time cluster. ROC analysis of the higher cluster-membership and elapsed cold ischemic time demonstrated good discriminatory capacity (ROC AUC 0.772, P = 0.004), with Youden's J statistic indicating an estimated cold ischemic time cutoff of 495 minutes for increased nuclear cell-free DNA release (**Figure 16**). No significant clustering was identified for mitochondrial cell-free DNA.

Among recipients with available sC5b-9 data (n = 58), cold ischemic time was similarly associated with immediate sC5b-9 generation (ROC AUC 0.771, P = 0.001), yielding an estimated cold ischemic time cutoff of 522.5 minutes for increased 1-minute sC5b-9 release (**Figure 16**).

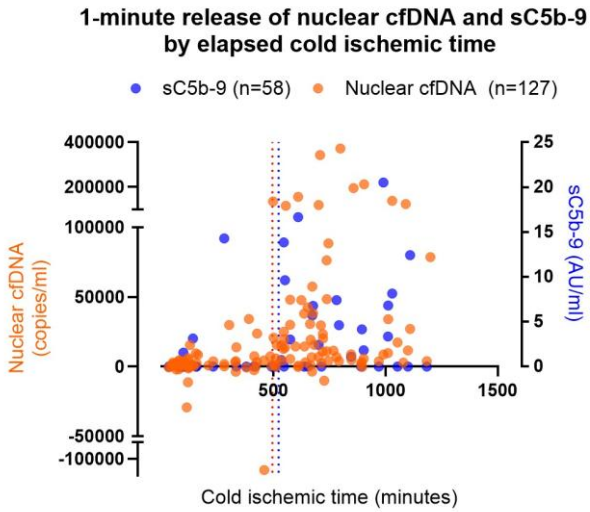

Figure 16. 1-minute release of nuclear cell-free DNA (n=127) and sC5b-9 (n=58) by cold ischemic time. Scatter plot presenting baseline-subtracted 1-minute release of nuclear cfDNA (orange) and sC5-9 (blue) by elapsed cold ischemic time. Orange and blue vertical dotted lines indicate Youden's J-esimated cutoffs from receiver operating characteristics for increased 1-minute release at 495.0 and 522.5 minutes of cold ischemic time, respectively. cfDNA = cell-free DNA, sC5b-9 = soluble C5b-9.

Cell culture necrosis model and C5b-9

A necrosis model on human proximal tubular cells (HK-2) was incorporated to further elaborate on possible mechanistic links from findings of increased nuclear cell-free DNA release, predominantly in DD kidneys, and correlations with elapsed cold ischemic time and sC5b-9.

After induction of necrosis, C5b-9 deposition was assessed by flow cytometry and confocal microscopy. Necrotic and live cells were identified by Annexin V and viability dye staining and incubated with buffer alone or 10% NHS. Necrotic cells exposed to NHS showed markedly increased C5b-9 deposition compared with buffer-treated necrotic cells, whereas live cells exhibited minimal C5b-9 deposition under both conditions. Confocal microscopy confirmed extensive C5b-9 staining on necrotic cells, with no deposition on live controls (**Figure 17**).

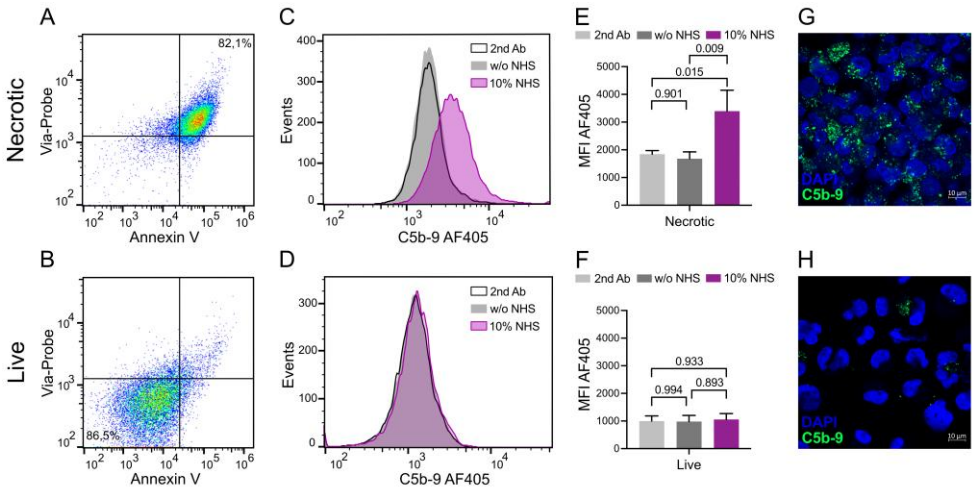

Figure 17. C5b-9 deposition on live and necrotic HK-2 cells assessed by flow cytometry and confocal microscopy. Annexin V and Via-Probe were used to gate live (AV-, Via-) and necrotic cells (AV+, Via+) (A-B). C5b-9 deposition was determined on cells incubated with buffer only or NHS. Cells incubated with NHS but without primary antibody were used as an additional negative control. Representative histograms are presented (C-D). MFI of n = 3 repeats was used for comparison between the necrotic cells and negative controls (E) and live cells and negative controls (F). Graphs depict mean with standard deviation. P values from one-way ANOVA are presented (E-F). C5b-9 deposition (green) on live and necrotic HK-2 cells visualized by confocal microscopy. Nuclei were counterstained with DAPI (blue). Scale bar corresponds to 10 µm (g-h). w/o = without, NHS = normal human serum, MFI = mean fluorescence intensity.

Paper IV – main findings

Characteristics and general outcomes

In DD kidney-transplant recipients, donor and recipient ages, as well as cold ischemic times, were higher compared to recipients of LD kidneys. Hypothermic machine perfusion preservation was used in 52.4% of DD kidneys and 0% of LD kidneys (**Table 11**). Six cases of delayed graft function occurred in the DD group. No death-censored graft failure occurred in the study cohort. Two patients in the DD group died on days 785 and 494 due to acute subdural hematoma and respiratory failure with cytomegalovirus infection, respectively. At four years follow-up, there were no statistical differences between recipients of LD and DD kidneys in plasma-creatinine and eGFR, nor the incidence of patient death or biopsy-proven acute rejections of any type (**Table 12**).

Table 11. Donor and recipient characteristics (Paper IV) stratified by transplant modality.

Characteristics and outcome		Study population (n=29)		P value
Median (1st-3rd quartile) or frequencies (percent)		LD-KT (n=8)	DD-KT (n=21)	
Sex – male		4 (50.0)	14 (66.7)	0.433
Recipient Age		43.5 (32.0-60.0)	59.0 (54.0-65.0)	0.036
Donor Age		51.5 (44.0-55.0)	63.0 (54.0-70.0)	0.016
Cold ischemic time		139.5 (69.0-223.0)	569.0 (495.0-868.0)	< 0.001
Preservation method	Static cold storage	8 (100)	10 (47.6)	0.012
	Hypothermic machine perfusion	0 (0.0)	11 (52.4)	0.012
Dialysis type	Preemptive	1 (12.5)	2 (9.5)	1.000
	Hemodialysis	4 (50.0)	14 (66.7)	0.433
	Peritoneal dialysis	3 (37.5)	5 (23.8)	0.646
Induction therapy	Solumedrol + basiliximab	5 (62.5)	21 (100.0)	0.015
	Solumedrol + basiliximab + rituximab	3 (37.5)	0 (0.0)	0.015

Values are presented as median (1st-3rd quartile) or frequencies (percent). P values are presented for differences between transplant modalities. Bold text highlights P values < 0.05. LD = living-donor, DD = deceased-donor, KT = kidney transplantation.

Table 12. Outcomes by 4 years follow-up stratified by transplant modalities.

Outcome by 4 years		LD-KT (n=8)	DD-KT (n=21)	*P* value
Delayed graft function		0 (0.0)	6 (28.6)	*0.148*
Plasma-creatinine at 4 years		122.0 (97.5-168.5)	114 (85.0-145.0)	*0.481*
eGFR at 4 years		48.7 (31.3-65.0)	52.6 (41.7-69.8)	0.549
Patient death		0 (0.0)	2 (9.5)	1.000
Graft failure (death-censored)		0 (0.0)	0 (0.0)	N/A
Biopsy-proven acute rejection	TCMR (including borderline)	2 (25.0)	8 (38.1)	0.675
	ABMR	1 (12.5)	3 (14.3)	1.000

P values present differences between transplant modalities. ABMR = antibody-mediated rejection, eGFR = estimated glomerular filtration rate, LD = living-donor, DD = deceased-donor, KT = kidney transplantation, TCMR = T cell-mediated rejection.

Leukocyte compositions by sampling time and transplant modality

We initially screened relative between-subject effects to evaluate temporal changes in leukocyte subset concentrations according to transplant modality (LD vs DD). All subsets, except granulocytes, decreased post-reperfusion relative to pre-implantation levels. A significant time-dependent effect on cell concentrations was observed for all populations in the ART-ANOVA (**Figure 18**).

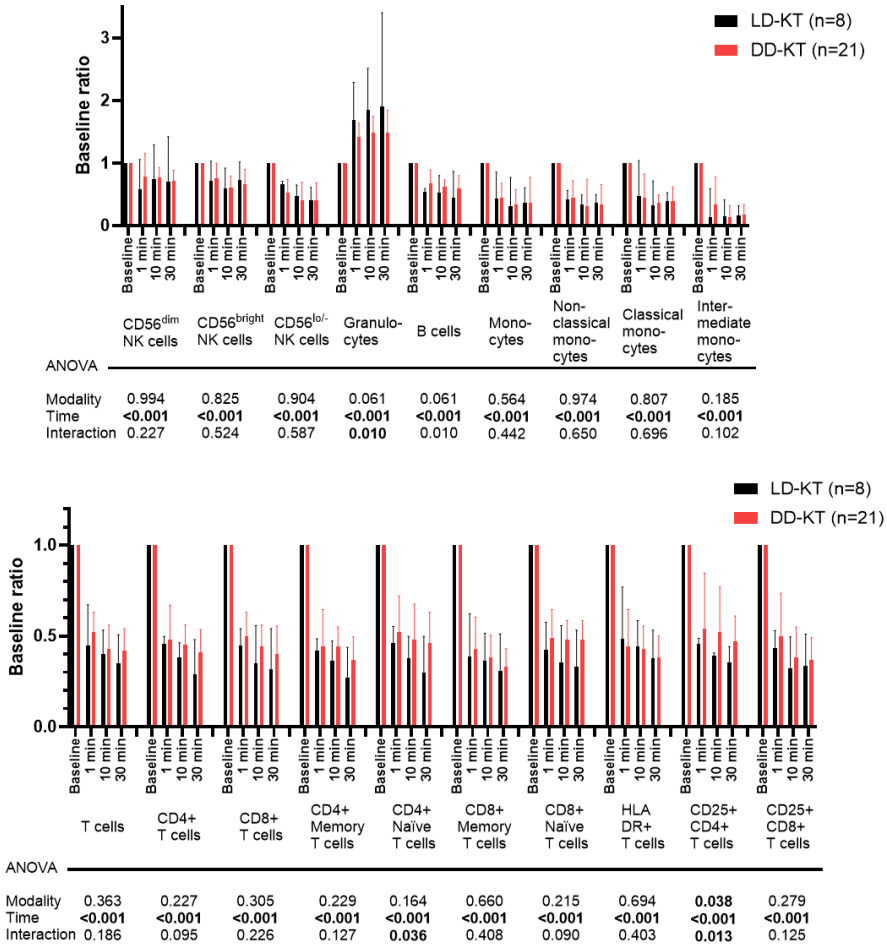

Figure 18. Leukocyte compositions by sampling time and transplant modality.
Bar charts depicting median (interquartile range) of baseline-adjusted levels of cells/mL by leukocyte subsets and sampling time points, sorted by LD (black) and DD (red) transplant modalities. P values from ART ANOVAs are presented below each cell subset. LD = living-donor, DD = deceased-donor, KT = kidney transplantation.

Leukocyte trajectories by induction therapy and the reperfusion exposure

The joint pattern of sampling time-dependent general decline in concentrations of the assessed leukocyte subsets in static levels was observed in all recipients, regardless of donor type, where the majority of cells did not show significant variation by the interacting effect of transplant modality on elapsed time.

To further delineate dominating exposures within this early transplant timeframe, we considered the common exposures of induction therapy with methylprednisolone as well as the reperfusion event, present in all patients.

As corticosteroids are known to cause intravascular redistribution of immune cells[163–165], we first performed a screening analysis on granulocytes and T cells by elapsed time from methylprednisolone administration to verify that this influence could be present. Here, significant trends on concentrations by time from methylprednisolone were observed for granulocytes which exhibited a general increase, while T cells generally decreased (**Supplementary Figure S1**).

To further determine the dominating exposure on cell trajectories, monophasic (baseline–30 min) and biphasic (baseline–1 min and 1–30 min) linear regression models were compared along a shared time axis. Monophasic models reflected corticosteroid-driven redistribution, whereas biphasic models incorporated a reperfusion-associated breakpoint. Model performance was evaluated using leave-one-out cross-validation and log-RMSE ratios to identify cell populations in which a reperfusion-driven trajectory provided superior fit.

In the full cohort (n = 29), non-classical monocytes ($CD14^{dim}CD16^{++}$), $CD56^{dim}$ NK cells, $CD8^{+}CD45RO^{+}$ memory T cells, and $CD8^{+}CD25^{+}$ T cells demonstrated accelerated depletion rates following reperfusion, consistent with a dominant reperfusion pattern (**Figure 19**).

To visualize the model-derived directional trends of biphasic reperfusion-splits in cell depletion for these cells together with the raw linear data, we superimposed the estimated median slopes per cell type in a composite graph including linear cell counts/mL data along an individually reperfusion-aligned time axis (**Figure 20**).

In exploratory stratified analyses, DD kidney-transplant recipients displayed a reperfusion-associated pattern in the depletion rates of non-classical monocytes, $CD8^{+}CD45RO^{+}$ memory T cells, and $CD8^{+}CD25^{+}$T cells. In contrast, LD kidney-transplant recipients showed no evidence of reperfusion-dominated shifts; instead, cellular redistribution patterns were more consistent with monophasic corticosteroid-driven effects across multiple lymphocyte subsets, including non-classical monocytes, $CD8^{+}$ T cells, $CD8^{+}$ memory T cells, $CD8^{+}CD25^{+}$T cells, and $CD56^{bright}$ NK cells. Detailed slope estimates and model performance metrics are provided in **Supplementary Tables S4-S6.**

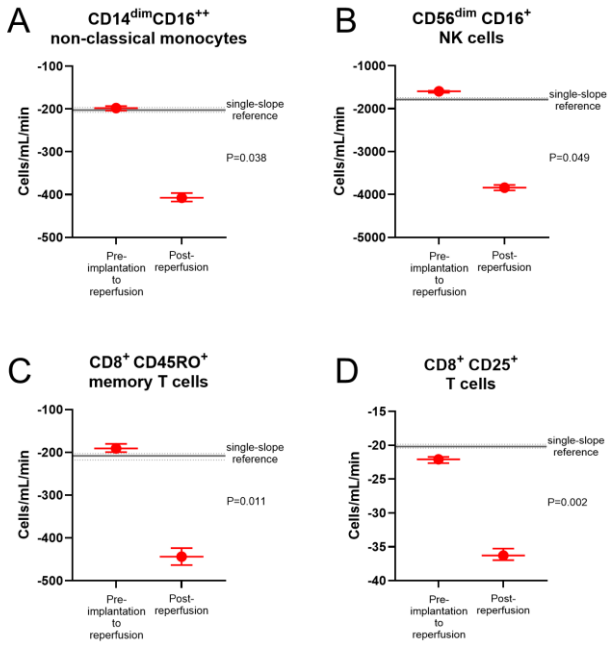

Figure 19. Estimated median slopes of cell subsets pre- and post-reperfusion. Dot and-whisker plots of cross validation-derived slopes (cells/mL/minute from the time-axis of minutes from methylprednisolone induction) for CD14dim CD16++ non-classical monocytes (A), CD56dim CD16+ NK cells (B), CD8+ memory T cells (C), and CD8+ CD25+ T cells (D). Dots with broad horizontal bars depict median and 95% bootstrapped CI:s are indicated by short horizontal bars. A grey single-slope reference (baseline to 30 minutes) is indicated by a dashed line (median) with dotted lines for its 95% bootstrapped CI. P values report Wilcoxon signed-rank tests on log(biphasic slope RMSE/monophasic slope RMSE), assessing consistent model superiority of the reperfusion-split biphasic (baseline to 1 minute and 1 minute to 30 minutes) over the monophasic (baseline to 30 minutes) single-slope fit.

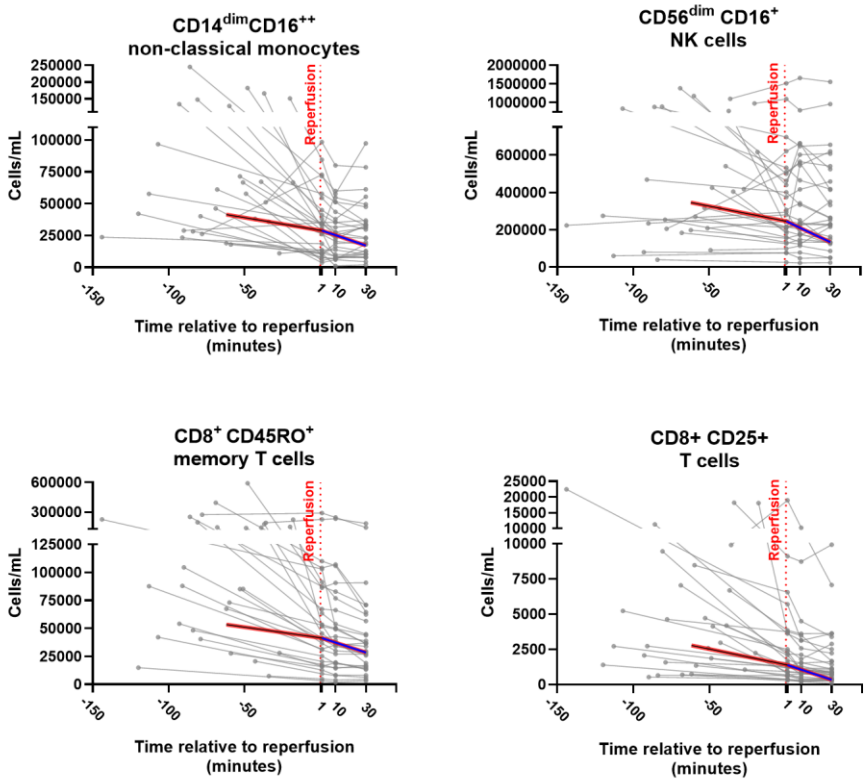

Figure 20. Cell subset dynamics by sampling time centered around reperfusion and superimposed estimated median slopes.

Connected scatter plots of cell counts/mL by time centered around the reperfusion event in all patients (n=29) for CD14dim CD16++ non-classical monocytes, CD56dim CD16+ NK cells, CD8+CD45RO+ T cells, and CD8+CD25+ T cells. Estimated median slopes from the leave-one-out cross-validation model – pre-reperfusion (baseline–1 min) and post-reperfusion (1–30 min) – are superimposed on the raw linear data and anchored at the cohort median 1 minute value. A black line with red outline depicts the estimated pre-reperfusion slope in cells/mL/min, while a blue line with red outline depicts the estimated post-reperfusion slope. A vertical dotted red line indicates the reperfusion event on the x-axis.

Supplementary material

Paper III

Supplementary Table S1. Spearman correlations of cell-free DNA and NETs markers

Spearman correlations			
		HNE-DNA	**Citrullinated histone H3**
Nuclear cfDNA	1 min	0.212 (*P* = 0.121)	-0.132 (*P* = 0.335)
	10 min	0.607 (*P* < *0.001*)	-0.140 (*P* = 0.314)
	30 min	0.475 (*P* < *0.001*)	-0.181 (*P* = 0.191)
Mitochondrial cfDNA	1 min	0.340 (*P* = 0.011)	0.095 (*P* = 0.491)
	10 min	0.241 (*P* = 0.080)	0.217 (*P* = 0.115)
	30 min	0.056 (*P* = 0.687)	0.285 (*P* = 0.037)
Spearman correlation coefficients of baseline-subtracted levels of HNE-DNA or citrullinated histone H3 and both nuclear and mitochondrial cfDNA levels at 1-, 10-, and 30-minutes post-reperfusion. Bold text indicates 2-tailed P < 0.05. cfDNA = cell-free DNA, HNE-DNA = human neutrophil elastase-DNA.			

Supplementary Table S2. Spearman correlations of NETs markers

Spearman correlations		
		HNE-DNA
Citrullinated histone H3	1 min	0.210 (*P* = 0.124)
	10 min	-0.028 (*P* = 0.842)
	30 min	0.051 (*P* = 0.712)
Spearman correlation coefficients of baseline-subtracted levels HNE-DNA and citrullinated histone H3 at 1-, 10-, and 30-minutes post-reperfusion. HNE-DNA = human neutrophil elastase-DNA.		

Supplementary Table S3. Spearman correlations of cell-free DNA and sC5b-9

Spearman correlations			
		Nuclear cfDNA	**Mitochondrial cfDNA**
sC5b-9	1 min	0.460 (P < 0.001)	0.243 (P = 0.066)
	10 min	0.373 (P = 0.004)	0.286 (P = 0.031)
	30 min	0.160 (P = 0.24)	-0.011 (P = 0.937)
Spearman correlation coefficients of baseline-subtracted levels of nuclear or mitochondrial cfDNA levels and sC5b-9 at 1-, 10-, and 30-minutes post-reperfusion. Bold text indicates 2-tailed P < 0.05. cfDNA = cell-free DNA, sC5b-9 = soluble sC5b-9.			

Paper IV

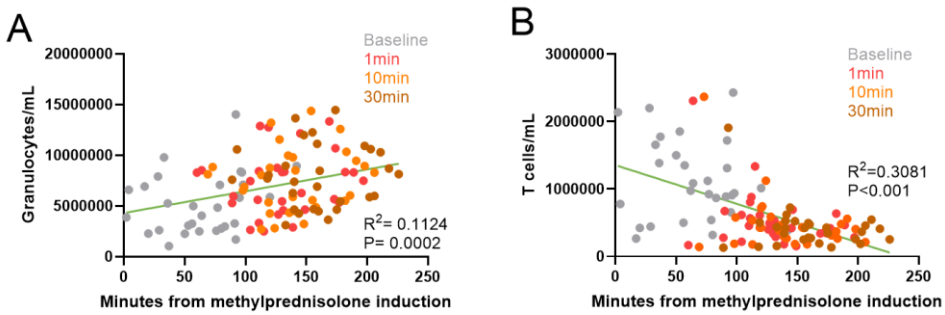

Supplementary Figure S1. Concentrations of granulocytes (A) and T cells (B) at different sampling times by elapsed time from methylprednisolone induction. Sampling time points are color coded by grey (baseline), red (1 minute), orange (10 minutes), and brown (30 minutes). A green line indicates the linear regression slope.

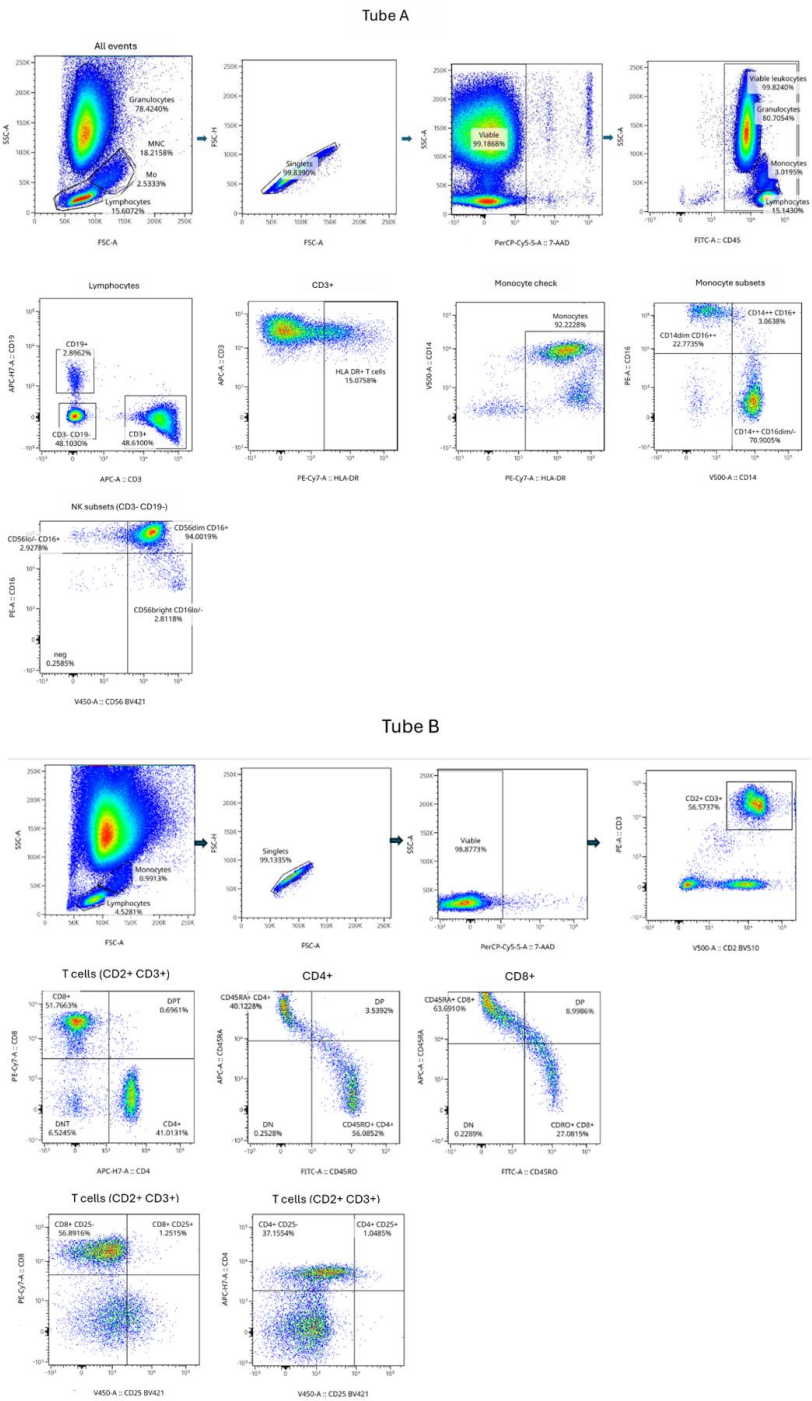

Supplementary Figure S2. Gating strategy for Tube A and Tube B.

Supplementary Table S4. Leukocyte change rates by biphasic or monophasic linear regression modeling in the entire study population (n=29).

Comparison of reperfusion versus induction treatment exposures on cell trajectories in the entire cohort (n=29)					
Cell type	**Change rate (cells/mL/min) Median (95% bootstrapped CI)**			**Log-RMSE ratio Model fit superiority biphasic: <0 monophasic: >0**	**P value**
	Biphasic (redistribution upon reperfusion)		Monophasic (corticosteroid induction pattern alone)		
	Baseline-1min	1min-30min	Baseline-30min		
Non-classical monocytes ($CD14^{dim}$ $CD16^{++}$)	−197.777 (−203.802 to −193.329)	−407.443 (−416.321 to −396.590)	−202.441 (−207.799 to −196.557)	−0.03871 (−0.12400 to 0.00042)	0.0379
$CD56^{dim}$ NK cells ($CD56^{dim}$ $CD16^{+}$)	−1594.702 (−1629.866 to −1580.622)	−3840.689 (−3904.797 to −3777.802)	−1783.414 (−1804.159 to −1740.721)	−0.03812 (−0.10436 to −0.00532)	0.0491
$CD8^{+}$ ($CD45RO^{+}$) Memory T cells	−190.704 (−199.412 to −180.288)	−443.891 (−463.480 to −423.890)	−208.279 (−217.931 to −202.941)	−0.02056 (−0.05637 to −0.00272)	0.0114
$CD8^{+}CD25^{+}$	−22.068 (−22.636 to −21.721)	−36.274 (−36.970 to −35.259)	−20.180 (−20.397 to −19.849)	−0.05034 (−0.13623 to −0.00482)	0.00185
Granulocytes	5714.636 (5131.202 to 5914.058)	983.744 (−145.468 to 1509.412)	2936.270 (2472.517 to 3094.106)	0.00654 (0.00181 to 0.01390)	0.0010
B cells	−171.476 (−180.231 to −166.309)	−268.740 (−279.230 to −263.671)	−152.149 (−158.346 to −148.281)	−0.01145 (−0.04471 to 0.00331)	0.2259
Monocytes (all)	−1266.585 (−1317.588 to −1256.925)	−2582.773 (−2692.367 to −2568.414)	−1292.184 (−1341.505 to −1283.764)	0.00105 (−0.03164 to 0.02191)	0.9655
Classical monocytes ($CD14^{++}$ $CD16^{dim/-}$)	−874.340 (−909.219 to −851.231)	−1881.046 (−1959.956 to −1867.276)	−920.742 (−942.161 to −899.555)	0.00307 (−0.03063 to 0.02107)	0.9483
Intermediate monocytes ($CD14^{++}$ $CD16^{+}$)	−48.605 (−55.707 to −43.485)	−118.150 (−124.165 to −113.086)	−54.742 (−60.495 to −52.543)	0.00094 (−0.05056 to 0.01066)	0.4755
HLA-DR^{+} T cells	163.614 (128.722 to 191.856)	435.143 (320.284 to 444.214)	200.135 (155.647 to 227.632)	0.00175 (−0.00232 to 0.00983)	0.3199

T cells (all)	−1476.777 (−1498.153 to −1430.135)	−2523.078 (−2593.497 to −2406.701)	−1360.199 (−1391.078 to −1317.577)	−0.01193 (−0.03878 to −0.00230)	0.0799
$CD4^+$ T cells	−1155.319 (−1167.008 to −1119.865)	−1982.854 (−2011.626 to −1921.708)	−1069.213 (−1089.870 to −1042.783)	−0.02448 (−0.09375 to 0.01978)	0.1872
$CD4^+$ ($CD45RO^+$) Memory T cells	−834.395 (−852.003 to −820.623)	−1567.127 (−1603.857 to −1545.561)	−809.378 (−828.839 to −802.470)	−0.02225 (−0.09233 to 0.00988)	0.1599
$CD4^+$ ($CD45RA^+$) naïve T cells	−428.770 (−453.293 to −404.679)	−789.086 (−818.056 to −727.499)	−415.207 (−433.091 to −385.216)	−0.00918 (−0.01885 to 0.01554)	0.8457
$CD4^+$ $CD25^+$ T cells	−89.468 (−91.882 to −88.398)	−102.296 (−104.630 to −97.582)	−68.982 (−70.988 to −66.879)	−0.01563 (−0.04957 to 0.00730)	0.0629
CD8+ T cells	−183.836 (−210.336 to −154.774)	−585.686 (−608.053 to −507.579)	−238.347 (−260.746 to −217.412)	−0.00154 (−0.00954 to 0.00422)	0.8120
$CD8^+$ ($CD45RA^+$) naïve T cells	−51.184 (−62.200 to −32.570)	−284.574 (−301.066 to −255.657)	−98.438 (−109.881 to −83.510)	0.00165 (−0.00899 to 0.00680)	0.6971
$CD56^{bright}$ NK cells ($CD56^{bright}$ $CD16^{lo/-}$)	−81.718 (−84.738 to −80.718)	−138.330 (−141.973 to −137.888)	−75.562 (−77.538 to −74.610)	−0.01788 (−0.08958 to 0.00310)	0.5306
$CD56^{lo/-}$ NK cells ($CD56^{lo/-}$ $CD16^+$)	−62.783 (−66.150 to −60.770)	−83.911 (−89.326 to −79.101)	−51.642 (−55.114 to −50.115)	−0.00005 (−0.04643 to 0.00964)	0.6038

Values are expressed as estimated median slopes of cells/mL/min and 95% bootstrapped confidence intervals. P values denote log-RMSE ratios significantly distinct from 0. A negative log RMSE-ratio value indicates superior fit of the biphasic (reperfusion) model and a positive value indicates superior fit of the monophasic (induction therapy) model. Bold text indicates cell types with significant P values. RMSE = root mean square error.

Supplementary Table S5. Immune cell change rates by biphasic or monophasic linear regression modelling in the DD-KT subgroup (n=21)

Comparison of the reperfusion exposure versus methylprednisolone exposure on cell trajectories in the DD-KT subgroup (n=21)					
Cell type	**Change rate (cells/mL/min) Median (95% bootstrapped CI)**			**Log-RMSE ratio Model fit superiority biphasic: <0 monophasic: >0**	**P value**
	Biphasic (redistribution upon reperfusion)		Monophasic (corticosteroid induction pattern alone)		
	Baseline-1min	1min-30min	Baseline-30min		
Non-classical monocytes ($CD14^{dim}$ $CD16^{++}$)	-238.09 (-248.42 to -226.17	-472.99 (-503.08 to -447.96)	-251.56 (-270.21 to -238.94)	-0.046 (-0.152 to -0.013)	0.044
$CD8^+$ ($CD45RO^+$) Memory T cells	-161.52 (-168.67 to -136.77)	-363.87 (-380.73 to -348.43)	-183.67 (-190.16 to -170.10	-0.033 (-0.065 to -0.014)	0.022
$CD8^+CD25^+$	-32.44 (-33.36 to -31.97)	-33.35 (-33.92 to -31.92)	-25.06 (-25.55 to -24.25)	-0.086 (-0.141 to -0.060)	0.002
Granulocytes	4995.54 (4014.12 to 5400.72)	-3180.74 (-5728.71 to -2446.17)	1276.89 (161.02 to 1611.22)	0.006(-0.002 to 0.009)	0.175
B cells	-173.03(-182.99 to -167.71)	-318.61 (-338.65 to -312.92)	-174.66 (-185.74 to -172.63)	-0.026 (-0.096 to 0.000)	0.211
Monocytes (all)	-1740.46 (-1854.88 to -1684.07)	-3008.95 (-3123.93 to -2832.12)	-1705.38 (-1792.41 to -1592.68)	-0.010 (-0.082 to 0.030)	0.808
Classical monocytes ($CD14^{++}$ $CD16^{dim/-}$)	-1260.50 (-1323.79 to -1214.79)	-2201.86 (-2294.84 to -2159.08)	-1242.39 (-1306.15 to -1187.34)	-0.020 (-0.087 to 0.026)	0.728
Intermediate monocytes ($CD14^{++}$ $CD16^+$)	-95.11 (-105.65 to -94.17)	-126.40 (-137.68 to -112.88)	-82.88 (-91.40 to -76.52)	-0.011 (-0.070 to -0.001)	0.175
HLA-DR^+ T cells	104.94 (19.53 to 142.99)	314.66 (166.81 to 356.40)	145.37 (44.28 to 176.07)	0.003 (-0.003 to 0.013)	0.198
T cells (all)	-1472.22 (-1543.78 to -1449.44)	-1891.95 (-2050.29 to -1727.65)	-1245.29 (-1292.52 to -1188.84)	-0.004 (-0.024 to 0.010)	0.781
$CD4^+$ T cells	-1152.73 (-1250.62 to -1142.12)	-1414.99 (-1562.22 to -1374.84)	-954.41 (-1037.79 to -927.26)	-0.017 (-0.055 to 0.011)	0.281
$CD4^+$ ($CD45RO^+$) Memory T cells	-1055.45 (-1095.39 to -1045.25)	-1570.03 (-1684.63 to -1558.87)	-962.32 (-984.81 to -954.28)	-0.031 (-0.145 to 0.018)	0.198
$CD4^+$ ($CD45RA^+$) naïve T cells	-214.35 (-267.27 to -206.44)	-224.40 (-319.30 to -198.79)	-164.11 (-217.48 to -148.99)	0.009 (-0.013 to 0.018)	0.266
$CD4^+$ $CD25^+$ T cells	-82.51 (-85.70 to -81.55)	-47.49 (-61.17 to -45.70)	-51.67 (-56.29 to -50.93)	0.005 (-0.013 to 0.017)	0.237

CD8+ T cells	-253.44 (-321.65 to -232.98)	-557.45 (-647.68 to -459.80)	-283.20 (-339.45 to -248.22)	-0.003 (-0.010 to 0.005)	0.972
$CD8^+$ ($CD45RA^+$) naïve T cells	-147.54 (-263.46 to -136.85)	-348.85 (-469.87 to -286.28)	-173.95 (-277.29 to -143.49)	-0.001 (-0.009 to 0.007)	1.000
$CD56^{dim}$ NK cells ($CD56^{dim}$ $CD16^+$)	-1726.94 (-1803.82 to -1696.66)	-4074.46 (-4225.38 to -4034.18)	-2035.50 (-2083.42 to -1999.08)	-0.036 (-0.127 to -0.012)	0.224
$CD56^{bright}$ NK cells ($CD56^{bright}$ $CD16^{lo/-}$)	-88.26 (-94.23 to -87.08)	-140.12 (-143.26 to -137.08)	-82.46 (-87.35 to -82.06)	-0.005 (-0.094 to 0.026)	0.972
$CD56^{lo/-}$ NK cells ($CD56^{lo/-}$ $CD16^+$)	-65.51 (-75.77 to -63.71)	-90.39 (-102.28 to -86.03)	-58.64 (-65.17 to -54.03)	-0.014 (-0.070 to 0.018)	0.404

Values are expressed as estimated median slopes of cells/mL/min and 95% bootstrapped confidence intervals. P values denote log-RMSE ratios significantly distinct from 0. A negative log-RMSE ratio value indicates superior fit of the biphasic (reperfusion) model and a positive value indicates superior fit of the monophasic (induction therapy) model. Bold text indicates cell types with significant P values. RMSE = root mean square error, DD-KT = deceased-donor kidney transplantation.

Supplementary Table S6. Immune cell change rates by biphasic or monophasic linear regression modelling in the LD-KT subgroup (n=8)

Comparison of the reperfusion exposure versus methylprednisolone exposure on cell trajectories in the LD-KT subgroup (n=8)					
Cell type	Change rate (cells/mL/min) Median (95% bootstrapped CI)			Log-RMSE ratio Model fit superiority biphasic: <0 monophasic: >0	P value
	Biphasic (redistribution upon reperfusion)		Monophasic (corticosteroid induction pattern alone)		
	Baseline-1min	1min-30min	Baseline-30min		
Non-classical monocytes ($CD14^{dim}$ $CD16^{++}$)	-84.57 (-121.47 to -42.30)	282.86 (-38.35 to 407.76)	-20.70 (-62.01 to 14.48)	0.070 (-0.006 to 0.118)	0.042
CD8+ T cells	384.21 (-196.48 to 562.41)	417.88 (-549.85 to 990.85)	194.76 (-40.59 to 347.20)	0.016 (0.002 to 0.056)	0.030
$CD8^+$ ($CD45RO^+$) Memory T cells	-82.26 (-145.19 to 76.89)	-14.26 (-758.36 to 333.51)	-45.35 (-160.87 to 64.31)	0.029 (0.023 to 0.052)	0.021
$CD8^+CD25^+$	53.02 (36.50 to 57.51)	68.64 (6.87 to 94.37)	32.48 (20.69 to 34.36)	0.029 (0.000 to 0.079)	0.042
$CD56^{bright}$ NK cells ($CD56^{bright}$ $CD16^{lo/-}$)	-28.78 (-43.76 to -19.95)	30.98 (-13.88 to 96.78)	-12.45 (-22.81 to -2.23)	0.076 (0.020 to 0.113)	0.014
Granulocytes	768.69 (-6615.43 to 2116.59)	10963.21 (-11027.54 to 23143.73)	1421.50 (-2517.43 to 2376.52)	0.033 (0.003 to 0.071)	0.059
B cells	-209.05 (-295.55 to -129.58)	483.07 (-141.59 to 602.91)	-68.55 (-154.71 to -26.78)	0.057 (-0.010 to 0.231)	0.080
Monocytes (all)	1095.24 (855.78 to 1274.80)	4918.96 (4807.04 to 5210.80)	976.79 (872.55 to 1026.98)	-0.076 (-0.197 to 0.012)	0.441
Classical monocytes ($CD14^{++}$ $CD16^{dim/-}$)	1251.15 (978.16 to 1436.51)	4884.60 (4665.71 to 5487.92)	1048.35 (820.87 to 1147.20)	-0.017 (-0.126 to 0.016)	0.529
Intermediate monocytes ($CD14^{++}$ $CD16^{+}$)	317.39 (199.82 to 336.26)	920.01 (644.33 to 972.43)	234.34 (153.22 to 243.79)	0.005 (-0.138 to 0.205)	0.624
$HLA\text{-}DR^+$ T cells	-39.20 (-277.08 to 118.51)	-291.71 (-1732.44 to 280.94)	-67.27 (-321.82 to 54.66)	0.020 (-0.042 to 0.063)	0.234
T cells (all)	313.63 (-906.22 to 696.78)	-2687.37 (-5040.32 to -1457.91)	-100.10 (-864.37 to 168.40)	0.008 (-0.058 to 0.122)	0.441
$CD4^+$ T cells	124.27 (-427.67 to 228.77)	-5175.44 (-5785.01 to -4438.31)	-362.81 (-607.45 to -267.65)	-0.012 (-0.133 to 0.018)	0.294

$CD4^+$ ($CD45RO^+$) Memory T cells	227.02 (-139.42 to 332.91)	-1796.44 (-2746.72 to -954.27)	-57.79 (-121.70 to 32.02)	0.025 (0.001 to 0.243)	0.107
$CD4^+$ ($CD45RA^+$) naïve T cells	-101.11 (-352.52 to -45.18)	-2963.96 (-3762.62 to -2532.88)	-294.23 (-467.08 to -235.15)	-0.039 (-0.084 to 0.054)	0.624
$CD4^+$ $CD25^+$ T cells	33.53 (15.50 to 51.16)	78.37 (-61.40 to 132.35)	19.12 (12.86 to 36.75)	0.022 (-0.064 to 0.041)	0.363
$CD8^+$ ($CD45RA^+$) naïve T cells	451.05 (135.23 to 473.93)	643.24 (157.71 to 764.91)	261.86 (225.47 to 293.54)	0.005 (-0.008 to 0.188)	0.234
$CD56^{dim}$ NK cells ($CD56^{dim}$ $CD16^+$)	-207.13 (-657.41 to 388.02)	5018.76 (1942.40 to 6981.11)	243.29 (-78.99 to 761.12)	0.014 (-0.014 to 0.186)	0.294
$CD56^{lo/-}$ NK cells ($CD56^{lo/-}$ $CD16^+$)	-20.36 (-44.07 to 10.18)	340.89 (251.51 to 443.77)	16.78 (3.32 to 37.72)	0.040 (-0.062 to 0.159)	0.363

Values are expressed as estimated median slopes of cells/mL/min and 95% bootstrapped confidence intervals. P values denote log-RMSE ratios significantly distinct from 0. A negative log-RMSE ratio value indicates superior fit of the biphasic (reperfusion) model and a positive value indicates superior fit of the monophasic (induction therapy) model. Bold text indicates cell types with significant P values. RMSE = root mean square error, LD-KT = living-donor kidney transplantation.

Discussion

Ischemia-reperfusion injury in clinical kidney transplantation remains a primary and unavoidable contributor to impaired allograft function[25,139,166]. The concept is well established and the molecular architecture of ischemia-reperfusion injury is well described in experimental systems, yet investigations on its immediate biological manifestation in human allografts under routine clinical conditions remain limited.

Despite substantial advance in alloimmune control, donor evaluation and preservation strategies throughout the years, the persistent impact of ischemia-reperfusion injury is underscored by enduring disparities between living-donor and deceased-donor kidney transplants and by observations that rates of delayed graft function have remained largely unchanged throughout the years[149].

This thesis addresses this gap by presenting a multi-platform characterization of the earliest reperfusion phase of clinical kidney transplantation. By integrating complementary analyses of intravascular innate immune activation, inflammatory and injury-related proteomic signatures, cell-free DNA kinetics, and leukocyte redistribution patterns, the work provides a comprehensive view of early events that occur during ischemia-reperfusion injury. Through direct sampling of local allograft venous effluent during the first 30 minutes after reperfusion, these studies relate prompt biological signals within the allograft microenvironment to donor modality, ischemic burden and subsequent allograft function.

A consistent finding across analyses was that deceased-donor kidneys exhibited prompt expression of structural injury markers within one minute of reperfusion. In **Paper III**, nuclear cell-free DNA, a DAMP associated with cell death[167], rose immediately and remained elevated throughout the first 30 minutes. Proteomic profiling in **Paper II** provided complementary evidence of early ischemia-reperfusion injury in deceased-donor kidneys, revealing a prompt post-reperfusion surge of HGF. Although HGF is generally regarded as a protective and reparative mediator[168–170], its prompt appearance in the immediate reperfusion phase is more consistent with ischemia-induced disruption of cell surface structures. HGF is known to bind with high affinity to heparan sulfate within the endothelial glycocalyx[127,128,171], and ischemia-induced glycocalyx degradation could result in immediate intravascular release of surface-bound HGF. Similar early patterns of HGF release have been reported in myocardial infarction and experimental renal ischemia-reperfusion injury, supporting this interpretation[172–175]. In this context, the

early HGF signal is therefore best interpreted as a displacement marker, reflecting physical release from disrupted endothelial surface structures rather than active induction.

In parallel, IL-33, a potent nuclear alarmin released upon endothelial and epithelial injury or necrosis and capable of activating both myeloid and lymphoid immune cells[176,177], showed a progressive increase over the first 30 minutes of reperfusion. This temporal pattern aligns with preclinical findings in renal ischemia-reperfusion injury demonstrating early microvascular IL-33 expression in peritubular and periglomerular compartments, where it contributes to downstream innate immune activation[178].

Together, the sequential emergence of nuclear cell-free DNA as a marker of cell death, prompt HGF release potentially reflecting glycocalyx degradation, and subsequent IL-33 expression supports the model in which structural injury precedes the activation of inflammatory signaling pathways during early reperfusion. These patterns were absent in living-donor kidneys despite the same surgical routines and perioperative care, reinforcing a biological rather than procedural origin for these patterns. Importantly, the cumulative release of nuclear cell-free DNA, HGF, and IL-33 showed associations with delayed graft function, linking structural and alarmin signaling to clinically relevant injury burden.

Although NETs have been implicated as a source of circulating cell-free DNA in ischemia-reperfusion injury[179], their temporal dynamics and anatomical distribution are critical for interpretation. Experimental studies consistently demonstrate that NET formation peaks several hours after reperfusion and occurs predominantly within tissue compartments, rather than in the intravascular space as neutrophils extravasate into injured tissue[180–182]. In **Paper III**, intravascular NET-associated markers neither differed by donor type nor correlated with each other, in clear contrast to rapid and sustained kinetics observed for nuclear cell-free DNA. Rather than undermining interpretability, these findings support the conclusion that nuclear cell-free DNA detected in allograft venous effluent likely reflects immediate parenchymal injury at reperfusion, whereas NET-driven nuclear cell-free DNA release likely emerges later or within tissue compartments not captured by early intravascular sampling.

In **Paper I**, activation of intravascular innate immune system occurred within the 30-minute window of reperfusion in deceased-donor kidneys. Most prominently, formation of the soluble terminal complement complex sC5b-9 coincided with concurrent activation of components in the coagulation and kallikrein-kinin systems, indicative of coordinated rather than isolated pathway activation. Importantly, sC5b-9 levels closely correlated with activation markers across all three cascade systems, prompting its interpretation in this work as an integrated response marker of thromboinflammation rather than a readout of complement activation alone.

These findings extend earlier kidney transplantation studies that have largely emphasized complement activation as a dominant effector pathway by demonstrating that ischemia-reperfusion injury instead triggers coordinated activation of all intravascular innate immune cascade systems resulting in a complex thrombo-inflammatory response[183,184].

The clinical impact of this inflammatory response was evident in recipients with elevated sC5b-9 levels at 30 minutes, who exhibited a progressive decline in long-term allograft function in **Papers I** and **III**. Notably, deceased-donor kidneys preserved with hypothermic machine perfusion showed attenuated thrombo-inflammatory response and preserved mid- to long-term allograft function, despite comparable KDRI score and cold ischemic times relative to static cold-stored deceased-donor kidneys.

Furthermore, **Paper III** indicated that elevated sC5b-9 levels post-reperfusion occurred more frequently in patients with higher cumulative release of nuclear cell-free DNA, indicating a close temporal relationship between structural cell injury and innate immune activation. Supporting this biological plausibility, *in vitro* experiments in **Paper III** demonstrated that C5b-9 selectively deposits on necrotic, but not viable, human tubular epithelial cells consistent with the concept that structural renal cell injury promotes activation of the intravascular innate immune system.

While hypothermic machine perfusion of deceased-donor kidneys influenced the magnitude of intravascular innate immune system activation after reperfusion, it did not alter the release of early markers of intragraft injury. Here, nuclear cell-free DNA release during the 30 minutes of reperfusion was comparable between hypothermic machine-perfused and static cold-stored kidneys. Likewise, neither HGF nor IL-33 levels differed between preservation modalities in **Paper II**. These findings indicate that hypothermic machine perfusion might not prevent ischemia-induced cellular injury that becomes apparent at reperfusion, but rather modulates how this injury is translated into downstream inflammatory responses. Thus, although structural cell injury appears to be a prerequisite for post-reperfusion innate immune activation, the magnitude of this response remains amenable to modulation by preservation strategy. At the same time, the observed association between early HGF release and reduced long-term allograft function, paralleling that observed for sC5b-9, suggests that the extent of structural cell injury may remain relevant for long-term graft outcomes, even when early inflammatory amplification is partially mitigated.

Collectively, these findings support a conceptual model in which ischemia establishes the injury substrate, whereas reperfusion modulates the extent of downstream inflammatory response. These processes appear to be mechanistically linked, yet differentially susceptible to modulation.

This interpretation is further supported by the close alignment between ischemic burden and early expression of multiple injury-associated biomarkers. Across **Papers I-III**, cold ischemic time modulated the release of the most prominently upregulated injury markers in a threshold-like manner. Inflection points for increased and immediate 1-minute expression of nuclear cell-free DNA, HGF, and sC5b-9 all converged within a narrow timeline of 475 to 522 minutes. This convergence across studies and different patient populations suggests that once ischemic duration exceeds a critical tipping point in this clinical setting, the downstream inflammatory response to reperfusion becomes disproportionately amplified.

Beyond early soluble ischemia-reperfusion injury signals, leukocyte engagement occurred within the same temporal window. In **Paper IV**, time-aligned modelling, that accounted for expected corticosteroid-induced systemic redistribution, demonstrated that reperfusion coincided with an accelerated decline in circulating non-classical monocytes, $CD56^{dim}$ NK cells (constituting the majority of NK cells), and $CD8^{+}$ T-cell subsets, consistent with prompt engagement within the kidney allograft.

These cell types have previously been implicated in experimental ischemia-reperfusion injury models showing early recruitment of NK cells and $CD8^{+}$ T cells into post-ischemic kidney tissue, and early margination of non-classical monocytes within damaged microvasculature[185–189].

The selective decline of these circulating subsets is further supported by observations from other conditions closely resembling ischemia-reperfusion injury. In myocardial infarction and stroke, prompt declines in circulating non-classical monocytes, vascular patrollers that may rapidly adhere to injured endothelium[190,191], have been shown to correlate with infarct size and adverse outcomes[189,192]. Similarly, clinical studies on myocardial reperfusion report prompt reductions in circulating NK cells and $CD8^{+}$ T cells, accompanied by trans-coronary arterial-venous gradients indicative of tissue margination, with the magnitude of systemic depletion relating to microvascular obstruction[193].

Mechanistically, non-classical monocytes and $CD56^{dim}$ NK cells are described as key early innate responders to sterile damage, rapidly engaging injured endothelium and mediating cytotoxic and pro-inflammatory effector functions, while NK cells also modulate subsequent adaptive immune responses[194]. In parallel, T cells are recognized as contributors to sterile injury settings such as ischemia-reperfusion injury, with early involvement proposed to occur independently of classical antigen-specific activation pathways[195].

Further supporting the relevance of these cell subsets in clinical kidney transplantation, post-operative systemic measurements of CD8+ T cells, NK cells, and monocytes within days following kidney transplantation have shown

associations between variations in quantities of these cell types and delayed graft function[196,197].

Taken together, these findings suggest that ischemia-reperfusion injury in clinical kidney transplantation involves prompt margination of tissue engagement of cell subsets within the first 30 minutes after reperfusion. This cellular response occurs in parallel with soluble injury signals and coordinated activation of intravascular innate immune cascade systems, underscoring the complexity of ischemia-reperfusion injury.

Across all studies, a consistent donor type-dependent divergence in biological responses emerged at the time of kidney allograft reperfusion. Deceased-donor kidneys consistently exhibited upregulation of injury-associated markers, pro-inflammatory proteins and activation of intravascular innate immune cascades, together with evidence of early immune cell engagement. In contrast, living-donor kidneys showed minimal or absent expression of these injury or inflammatory signals during the same reperfusion window.

Notably, in **Paper II**, living-donor kidneys instead exhibited a distinct proteomic signature enriched for regulatory or reparative mediators, including TRANCE, IL-6 family signaling (IL-6 and LIF) and FGF-23.

These findings are consistent with observations from other ischemia-reperfusion injury contexts in which early activation of specific mediators has been linked to tissue protection and repair. In murine stroke, higher TRANCE levels have been associated with reduced cerebral infarct size[198], while IL-6 signaling has been shown to exert protective effects in experimental renal ischemia-reperfusion injury models[199]. In addition, exogenous FGF-23 administration in murine renal ischemia-reperfusion injury enhances tubular regeneration while limiting cell necrosis and microvascular injury[200].

Against this background, the distinct early responses observed between living- and deceased-donor kidney transplantation highlight a fundamental aspect of ischemia-reperfusion injury: it represents a biologically ambivalent process with the potential to drive both tissue repair and tissue damage. In the living-donor setting, where ischemic burden is limited, reperfusion appears to preferentially engage regulatory and reparative pathways, consistent with it functioning as a necessary trigger for healing. In contrast, in deceased-donor transplantation, the greater ischemic burden appears to overwhelm these adaptive mechanisms, tipping the response toward exaggerated innate immune activation and destructive thrombo-inflammatory processes that impair allograft function.

Conclusion

Collectively, this work demonstrates that the ischemia–reperfusion injury in clinical kidney transplantation is initiated promptly and is biologically tractable within the first 30 minutes after reperfusion. This brief but critical interval captures the earliest convergence of parenchymal injury, complex inflammatory signaling, and immune-cell redistribution, all of which can be directly detected in the renal venous effluent of the transplanted kidney. These findings establish the first 30 minutes of reperfusion as a critical biological window during which early determinants of graft injury are both measurable and mechanistically interpretable, highlighting a time frame of particular relevance for diagnostic stratification and the development of effective therapeutic interventions.

Key conclusions:

- Ischemia–reperfusion injury can trigger a prompt, multifaceted, and interlinked activation of the intravascular innate immune systems, encompassing complement, coagulation, and contact system pathways. Soluble C5b-9 reflects an integrated thrombo-inflammatory response rather than isolated complement activation.

- Donor modality shapes the earliest reperfusion response during kidney transplantations. Within minutes after reperfusion, living-donor kidneys exhibit regulatory and reparative protein signatures, whereas deceased-donor kidneys distinctly display injury and inflammation-dominated profiles, reflecting fundamentally different biological trajectories.

- Reperfusion is accompanied by prompt, subset-specific redistribution of circulating immune cells, consistent with early margination and tissue interaction. This response is likely pronounced in deceased-donor grafts, indicating possible donor-dependent differences in early immune cell engagement.

Methodological considerations

The present work is based on renal venous sampling and captures biological processes during ischemia-reperfusion injury that are accessible within the intravascular compartment at the moment of reperfusion. Consequently, tissue-resident processes may not be fully represented by these measurements, and the findings should be interpreted as reflecting events occurring at the vascular–tissue interface rather than within the parenchyma alone.

The studies were conducted at a single center with a comparatively large and well-characterized cohort of kidney transplant recipients, but with relatively short cold ischemic times and a limited proportion of donation-after-circulatory-death allografts. These factors may limit generalizability to transplant settings characterized by larger ischemic exposure or higher prevalence of donation-after-circulatory-death donors. In addition, the absence of paired arterial, systemic, or histological sampling restricts spatial resolution and precludes direct localization of inflammatory and cellular events within specific tissue compartments.

Despite these limitations, several features support the robustness and interpretability of the findings. All analyses were based on blood sampled directly from the renal venous effluent of the transplanted kidney rather than from the systemic circulation. This approach increases biological resolution by capturing signals originating from the allograft itself and minimizes dilution and confounding effects inherent to systemic sampling. Independent multimodal analyses consistently demonstrated early and convergent changes in injury markers, inflammatory mediators, innate immune cascade activation products, and immune cell dynamics within the same narrow post-reperfusion window. These responses reproducibly differed by donor modality and showed that multiple independent biomarkers of injury and inflammation increased in a threshold-like manner at comparable cold ischemia durations across studies, supporting a biologically coherent response rather than random or nonspecific variation.

Future perspectives

A central finding in this work is that prolonged cold ischemic time, particularly beyond approximately 8 hours, is associated with detectable ischemia-reperfusion injury. This observation suggests that duration of ischemia may function not merely as a linear quantitative stressor but as a threshold determinant that increases the susceptibility of cells to coordinated inflammatory and injury-related pathways upon reperfusion.

Accordingly, the most direct and effective strategy to mitigate ischemia-reperfusion injury remains prevention through minimization of ischemic exposure. Continued efforts to reduce cold ischemic time, through optimized logistics, effective allocation strategies, decentralized transplant activity, and coordinated collaboration between transplant centers to leverage shared regional resources remain fundamental.

In clinical scenarios where prolonged ischemia cannot be avoided, the present findings suggest that therapeutic strategies focused on single effector pathways may not be sufficient to effectively attenuate ischemia-reperfusion injury. Once initiated, ischemia-reperfusion injury rapidly evolves into a complex, multimodal, and tightly interlinked process involving multiple effector pathways. This highlights the inherent challenges of therapeutic drug development in this setting. Consequently, alternative strategies aimed at preventing or attenuating the initial triggering of ischemia–reperfusion injury, such as limiting direct interactions between circulating blood components and ischemia-injured cellular surfaces, may represent a more effective approach, as exemplified by the ongoing first-in-human trial (ATMIRe NCT05246618) evaluating a polymer-based *ex vivo* allograft surface-shielding strategy in kidney transplantation.

Finally, a key enabling aspect of this work is the use of direct serial renal venous effluent sampling during transplantation, a procedure that was safely integrated into routine surgical workflows without added risk to the patients. This novel approach provides high-resolution access to the earliest reperfusion phase, capturing biological events at the interface between the post-ischemic allograft and the incoming recipient circulation, and enables direct investigation of the initial molecular and cellular processes underlying ischemia-reperfusion injury in humans.

Populärvetenskaplig sammanfattning

Njurtransplantation är idag den föredragna behandlingen för patienter med terminal njursvikt och medför förbättrad överlevnad, livskvalitet och lägre samhällskostnader jämfört med dialys. Trots stora framsteg inom kirurgi, organbevaring och immunförsvarsdämpande behandling kvarstår dock betydande utmaningar som begränsar transplantatets livslängd. En viktig orsak är den tidiga vävnadsskadan som uppstår i samband med själva transplantationen.

Alla njurar som transplanteras utsätts för en period utan syretillförsel (ischemi) under organuttag och förvaring. När njuren sedan kopplas in hos mottagaren återställs blodflödet abrupt (reperfusion), vilket utlöser en skadlig biologisk reaktion kallad ischemi-reperfusionsskada. Denna process är nödvändig för att njuren ska återhämta sig och fungera, men kan samtidigt orsaka betydande skada och inflammation. Kroppens medfödda immunförsvar, som bland annat består av immunförsvarsceller och proteiner i blodbanan, har en viktig roll i vår kropps förmåga att omedelbart känna igen infektioner och vävnadsskada, påbörja bekämpning och inflammatoriskt svar på dessa samt främja läkning. Men om allt för många aktiveringssignaler förekommer utan att det samtidigt finns tillräckligt med hämmande och reglerande funktioner i omgivningen så kan reaktionen i sig vara skadande och förvärra vävnadens tillstånd.

Njurtransplantation sker med njurar från levande eller avlidna donatorer. Ischemi-reperfusionsskadan är i regel mer uttalad i njurar från avlidna donatorer och dessa njurar har ofta utsatts för längre perioder av syrebrist och donators-relaterad fysiologisk stress före transplantationen. I praktiken utmärker detta sig genom att dessa njurar ibland har en fördröjd funktionsstart och mottagaren kan behöva dialys i väntan på njurens återhämtning tills den börjar fungera igen efter transplantationen. Därtill är njurtransplantatets funktionella livslängd ofta kortare hos njurar från avlidna donatorer jämfört med de från levande donatorer.

Trots att biologin kring ischemi-reperfusionsskada är välstuderad i experimentella modeller så finns det inga godkända läkemedel mot denna skada och kunskapen är begränsad kring vad som faktiskt händer i mänskliga njurar under de allra första minuterna efter att blodflödet återställs och skadan sätter igång. Syftet med denna avhandling var därför att undersöka de tidigaste biologiska händelserna vid njurtransplantation genom att analysera det venösa utflödet av det blod som cirkulerat in i njuren under de första 30 minuterna efter att blodflödet har återställts.

Studierna genomfördes vid Skånes universitetssjukhus i Malmö och inkluderade patienter som inkom för njurtransplantation i antingen planerat eller akut skede. Blodprover togs under operationen från mottagarens bäcken-ven innan njuren börjat sys in, samt direkt från den transplanterade njurens ven vid tidpunkterna 1, 10 och 30 minuter efter att blodflödet återställts. På så sätt kunde lokala signaler från den transplanterade njuren studeras genom att vidare analysera blodet med laborativa metoder. Analyserna omfattade mätningar av aktiveringen av kroppens medfödda immunförsvar, halterna av inflammatoriska och skaderelaterade proteiner, förekomst av fritt cirkulerande material av arvsmassa (DNA) som läckt ut ur celler som tecken på skada, samt mängden av olika immunförsvarsceller.

Resultaten visade att njurar från avlidna donatorer uppvisade tydliga tecken på akut cellskada redan inom en minut efter att blodflödet återställts. Detta avspeglades bland annat genom en snabb frisättning av fritt DNA från cellkärnor, vilket indikerar irreversibel cellskada. Samtidigt sågs tidig frisättning av proteiner som är kopplade till vävnadsskada och inflammation. Dessa tidiga signaler var i stort sett frånvarande i njurar från levande donatorer. Mängden DNA som släpptes ut var kopplad till fördröjd funktionsstart av njuren.

Parallellt med dessa fynd såg vi att kroppens medfödda immunförsvars kaskadssystem aktiveras i njurar från avlidna donatorer. Detta omfattade aktivering av det så kallade komplementsystemet, koagulationssystemet och kontakt/kallikrein-kininsystemet. Dessa system är normalt viktiga för att hantera skada och infektion, men kan vid kraftig aktivering bidra till inflammation och ytterligare vävnadsskada. Ett centralt fynd var att denna aktivering inte skedde isolerat, utan som en sammanhängande respons där graden av tidig aktivering var kopplad till fördröjd funktionsstart. Därtill noterades att de patienter som uppvisade kvarstående aktivering av dessa system efter 30 minuter också hade sämre njurfunktion på sikt (2 år). Denna tidiga biologiska responsen speglade därmed inte bara akut skada utan hade även en koppling till njurens fortsatta funktion.

Därtill såg vi att njurar från avlidna och levande donatorer uttrycker helt olika uppsättningar av inflammationsproteiner efter påsläpp av blodflödet. I avlidna donatorsnjurar utgjordes denna sammansättning av inflammationsbefrämjande och skaderelaterade proteiner, medan de levande donatorsnjurarna uppvisade inflammationsreglerande och antiinflammatoriska proteiner. Nivåerna av de skade- och inflammationsrelaterade proteiner som uttrycktes i avlidna donatorsnjurar var kopplade till fördröjd funktionsstart och försämrad njurfunktion över fyra års tid.

Utöver lösliga markörer i blodet observerades även snabba förändringar i halten av immunförsvarsceller i samband med att blodflödet återställdes. Vissa celltyper, särskilt icke-klassiska monocyter och naturliga mördarceller (NK-celler), uppmätta i det venösa återflödet från transplantatnjuren, minskade i antal över tid från att njuren återfått blodcirkulation. Detta talar för att dessa celler tidigt kan involveras i den transplanterade njuren.

Ett genomgående mönster var att aktiveringen av dessa tidiga biologiska förändringar var starkt kopplad till hur lång tid njuren varit utsatt för syrebrist i samband med kall förvaring i väntan på transplantation. När denna tid översteg cirka 8 timmar ökade frisättningen av skademarkörer och inflammationsaktiveringen markant. Detta tyder på att varaktigheten som en njure förvarats i syrebrist till slut uppnår en gräns för när njuren plötsligt blir mer känslig för angrepp från mottagarens immunförsvar i samband med att den återfår blodflödet.

Sammanfattningsvis visar denna avhandling att de första 30 minuterna vid njurtransplantation utgör en kritisk tidsperiod då avgörande biologiska processer omedelbart initieras. Under denna korta fas kan strukturell cellskada, inflammation, aktivering av medfödda försvarssystem, samt stimulering av immunförsvarsceller mätas under den pågående ischemi-reperfusionsskadan i samband med klinisk njurtransplantation. Denna mångfacetterade respons uppstod i njurar från avlidna donatorer men inte i de från levande donatorer. Kopplingen till både tidigt och långsiktigt försämrad njurfunktion visar även på relevansen av denna mycket tidiga aktivering. Detta betonar den avgörande betydelsen av denna omedelbara händelse i njurtransplantation.

Sammantaget visar resultaten att avgörande biologiska förlopp vid njurtransplantation initieras omedelbart efter att blodflödet återställts. Denna mycket tidiga fas kan ha långvarig betydelse för transplantatets funktion. Genom att identifiera och beskriva dessa tidiga processer bidrar arbetet till ökad förståelse kring vad ischemi-reperfusionsskadan utgörs av i den kliniska verkligheten. Dessa fynd kan på sikt ligga till grund för bättre prognostiska bedömningar för njurtransplanterade. Studierna tillför även nyttig information som kan vara av värde för utveckling av riktade strategier för att minska transplantationsrelaterad skada och förbättra resultaten efter njurtransplantation.

Acknowledgements

I would like to express my sincere gratitude to **Ali-Reza Biglarnia**, my main supervisor, for your endless patience, commitment, and unwavering support throughout the years. Your invaluable guidance, inspiration, and extensive scientific knowledge have been fundamental in shaping both my development and this thesis.

I am also grateful to **Anna Blom**, my co-supervisor, for your guidance, support, and insightful feedback over the years. Your quick thinking and ability to consistently provide constructive ideas and solutions have been greatly appreciated.

A big thank you to **David Berglund**, my co-supervisor for this thesis and my first supervisor, who introduced me to research during my student years. Your expertise, problem-solving mindset, and enthusiasm were instrumental in bringing me into the field of transplantation.

My sincere thanks to **Clara Paul**, my head of department, for your support, understanding, and for providing me with time and opportunity to work on this thesis alongside my clinical duties.

Thank you**, Bo Nilsson,** for sharing your extensive knowledge and for your invaluable scientific contributions to this work.

I am also grateful to **Carl Öberg**, for your statistical expertise, support, and for sparking my interest in statistics.

I would also like to thank all my co-authors: **Carl Raihle**, **Oleg Slivca**, **Rebecca Trattner**, **Felix Sellberg**, **Myriam Martin**, **Mårten Segelmark**, **Anders Christensson**, **Shahnawaz Alam**, **Ann-Sofie Liedberg**, **Annika Hult**, and **Sara Axman** – for your valuable contributions for this thesis.

To **my colleagues** at the Departments of Transplantation and Surgery at Skåne University Hospital: thank you for your collegiality, professionalism, and for making the daily clinical work both meaningful and enjoyable throughout the years.

Finally, I owe my deepest gratitude to **my family**, and above all to my wife **Sofie**, for your unwavering support, patience, and understanding. To our wonderful children, **Albin** and **Ellen**, thank you for your joy, curiosity, and for always wanting to keep me company, even during long hours of writing. I look forward to sharing many more experiences and adventures with you in the years to come.

References

1. Tonelli M, Wiebe N, Knoll G, et al. Systematic Review: Kidney Transplantation Compared With Dialysis in Clinically Relevant Outcomes. *American Journal of Transplantation*. 2011;11(10):2093-2109. doi:10.1111/j.1600-6143.2011.03686.x

2. Chaudhry D, Chaudhry A, Peracha J, Sharif A. Survival for waitlisted kidney failure patients receiving transplantation versus remaining on waiting list: systematic review and meta-analysis. *BMJ*. 2022;376:e068769. doi:10.1136/bmj-2021-068769

3. de Boer SE, Knobbe TJ, Kremer D, et al. Kidney Transplantation Improves Health-Related Quality of Life in Older Recipients. *Transpl Int*. 2024;37:12071. doi:10.3389/ti.2024.12071

4. Nyokabi P, Youngkong S, Bagepally BS, et al. A systematic review and quality assessment of economic evaluations of kidney replacement therapies in end-stage kidney disease. *Sci Rep*. 2024;14(1):23018. doi:10.1038/s41598-024-73735-8

5. Novacescu D, Latcu SC, Raica M, et al. Surgical Strategies for Renal Transplantation: A Pictorial Essay. *Journal of Clinical Medicine*. 2024;13(14):4188. doi:10.3390/jcm13144188

6. Mundt HM, Yard BA, Krämer BK, Benck U, Schnülle P. Optimized donor management and organ preservation before kidney transplantation. *Transplant International*. 2016;29(9):974-984. doi:10.1111/tri.12712

7. Hosgood SA, Brown RJ, Nicholson ML. Advances in Kidney Preservation Techniques and Their Application in Clinical Practice. *Transplantation*. 2021;105(11):e202. doi:10.1097/TP.0000000000003679

8. Chen Y, Shi J, Xia TC, Xu R, He X, Xia Y. Preservation Solutions for Kidney Transplantation: History, Advances and Mechanisms. *Cell Transplant*. 2019;28(12):1472-1489. doi:10.1177/0963689719872699

9. Lim MA, Kohli J, Bloom RD. Immunosuppression for kidney transplantation: Where are we now and where are we going? *Transplantation Reviews*. 2017;31(1):10-17. doi:10.1016/j.trre.2016.10.006

10. Global Observatory on Donation and Transplantation (2024-2024 Global Data). GODT. https://www.transplant-observatory.org/

11. Annual_Scandiatransplant_data_report_2024.pdf. https://www.scandiatransplant.org/resources/annual-report/Annual_Scandiatransplant_data_report_2024.pdf

12. Nashan B. Antibody Induction Therapy in Renal Transplant Patients Receiving Calcineurin-Inhibitor Immunosuppressive Regimens. *BioDrugs*. 2005;19(1):39-46. doi:10.2165/00063030-200519010-00005

13. Khan MA, Hanna A, Sridhara S, et al. Maintenance Immunosuppression in Kidney Transplantation: A Review of the Current Status and Future Directions. *Journal of Clinical Medicine*. 2025;14(6):1821. doi:10.3390/jcm14061821

14. Ekberg H, Tedesco-Silva H, Demirbas A, et al. Reduced Exposure to Calcineurin Inhibitors in Renal Transplantation. *New England Journal of Medicine*. 2007;357(25):2562-2575. doi:10.1056/NEJMoa067411

15. Flechner SM, Glyda M, Cockfield S, et al. The ORION Study: Comparison of Two Sirolimus-Based Regimens versus Tacrolimus and Mycophenolate Mofetil in Renal Allograft Recipients. *American Journal of Transplantation*. 2011;11(8):1633-1644. doi:10.1111/j.1600-6143.2011.03573.x

16. Wojciechowski D, Wiseman A. Long-Term Immunosuppression Management: Opportunities and Uncertainties. *Clinical Journal of the American Society of Nephrology*. 2021;16(8):1264. doi:10.2215/CJN.15040920

17. Marcén R. Immunosuppressive Drugs in Kidney Transplantation. *Drugs*. 2009;69(16):2227-2243. doi:10.2165/11319260-000000000-00000

18. Carminatti M, Tedesco-Silva H, Silva Fernandes NM, Sanders-Pinheiro H. Chronic kidney disease progression in kidney transplant recipients: A focus on traditional risk factors. *Nephrology*. 2019;24(2):141-147. doi:10.1111/nep.13483

19. Poggio ED, Augustine JJ, Arrigain S, Brennan DC, Schold JD. Long-term kidney transplant graft survival—Making progress when most needed. *American Journal of Transplantation*. 2021;21(8):2824-2832. doi:10.1111/ajt.16463

20. Toapanta N, Comas J, Revuelta I, et al. Benefits of Living Over Deceased Donor Kidney Transplantation in Elderly Recipients. A Propensity Score Matched Analysis of a Large European Registry Cohort. *Transpl Int*. 2024;37:13452. doi:10.3389/ti.2024.13452

21. Murray J, Luke A, Wallace D, Callaghan C, Sharples LD. Comparison of outcomes after living and deceased donor kidney transplantation: UK national cohort study. *Br J Surg*. 2025;112(8):znaf162. doi:10.1093/bjs/znaf162

22. Aubert O, Reese PP, Audry B, et al. Disparities in Acceptance of Deceased Donor Kidneys Between the United States and France and Estimated Effects of Increased US Acceptance. *JAMA Intern Med*. 2019;179(10):1365-1374. doi:10.1001/jamainternmed.2019.2322

23. Wu DA, Watson CJ, Bradley JA, Johnson RJ, Forsythe JL, Oniscu GC. Global trends and challenges in deceased donor kidney allocation. *Kidney International*. 2017;91(6):1287-1299. doi:10.1016/j.kint.2016.09.054

24. Nieuwenhuijs-Moeke GJ, Pischke SE, Berger SP, et al. Ischemia and Reperfusion Injury in Kidney Transplantation: Relevant Mechanisms in Injury and Repair. *J Clin Med*. 2020;9(1):253. doi:10.3390/jcm9010253

25. Zhao H, Alam A, Soo AP, George AJT, Ma D. Ischemia-Reperfusion Injury Reduces Long Term Renal Graft Survival: Mechanism and Beyond. *EBioMedicine*. 2018;28:31-42. doi:10.1016/j.ebiom.2018.01.025

26. Dols LFC, Kok NFM, IJzermans JNM. Live donor nephrectomy: a review of evidence for surgical techniques. *Transplant International*. 2010;23(2):121-130. doi:10.1111/j.1432-2277.2009.01027.x

27. Musquera M, Peri L, D'Anna M, et al. Outcomes after 20 years of experience in minimally invasive living-donor nephrectomy. *World J Urol*. 2022;40(3):807-813. doi:10.1007/s00345-021-03912-1

28. Kourounis G, Tingle SJ, Hoather TJ, et al. Robotic versus laparoscopic versus open nephrectomy for live kidney donors - Kourounis, G - 2024 | Cochrane Library. 2025. https://www.cochranelibrary.com/cdsr/doi/10.1002/14651858.CD006124.pub3/full

29. Venkataraman K, Irish GL, Collins MG, Clayton PA. The Association Between Early Graft Function, Donor Type and Long-Term Kidney Transplant Outcomes. *Transpl Int*. 2025;38:14197. doi:10.3389/ti.2025.14197

30. Redfield RR, Scalea JR, Zens TJ, et al. Predictors and outcomes of delayed graft function after living-donor kidney transplantation. *Transplant International*. 2016;29(1):81-87. doi:10.1111/tri.12696

31. Socialstyrelsen. Fastställa döden med direkta kriterier – Nationellt kunskapsstöd till hälso- och sjukvårdspersonal inom intensivvården. Stockholm: Socialstyrelsen; 2024. Report No.: 2024-12-9348.

32. Socialstyrelsen. Organdonation – nya regler från 1 juli 2022. Information till hälso- och sjukvården. Stockholm: Socialstyrelsen; 2022. Available from: https://www.socialstyrelsen.se/globalassets/sharepoint-dokument/dokument-webb/ovrigt/organdonation-nya-regler-1-juli-2022.pdf.

33. Poppelaars F, Seelen MA. Complement-mediated inflammation and injury in brain dead organ donors. *Molecular Immunology*. 2017;84:77-83. doi:10.1016/j.molimm.2016.11.004

34. Lopau K, Mark J, Schramm L, Heidbreder E, Wanner C. Hormonal changes in brain death and immune activation in the donor. *Transplant International*. 2000;13(S1):S282-S285. doi:10.1111/j.1432-2277.2000.tb02038.x

35. Lazzeri C, Bonizzoli M, Batacchi S, et al. Haemodynamic management in brain death donors: Influence of aetiology of brain death. *World Journal of Transplantation*. 2023;13(4):183-189. doi:10.5500/wjt.v13.i4.183

36. Pérez López S, Otero Hernández J, Vázquez Moreno N, Escudero Augusto D, Álvarez Menéndez F, Astudillo González A. Brain Death Effects on Catecholamine Levels and Subsequent Cardiac Damage Assessed in Organ Donors. *The Journal of Heart and Lung Transplantation*. 2009;28(8):815-820. doi:10.1016/j.healun.2009.04.021

37. Manara AR, Murphy PG, O'Callaghan G. Donation after circulatory death. *British Journal of Anaesthesia*. 2012;108:i108-i121. doi:10.1093/bja/aer357

38. Kootstra G, Daemen JH, Oomen AP. Categories of non-heart-beating donors. *Transplant Proc*. 1995;27(5):2893-2894.

39. Thuong M, Ruiz A, Evrard P, et al. New classification of donation after circulatory death donors definitions and terminology. *Transplant International*. 2016;29(7):749-759. doi:10.1111/tri.12776

40. Uppföljning av implementering av organdonation efter kontrollerat cirkulationsstillestånd (DCD) i Sverige 2023-6-8650.

41. Vävnadsrådet. Slutrapport DCD-projektet, 1.5 DCD Projektplan; 2020 2020-02-13.

42. Vävnadsrådet. Protocol for donation after circulatory death (DCD). National DCD Project Report. Stockholm: SKR;2020.

43. van Heurn LWE, Talbot D, Nicholson ML, et al. Recommendations for donation after circulatory death kidney transplantation in Europe. *Transplant International*. 2016;29(7):780-789. doi:10.1111/tri.12682

44. van de Leemkolk FEM, Schurink IJ, Dekkers OM, et al. Abdominal Normothermic Regional Perfusion in Donation After Circulatory Death: A Systematic Review and Critical Appraisal. *Transplantation*. 2020;104(9):1776. doi:10.1097/TP.0000000000003345

45. Sandes-Freitas TV de, Felipe CR, Aguiar WF, Cristelli MP, Tedesco-Silva H, Medina-Pestana JO. Prolonged Delayed Graft Function Is Associated with Inferior Patient and Kidney Allograft Survivals. *PLOS ONE*. 2015;10(12):e0144188. doi:10.1371/journal.pone.0144188

46. Johnston O, O'Kelly P, Spencer S, et al. Reduced graft function (with or without dialysis) vs immediate graft function—a comparison of long-term renal allograft survival. *Nephrol Dial Transplant*. 2006;21(8):2270-2274. doi:10.1093/ndt/gfl103

47. Lee APK, Abramowicz D. Is the Kidney Donor Risk Index a step forward in the assessment of deceased donor kidney quality? *Nephrol Dial Transplant*. 2015;30(8):1285-1290. doi:10.1093/ndt/gfu304

48. Rao PS, Schaubel DE, Guidinger MK, et al. A Comprehensive Risk Quantification Score for Deceased Donor Kidneys: The Kidney Donor Risk Index. *Transplantation*. 2009;88(2):231. doi:10.1097/TP.0b013e3181ac620b

49. Bae S, Massie AB, Luo X, Anjum S, Desai NM, Segev DL. Changes in Discard Rate After the Introduction of the Kidney Donor Profile Index (KDPI). *American Journal of Transplantation*. 2016;16(7):2202-2207. doi:10.1111/ajt.13769

50. Salguero J, Chamorro L, Gómez-Gómez E, de Benito P, Robles JE, Campos JP. Kidney Survival Impact of Delayed Graft Function Depends on Kidney Donor Risk Index: A Single-Center Cohort Study. *Journal of Clinical Medicine*. 2023;12(19):6397. doi:10.3390/jcm12196397

51. Zens TJ, Danobeitia JS, Leverson G, et al. The impact of kidney donor profile index on delayed graft function and transplant outcomes: A single-center analysis. *Clinical Transplantation*. 2018;32(3):e13190. doi:10.1111/ctr.13190

52. Han M, Jeong JC, Koo TY, et al. Kidney donor risk index is a good prognostic tool for graft outcomes in deceased donor kidney transplantation with short, cold ischemic time. *Clinical Transplantation*. 2014;28(3):337-344. doi:10.1111/ctr.12318

53. Hernandez RA, Malek SK, Milford EL, Finlayson SRG, Tullius SG. The Combined Risk of Donor Quality and Recipient Age: Higher-Quality Kidneys May Not Always Improve Patient and Graft Survival. *Transplantation*. 2014;98(10):1069. doi:10.1097/TP.0000000000000181

54. Darema M, Athanasopoulou D, Bellos I, et al. Evaluation of Kidney Donor Risk Index/Kidney Donor Profile Index as Predictor Tools of Deceased-Donor Kidney Transplant Outcomes in a Greek Cohort. *Journal of Clinical Medicine*. 2023;12(6):2439. doi:10.3390/jcm12062439

55. Dahmen M, Becker F, Pavenstädt H, Suwelack B, Schütte-Nütgen K, Reuter S. Validation of the Kidney Donor Profile Index (KDPI) to assess a deceased donor's kidneys' outcome in a European cohort. *Sci Rep*. 2019;9(1):11234. doi:10.1038/s41598-019-47772-7

56. Peters-Sengers H, Houtzager J, Idu M, et al. Impact of Cold Ischemia Time on Outcomes of Deceased Donor Kidney Transplantation: An Analysis of a National Registry. *Transplantation Direct*. 2019;5. doi:10.1097/txd.0000000000000888

57. Mikhalski D, Wissing K, Ghisdal L, et al. Cold Ischemia is a Major Determinant of Acute Rejection and Renal Graft Survival in the Modern Era of Immunosuppression. *Transplantation*. 2008;85:3-9. doi:10.1097/tp.0b013e318169c29e

58. Debout A, Foucher Y, Trébern-Launay K, et al. Each additional hour of cold ischemia time significantly increases the risk of graft failure and mortality following renal transplantation. *Kidney International*. 2015;87(2):343-349. doi:10.1038/ki.2014.304

59. Krishnan A, Wong G, Chapman J, et al. Prolonged Ischemic Time, Delayed Graft Function, and Graft and Patient Outcomes in Live Donor Kidney Transplant Recipients. *American Journal of Transplantation*. 2016;16:2714-2723. doi:10.1111/ajt.13817

60. Verstraeten L, Den abt R, Ghesquière B, Jochmans I. Current Insights into the Metabolome during Hypothermic Kidney Perfusion—A Scoping Review. *Journal of Clinical Medicine*. 2023;12(11):3613. doi:10.3390/jcm12113613

61. Eskla KL, Vellama H, Tarve L, et al. Hypothermia Alleviates Reductive Stress, a Root Cause of Ischemia Reperfusion Injury. *International Journal of Molecular Sciences*. 2022;23(17):10108. doi:10.3390/ijms231710108

62. Bellini MI, Tortorici F, Amabile MI, D'Andrea V. Assessing Kidney Graft Viability and Its Cells Metabolism during Machine Perfusion. *International Journal of Molecular Sciences*. 2021;22(3):1121. doi:10.3390/ijms22031121

63. Ran Q, Zhang J, Zhong J, et al. Organ preservation: current limitations and optimization approaches. *Front Med*. 2025;12. doi:10.3389/fmed.2025.1566080

64. Yuan X, Theruvath AJ, Ge X, et al. Machine perfusion or cold storage in organ transplantation: indication, mechanisms, and future perspectives. *Transplant International*. 2010;23(6):561-570. doi:10.1111/j.1432-2277.2009.01047.x

65. Jiao B, Liu S, Liu H, Cheng D, Cheng Y, Liu Y. Hypothermic Machine Perfusion Reduces Delayed Graft Function and Improves One-Year Graft Survival of Kidneys from Expanded Criteria Donors: A Meta-Analysis. *PLOS ONE*. 2013;8(12):e81826. doi:10.1371/journal.pone.0081826

66. Gasteiger S, Berchtold V, Bösmüller C, et al. A Retrospective Propensity Score Matched Analysis Reveals Superiority of Hypothermic Machine Perfusion over Static Cold Storage in Deceased Donor Kidney Transplantation. *Journal of Clinical Medicine*. 2020;9(7):2311. doi:10.3390/jcm9072311

67. Patel K, Nath J, Hodson J, Inston N, Ready A. Outcomes of donation after circulatory death kidneys undergoing hypothermic machine perfusion following static cold storage: A UK population-based cohort study. *American Journal of Transplantation*. 2018;18(6):1408-1414. doi:10.1111/ajt.14587

68. Foguenne M, MacMillan S, Kron P, et al. Current Evidence and Future Perspectives to Implement Continuous and End-Ischemic Use of Normothermic and Oxygenated Hypothermic Machine Perfusion in Clinical Practice. *Journal of Clinical Medicine*. 2023;12(9):3207. doi:10.3390/jcm12093207

69. Hendriks KDW, Brüggenwirth IMA, Maassen H, et al. Renal temperature reduction progressively favors mitochondrial ROS production over respiration in hypothermic kidney preservation. *J Transl Med*. 2019;17(1):265. doi:10.1186/s12967-019-2013-1

70. Calva Lopez A, Robles Garcia JE, Yanez Ruiz CA, et al. Does Oxygen Work? Evidence for Oxygenation During Kidney Graft Preservation: A Review. *Journal of Clinical Medicine*. 2025;14(6):1927. doi:10.3390/jcm14061927

71. Wang R, Lan C, Benlagha K, et al. The interaction of innate immune and adaptive immune system. *MedComm*. 2024;5(10):e714. doi:10.1002/mco2.714

72. Kubelkova K, Bostik V, Joshi L, Macela A. Innate Immune Recognition, Integrated Stress Response, Infection, and Tumorigenesis. *Biology*. 2023;12(4):499. doi:10.3390/biology12040499

73. DeWolf SE, Kasimsetty SG, Hawkes AA, Stocks LM, Kurian SM, McKay DB. DAMPs Released From Injured Renal Tubular Epithelial Cells Activate Innate Immune Signals in Healthy Renal Tubular Epithelial Cells. *Transplantation*. 2022;106(8):1589. doi:10.1097/TP.0000000000004038

74. Murao A, Aziz M, Wang H, Brenner M, Wang P. Release mechanisms of major DAMPs. *Apoptosis*. 2021;26(3):152-162. doi:10.1007/s10495-021-01663-3

75. Land WG, Agostinis P, Gasser S, Garg AD, Linkermann A. Transplantation and Damage-Associated Molecular Patterns (DAMPs). *American Journal of Transplantation*. 2016;16(12):3338-3361. doi:10.1111/ajt.13963

76. Li D, Wu M. Pattern recognition receptors in health and diseases. *Sig Transduct Target Ther*. 2021;6(1):291. doi:10.1038/s41392-021-00687-0

77. Wicherska-Pawłowska K, Wróbel T, Rybka J. Toll-Like Receptors (TLRs), NOD-Like Receptors (NLRs), and RIG-I-Like Receptors (RLRs) in Innate Immunity. TLRs, NLRs, and RLRs Ligands as Immunotherapeutic Agents for Hematopoietic Diseases. *International Journal of Molecular Sciences*. 2021;22(24):13397. doi:10.3390/ijms222413397

78. Lim JJ, Grinstein S, Roth Z. Diversity and Versatility of Phagocytosis: Roles in Innate Immunity, Tissue Remodeling, and Homeostasis. *Front Cell Infect Microbiol*. 2017;7. doi:10.3389/fcimb.2017.00191

79. Mandel J, Casari M, Stepanyan M, Martyanov A, Deppermann C. Beyond Hemostasis: Platelet Innate Immune Interactions and Thromboinflammation. *International Journal of Molecular Sciences*. 2022;23(7):3868. doi:10.3390/ijms23073868

80. Ribeiro LS, Migliari Branco L, Franklin BS. Regulation of Innate Immune Responses by Platelets. *Front Immunol*. 2019;10. doi:10.3389/fimmu.2019.01320

81. Shishido SN, Varahan S, Yuan K, Li X, Fleming SD. Humoral innate immune response and disease. *Clinical Immunology*. 2012;144(2):142-158. doi:10.1016/j.clim.2012.06.002

82. Ekdahl KN, Fromell K, Mannes M, et al. Therapeutic regulation of complement activation in extracorporeal circuits and intravascular treatments with special reference to the alternative pathway amplification loop. *Immunological Reviews*. 2023;313(1):91-103. doi:10.1111/imr.13148

83. Freeley S, Kemper C, Le Friec G. The “ins and outs” of complement-driven immune responses. *Immunological Reviews*. 2016;274(1):16-32. doi:10.1111/imr.12472

84. Nonaka M. Evolution of the Complement System. In: Anderluh G, Gilbert R, eds. *MACPF/CDC Proteins - Agents of Defence, Attack and Invasion*. Springer Netherlands; 2014:31-43. doi:10.1007/978-94-017-8881-6_3

85. Merle NS, Church SE, Fremeaux-Bacchi V, Roumenina LT. Complement System Part I – Molecular Mechanisms of Activation and Regulation. *Front Immunol*. 2015;6. doi:10.3389/fimmu.2015.00262

86. Ghai R, Waters P, Roumenina LT, et al. C1q and its growing family. *Immunobiology*. 2007;212(4):253-266. doi:10.1016/j.imbio.2006.11.001

87. Kishore U, Ghai R, Greenhough TJ, et al. Structural and functional anatomy of the globular domain of complement protein C1q. *Immunol Lett*. 2004;95(2):10.1016/j.imlet.2004.06.015. doi:10.1016/j.imlet.2004.06.015

88. Roumenina LT, Popov KT, Bureeva SV, et al. Interaction of the globular domain of human C1q with Salmonella typhimurium lipopolysaccharide. *Biochim Biophys Acta*. 2008;1784(9):1271-1276. doi:10.1016/j.bbapap.2008.04.029

89. Tissot B, Daniel R, Place C. Interaction of the C1 complex of Complement with sulfated polysaccharide and DNA probed by single molecule fluorescence microscopy. *European Journal of Biochemistry*. 2003;270(23):4714-4720. doi:10.1046/j.1432-1033.2003.03870.x

90. Matsushita M, Endo Y, Fujita T. Structural and Functional Overview of the Lectin Complement Pathway: Its Molecular Basis and Physiological Implication. *Arch Immunol Ther Exp*. 2013;61(4):273-283. doi:10.1007/s00005-013-0229-y

91. Farrar CA, Tran D, Li K, et al. Collectin-11 detects stress-induced L-fucose pattern to trigger renal epithelial injury. *J Clin Invest*. 126(5):1911-1925. doi:10.1172/JCI83000

92. Nilsson B, Nilsson Ekdahl K. The tick-over theory revisited: Is C3 a contact-activated protein? *Immunobiology*. 2012;217(11):1106-1110. doi:10.1016/j.imbio.2012.07.008

93. Pangburn MK, Schreiber RD, Müller-Eberhard HJ. Formation of the initial C3 convertase of the alternative complement pathway. Acquisition of C3b-like activities by spontaneous hydrolysis of the putative thioester in native C3. *J Exp Med*. 1981;154(3):856-867. doi:10.1084/jem.154.3.856

94. Pangburn MK. Initiation of the alternative pathway of complement and the history of "tickover." *Immunological Reviews*. 2023;313(1):64-70. doi:10.1111/imr.13130

95. Forneris F, Ricklin D, Wu J, et al. Structures of C3b in Complex with Factors B and D Give Insight into Complement Convertase Formation. *Science*. 2010;330(6012):1816-1820. doi:10.1126/science.1195821

96. van Essen MF, Schlagwein N, van den Hoven EMP, et al. Initial properdin binding contributes to alternative pathway activation at the surface of viable and necrotic cells. *European Journal of Immunology*. 2022;52(4):597-608. doi:10.1002/eji.202149259

97. Lammerts RGM, Talsma DT, Dam WA, et al. Properdin Pattern Recognition on Proximal Tubular Cells Is Heparan Sulfate/Syndecan-1 but Not C3b Dependent and Can Be Blocked by Tick Protein Salp20. *Front Immunol*. 2020;11. doi:10.3389/fimmu.2020.01643

98. Parente R, Clark SJ, Inforzato A, Day AJ. Complement factor H in host defense and immune evasion. *Cell Mol Life Sci*. 2017;74(9):1605-1624. doi:10.1007/s00018-016-2418-4

99. Williams B, Zou L, Pittet JF, Chao W. Sepsis-Induced Coagulopathy: A Comprehensive Narrative Review of Pathophysiology, Clinical Presentation, Diagnosis, and Management Strategies. *Anesthesia & Analgesia*. 2024;138(4):696. doi:10.1213/ANE.0000000000006888

100. Chu AJ. Tissue Factor, Blood Coagulation, and Beyond: An Overview. *Int J Inflam*. 2011;2011:367284. doi:10.4061/2011/367284

101. Rao LVM, Kothari H, Pendurthi UR. Tissue Factor encryption and decryption: Facts and controversies. *Thrombosis Research*. 2012;129:S13-S17. doi:10.1016/j.thromres.2012.02.021

102. Monroe DM, Hoffman M, Roberts HR. Platelets and Thrombin Generation. *Arteriosclerosis, Thrombosis, and Vascular Biology*. 2002;22(9):1381-1389. doi:10.1161/01.ATV.0000031340.68494.34

103. Palta S, Saroa R, Palta A. Overview of the coagulation system. *Indian Journal of Anaesthesia*. 2014;58(5):515. doi:10.4103/0019-5049.144643

104. Schmaier AH. The contact activation and kallikrein/kinin systems: pathophysiologic and physiologic activities. *Journal of Thrombosis and Haemostasis*. 2016;14(1):28-39. doi:10.1111/jth.13194

105. Graaf F van der, Koedam JA, Bouma BN. Inactivation of kallikrein in human plasma. *J Clin Invest*. 1983;71(1):149-158. doi:10.1172/JCI110743

106. Kuoppala A, Lindstedt KA, Saarinen J, Kovanen PT, Kokkonen JO. Inactivation of bradykinin by angiotensin-converting enzyme and by carboxypeptidase N in human plasma. *American Journal of Physiology-Heart and Circulatory Physiology*. 2000;278(4):H1069-H1074. doi:10.1152/ajpheart.2000.278.4.H1069

107. Schrottmaier WC, Assinger A. The Concept of Thromboinflammation. *Hamostaseologie*. 2024;44(01):021-030. doi:10.1055/a-2178-6491

108. Nilsson B, Eriksson O, Fromell K, Persson B, Ekdahl KN. How COVID-19 and other pathological conditions and medical treatments activate our intravascular innate immune system. *Front Immunol*. 2023;13. doi:10.3389/fimmu.2022.1030627

109. Maas C, Renné T. Coagulation factor XII in thrombosis and inflammation. *Blood*. 2018;131(17):1903-1909. doi:10.1182/blood-2017-04-569111

110. Irmscher S, Döring N, Halder LD, et al. Kallikrein Cleaves C3 and Activates Complement. *J Innate Immun*. 2018;10(2):94-105. doi:10.1159/000484257

111. Redecha P, Tilley R, Tencati M, et al. Tissue factor: a link between C5a and neutrophil activation in antiphospholipid antibody–induced fetal injury. *Blood*. 2007;110(7):2423-2431. doi:10.1182/blood-2007-01-070631

112. Martorell L, Martínez-González J, Rodríguez C, Gentile M, Calvayrac O, Badimon L. Thrombin and protease-activated receptors (PARs) in atherothrombosis. *Thromb Haemost*. 2008;99(02):305-315. doi:10.1160/TH07-08-0481

113. Huber-Lang M, Lambris JD, Ward PA. Innate immune responses to trauma. *Nat Immunol*. 2018;19(4):327-341. doi:10.1038/s41590-018-0064-8

114. Saparov A, Ogay V, Nurgozhin T, et al. Role of the immune system in cardiac tissue damage and repair following myocardial infarction. *Inflamm Res*. 2017;66(9):739-751. doi:10.1007/s00011-017-1060-4

115. Iadecola C, Buckwalter MS, Anrather J. Immune responses to stroke: mechanisms, modulation, and therapeutic potential. *J Clin Invest*. 2020;130(6):2777-2788. doi:10.1172/JCI135530

116. Biglarnia AR, Huber-Lang M, Mohlin C, Ekdahl KN, Nilsson B. The multifaceted role of complement in kidney transplantation. *Nat Rev Nephrol*. 2018;14(12):767-781. doi:10.1038/s41581-018-0071-x

117. Doni A, D'Amico G, Morone D, Mantovani A, Garlanda C. Humoral innate immunity at the crossroad between microbe and matrix recognition: The role of PTX3 in tissue damage. *Seminars in Cell & Developmental Biology*. 2017;61:31-40. doi:10.1016/j.semcdb.2016.07.026

118. Brazil JC, Quiros M, Nusrat A, Parkos CA. Innate immune cell–epithelial crosstalk during wound repair. *J Clin Invest*. 2019;129(8):2983-2993. doi:10.1172/JCI124618

119. Hirayama D, Iida T, Nakase H. The Phagocytic Function of Macrophage-Enforcing Innate Immunity and Tissue Homeostasis. *International Journal of Molecular Sciences*. 2018;19(1):92. doi:10.3390/ijms19010092

120. Tammaro A, Kers J, Scantlebery AML, Florquin S. Metabolic Flexibility and Innate Immunity in Renal Ischemia Reperfusion Injury: The Fine Balance Between Adaptive Repair and Tissue Degeneration. *Front Immunol*. 2020;11. doi:10.3389/fimmu.2020.01346

121. Perico N, Cattaneo D, Sayegh MH, Remuzzi G. Delayed graft function in kidney transplantation. *The Lancet*. 2004;364(9447):1814-1827. doi:10.1016/S0140-6736(04)17406-0

122. Mason J, Beck F, Dörge A, Rick R, Thurau K. Intracellular electrolyte composition following renal ischemia. *Kidney International*. 1981;20(1):61-70. doi:10.1038/ki.1981.105

123. Eltzschig HK, Eckle T. Ischemia and reperfusion—from mechanism to translation. *Nat Med*. 2011;17(11):1391-1401. doi:10.1038/nm.2507

124. Kezic A, Spasojevic I, Lezaic V, Bajcetic M. Mitochondria-Targeted Antioxidants: Future Perspectives in Kidney Ischemia Reperfusion Injury. *Oxidative Medicine and Cellular Longevity*. 2016;2016(1):2950503. doi:10.1155/2016/2950503

125. Granata S, Votrico V, Spadaccino F, et al. Oxidative Stress and Ischemia/Reperfusion Injury in Kidney Transplantation: Focus on Ferroptosis,

Mitophagy and New Antioxidants. *Antioxidants (Basel)*. 2022;11(4):769. doi:10.3390/antiox11040769

126. Moore KH, Murphy HA, George EM. The glycocalyx: a central regulator of vascular function. *American Journal of Physiology - Regulatory, Integrative and Comparative Physiology*. 2021;320(4):R508. doi:10.1152/ajpregu.00340.2020

127. Duni A, Liakopoulos V, Koutlas V, Pappas C, Mitsis M, Dounousi E. The Endothelial Glycocalyx as a Target of Ischemia and Reperfusion Injury in Kidney Transplantation—Where Have We Gone So Far? *Int J Mol Sci*. 2021;22(4):2157. doi:10.3390/ijms22042157

128. Reitsma S, Slaaf DW, Vink H, Zandvoort MAMJ van, Egbrink MGA oude. The endothelial glycocalyx: composition, functions, and visualization. *Pflugers Archiv*. 2007;454(3):345. doi:10.1007/s00424-007-0212-8

129. Chen J, John R, Richardson JA, et al. Toll-like receptor 4 regulates early endothelial activation during ischemic acute kidney injury. *Kidney International*. 2011;79(3):288-299. doi:10.1038/ki.2010.381

130. Combe C, Burton CJ, Dufourcq P, et al. Hypoxia induces intercellular adhesion molecule-1 on cultured human tubular cells. *Kidney International*. 1997;51(6):1703-1709. doi:10.1038/ki.1997.235

131. Zhao F, Wang X, Liang T, et al. Effect of Hyperbaric Oxygen on Tissue Damage and Expression of Adhesion Molecules and C3 in a Rat Model of Renal Ischemia-Reperfusion Injury After Kidney Transplantation. *Ann Transplant*. 2020;25:0-0. doi:10.12659/AOT.919385

132. Takada M, Nadeau KC, Shaw GD, Marquette KA, Tilney NL. The cytokine-adhesion molecule cascade in ischemia/reperfusion injury of the rat kidney. Inhibition by a soluble P-selectin ligand. *J Clin Invest*. 1997;99(11):2682-2690. doi:10.1172/JCI119457

133. Abassi Z, Armaly Z, Heyman SN. Glycocalyx Degradation in Ischemia-Reperfusion Injury. *The American Journal of Pathology*. 2020;190(4):752-767. doi:10.1016/j.ajpath.2019.08.019

134. Bianchi ME. DAMPs, PAMPs and alarmins: all we need to know about danger. *J Leukoc Biol*. 2007;81(1):1-5. doi:10.1189/jlb.0306164

135. Li J, Hu Z. Research progress on damage-associated molecular patterns in acute kidney injury. *Front Immunol*. 2025;16. doi:10.3389/fimmu.2025.1590822

136. Ekdahl KN, Teramura Y, Hamad OA, et al. Dangerous liaisons: complement, coagulation, and kallikrein/kinin cross-talk act as a linchpin in the events leading to thromboinflammation. *Immunological Reviews*. 2016;274(1):245-269. doi:10.1111/imr.12471

137. Biglarnia AR, Teramura Y, Asif S, et al. A new principle to attenuate ischemia-reperfusion injury in kidney transplantation. *American Journal of Transplantation*. 2025;0(0). doi:10.1016/j.ajt.2025.08.024

138. Wu J, Zhang F, Zheng X, et al. Identification of renal ischemia reperfusion injury subtypes and predictive strategies for delayed graft function and graft survival based on neutrophil extracellular trap-related genes. *Front Immunol*. 2022;13. doi:10.3389/fimmu.2022.1047367

139. Siedlecki A, Irish W, Brennan DC. Delayed Graft Function in the Kidney Transplant. *Am J Transplant*. 2011;11(11):2279-2296. doi:10.1111/j.1600-6143.2011.03754.x

140. Mallon DH, Summers DM, Bradley JA, Pettigrew GJ. Defining Delayed Graft Function after Renal Transplantation: Simplest Is Best. *Transplantation*. 2013;96(10):885. doi:10.1097/TP.0b013e3182a19348

141. Chapal M, Le Borgne F, Legendre C, et al. A useful scoring system for the prediction and management of delayed graft function following kidney transplantation from cadaveric donors. *Kidney International*. 2014;86(6):1130-1139. doi:10.1038/ki.2014.188

142. Helanterä I, Ibrahim HN, Lempinen M, Finne P. Donor Age, Cold Ischemia Time, and Delayed Graft Function. *Clinical Journal of the American Society of Nephrology*. 2020;15(6):813. doi:10.2215/CJN.13711119

143. Irish WD, McCollum DA, Tesi RJ, et al. Nomogram for Predicting the Likelihood of Delayed Graft Function in Adult Cadaveric Renal Transplant Recipients. *Journal of the American Society of Nephrology*. 2003;14(11):2967. doi:10.1097/01.ASN.0000093254.31868.85

144. Nagaraja P, Roberts GW, Stephens M, et al. Influence of Delayed Graft Function and Acute Rejection on Outcomes After Kidney Transplantation From Donors After Cardiac Death. *Transplantation*. 2012;94(12):1218. doi:10.1097/TP.0b013e3182708e30

145. Yarlagadda SG, Coca SG, Formica RN, Poggio ED, Parikh CR. Association between delayed graft function and allograft and patient survival: a systematic review and meta-analysis. *Nephrol Dial Transplant*. 2009;24(3):1039-1047. doi:10.1093/ndt/gfn667

146. Butala NM, Reese PP, Doshi MD, Parikh CR. Is Delayed Graft Function Causally Associated With Long-Term Outcomes After Kidney Transplantation? Instrumental Variable Analysis. *Transplantation*. 2013;95(8):1008. doi:10.1097/TP.0b013e3182855544

147. Ahlmark A, Sallinen V, Eerola V, Lempinen M, Helanterä I. Characteristics of Delayed Graft Function and Long-Term Outcomes After Kidney Transplantation From Brain-Dead Donors: A Single-Center and Multicenter Registry-Based Retrospective Study. *Transpl Int*. 2024;37:12309. doi:10.3389/ti.2024.12309

148. Josephson MA, Becker Y, Budde K, et al. Challenges in the management of the kidney allograft: from decline to failure: conclusions from a Kidney Disease: Improving Global Outcomes (KDIGO) Controversies Conference. *Kidney International*. 2023;104(6):1076-1091. doi:10.1016/j.kint.2023.05.010

149. Lentine KL, Smith JM, Lyden GR, et al. OPTN/SRTR 2023 Annual Data Report: Kidney. *American Journal of Transplantation*. 2025;25(2):S22-S137. doi:10.1016/j.ajt.2025.01.020

150. Gavriilidis P, Inston NG. Recipient and allograft survival following donation after circulatory death versus donation after brain death for renal transplantation: A systematic review and meta-analysis. *Transplantation Reviews*. 2020;34(4):100563. doi:10.1016/j.trre.2020.100563

151. Kok MJC de, Schaapherder AFM, Alwayn IPJ, et al. Improving outcomes for donation after circulatory death kidney transplantation: Science of the times. *PLOS ONE*. 2020;15(7):e0236662. doi:10.1371/journal.pone.0236662

152. Tingle SJ, Figueiredo RS, Moir JA, Goodfellow M, Talbot D, Wilson CH. Machine perfusion preservation versus static cold storage for deceased donor kidney transplantation. *Cochrane Database Syst Rev*. 2019;2019(3):CD011671. doi:10.1002/14651858.CD011671.pub2

153. Khan S, Zuluaga D, Ratner LE, Cogua LM, Wang H, Ortiz J. Emerging Therapeutic Strategies for Renal Ischemia-Reperfusion Injury in Kidney Transplantation: Progress and Challenges—A Systematic Review. *Clinical Transplantation*. 2025;39(8):e70263. doi:10.1111/ctr.70263

154. Kaabak M, Babenko N, Shapiro R, Zokoyev A, Dymova O, Kim E. A prospective randomized, controlled trial of eculizumab to prevent ischemia-reperfusion injury in pediatric kidney transplantation. *Pediatric Transplantation*. 2018;22(2):e13129. doi:10.1111/petr.13129

155. Schröppel B, Akalin E, Baweja M, et al. Peritransplant eculizumab does not prevent delayed graft function in deceased donor kidney transplant recipients:

Results of two randomized controlled pilot trials. *American Journal of Transplantation*. 2020;20(2):564-572. doi:10.1111/ajt.15580

156. Kassimatis T, Greenlaw R, Hunter JP, et al. Ex vivo delivery of Mirococept: A dose-finding study in pig kidney after showing a low dose is insufficient to reduce delayed graft function in human kidney. *American Journal of Transplantation*. 2021;21(3):1012-1026. doi:10.1111/ajt.16265

157. Björk J, Grubb A, Sterner G, Nyman U. Revised equations for estimating glomerular filtration rate based on the Lund-Malmö Study cohort. *Scandinavian Journal of Clinical and Laboratory Investigation*. Published online May 1, 2011. Accessed May 1, 2025. https://www.tandfonline.com/doi/abs/10.3109/00365513.2011.557086

158. Nyman U, Grubb A, Larsson A, et al. The revised Lund-Malmö GFR estimating equation outperforms MDRD and CKD-EPI across GFR, age and BMI intervals in a large Swedish population. *Clin Chem Lab Med*. 2014;52(6):815-824. doi:10.1515/cclm-2013-0741

159. Kozarcanin H, Lood C, Munthe-Fog L, et al. The lectin complement pathway serine proteases (MASPs) represent a possible crossroad between the coagulation and complement systems in thromboinflammation. *Journal of Thrombosis and Haemostasis*. 2016;14(3):531-545. doi:10.1111/jth.13208

160. Bäck J, Lood C, Bengtsson AA, Ekdahl KN, Nilsson B. Contact activation products are new potential biomarkers to evaluate the risk of thrombotic events in systemic lupus erythematosus. *Arthritis Res Ther*. 2013;15(6):R206. doi:10.1186/ar4399

161. Ekdahl KN, Nilsson B, Pekna M, Nilsson UR. Generation of iC3 at the Interface between Blood and Gas. *Scandinavian Journal of Immunology*. 1992;35(1):85-91. doi:10.1111/j.1365-3083.1992.tb02837.x

162. Bexborn F, Engberg AE, Sandholm K, Mollnes TE, Hong J, Nilsson Ekdahl K. Hirudin versus heparin for use in whole blood in vitro biocompatibility models. *Journal of Biomedical Materials Research Part A*. 2009;89A(4):951-959. doi:10.1002/jbm.a.32034

163. Nakagawa M, Terashima T, D'yachkova Y, Bondy GP, Hogg JC, van Eeden SF. Glucocorticoid-Induced Granulocytosis. *Circulation*. 1998;98(21):2307-2313. doi:10.1161/01.CIR.98.21.2307

164. Bloemena E, Weinreich S, Schellekens PT. The influence of prednisolone on the recirculation of peripheral blood lymphocytes in vivo. *Clin Exp Immunol*. 1990;80(3):460-466.

165. Cupps TR, Fauci AS. Corticosteroid-Mediated Immunoregulation in Man. *Immunological Reviews*. 1982;65(1):133-155. doi:10.1111/j.1600-065X.1982.tb00431.x

166. Nieuwenhuijs-Moeke GJ, Pischke SE, Berger SP, et al. Ischemia and Reperfusion Injury in Kidney Transplantation: Relevant Mechanisms in Injury and Repair. *J Clin Med*. 2020;9(1):253. doi:10.3390/jcm9010253

167. Magna M, Pisetsky DS. The Alarmin Properties of DNA and DNA-associated Nuclear Proteins. *Clin Ther*. 2016;38(5):1029-1041. doi:10.1016/j.clinthera.2016.02.029

168. Matsumoto K. Renotropic role and therapeutic potential of HGF in the kidney. *Nephrology Dialysis Transplantation*. 2002;17(90009):59-61. doi:10.1093/ndt/17.suppl_9.59

169. Imamura R, Matsumoto K. Hepatocyte growth factor in physiology and infectious diseases. *Cytokine*. 2017;98:97-106. doi:10.1016/j.cyto.2016.12.025

170. Zhou D, Tan RJ, Lin L, Zhou L, Liu Y. Activation of hepatocyte growth factor receptor, c-met, in renal tubules is required for renoprotection after acute kidney injury. *Kidney Int*. 2013;84(3):509-520. doi:10.1038/ki.2013.102

171. Xie M, Li J ping. Heparan sulfate proteoglycan – A common receptor for diverse cytokines. *Cellular Signalling*. 2019;54:115-121. doi:10.1016/j.cellsig.2018.11.022

172. Matsumori A, Furukawa Y, Hashimoto T, et al. Increased Circulating Hepatocyte Growth Factor in the Early Stage of Acute Myocardial Infarction. *Biochemical and Biophysical Research Communications*. 1996;221(2):391-395. doi:10.1006/bbrc.1996.0606

173. Ono K, Matsumori A, Shioi T, Furukawa Y, Sasayama S. Enhanced Expression of Hepatocyte Growth Factor/c-Met by Myocardial Ischemia and Reperfusion in a Rat Model. *Circulation*. 1997;95(11):2552-2558. doi:10.1161/01.CIR.95.11.2552

174. Konopka A, Janas J, Piotrowski W, Stępińska J. Hepatocyte growth factor—a new marker for prognosis in acute coronary syndrome. *Growth Factors*. 2010;28(2):75-81. doi:10.3109/08977190903403984

175. Mizuno S, Nakamura T. Prevention of Neutrophil Extravasation by Hepatocyte Growth Factor Leads to Attenuations of Tubular Apoptosis and Renal Dysfunction in Mouse Ischemic Kidneys. *Am J Pathol*. 2005;166(6):1895-1905. doi:10.1016/S0002-9440(10)62498-4

176. Cayrol C, Girard JP. Interleukin-33 (IL-33): A critical review of its biology and the mechanisms involved in its release as a potent extracellular cytokine. *Cytokine*. 2022;156:155891. doi:10.1016/j.cyto.2022.155891

177. Cayrol C, Girard JP. Interleukin-33 (IL-33): A nuclear cytokine from the IL-1 family. *Immunological Reviews*. 2018;281(1):154-168. doi:10.1111/imr.12619

178. Ferhat M, Robin A, Giraud S, et al. Endogenous IL-33 Contributes to Kidney Ischemia-Reperfusion Injury as an Alarmin. *J Am Soc Nephrol*. 2018;29(4):1272-1288. doi:10.1681/ASN.2017060650

179. Zhang F, Li Y, Wu J, et al. The role of extracellular traps in ischemia reperfusion injury. *Front Immunol*. 2022;13. doi:10.3389/fimmu.2022.1022380

180. Wu X, You D, Cui J, et al. Reduced Neutrophil Extracellular Trap Formation During Ischemia Reperfusion Injury in C3 KO Mice: C3 Requirement for NETs Release. *Front Immunol*. 2022;13. doi:10.3389/fimmu.2022.781273

181. Liu Y, Xin Y, Yuan M, et al. Sivelestat sodium protects against renal ischemia/reperfusion injury by reduction of NETs formation. *Archives of Biochemistry and Biophysics*. 2025;765:110318. doi:10.1016/j.abb.2025.110318

182. Awad AS, Rouse M, Huang L, et al. Compartmentalization of neutrophils in the kidney and lung following acute ischemic kidney injury. *Kidney International*. 2009;75(7):689-698. doi:10.1038/ki.2008.648

183. Błogowski W, Dołęgowska B, Sałata D, Budkowska M, Domański L, Starzyńska T. Clinical Analysis of Perioperative Complement Activity during Ischemia/Reperfusion Injury following Renal Transplantation. *Clinical Journal of the American Society of Nephrology*. 2012;7(11):1843. doi:10.2215/CJN.02200312

184. de Vries DK, van der Pol P, van Anken GE, et al. Acute But Transient Release of Terminal Complement Complex After Reperfusion in Clinical Kidney Transplantation. *Transplantation*. 2013;95(6):816. doi:10.1097/TP.0b013e31827e31c9

185. Zhang ZX, Wang S, Huang X, et al. NK cells induce apoptosis in tubular epithelial cells and contribute to renal ischemia-reperfusion injury. *J Immunol*. 2008;181(11):7489-7498. doi:10.4049/jimmunol.181.11.7489

186. Kim HJ, Lee JS, Kim A, et al. TLR2 signaling in tubular epithelial cells regulates NK cell recruitment in kidney ischemia-reperfusion injury. *J Immunol*. 2013;191(5):2657-2664. doi:10.4049/jimmunol.1300358

187. Jiang W, Tang TT, Zhang YL, et al. CD8 T cells induce the peritubular capillary rarefaction during AKI to CKD transition. *Int J Biol Sci*. 2024;20(8):2980-2993. doi:10.7150/ijbs.96812

188. Qiu L, Lai X, Wang J jing, et al. Kidney-intrinsic factors determine the severity of ischemia/reperfusion injury in a mouse model of delayed graft function. *Kidney International*. 2020;98(6):1489-1501. doi:10.1016/j.kint.2020.07.033

189. Marsh SA, Park C, Redgrave RE, et al. Rapid fall in circulating non-classical monocytes in ST elevation myocardial infarction patients correlates with cardiac injury. *The FASEB Journal*. 2021;35(5):e21604. doi:10.1096/fj.202100240R

190. Thomas G, Tacke R, Hedrick CC, Hanna RN. Nonclassical Patrolling Monocyte Function in the Vasculature. *Arterioscler Thromb Vasc Biol*. 2015;35(6):1306-1316. doi:10.1161/ATVBAHA.114.304650

191. Narasimhan PB, Marcovecchio P, Hamers AAJ, Hedrick CC. Nonclassical Monocytes in Health and Disease. *Annu Rev Immunol*. 2019;37(1):439-456. doi:10.1146/annurev-immunol-042617-053119

192. Urra X, Villamor N, Amaro S, et al. Monocyte subtypes predict clinical course and prognosis in human stroke. *J Cereb Blood Flow Metab*. 2009;29(5):994-1002. doi:10.1038/jcbfm.2009.25

193. Boag SE, Das R, Shmeleva EV, et al. T lymphocytes and fractalkine contribute to myocardial ischemia/reperfusion injury in patients. *J Clin Invest*. 2015;125(8):3063-3076. doi:10.1172/JCI80055

194. Dounousi E, Duni A, Naka KK, Vartholomatos G, Zoccali C. The Innate Immune System and Cardiovascular Disease in ESKD: Monocytes and Natural Killer Cells. *CVP*. 2020;19(1):63-76. doi:10.2174/1570161118666200628024027

195. Rao J, Lu L, Zhai Y. T cells in Organ Ischemia Reperfusion Injury. *Curr Opin Organ Transplant*. 2014;19(2):115-120. doi:10.1097/MOT.0000000000000064

196. Jahn N, Sack U, Stehr S, et al. The Role of Innate Immune Cells in the Prediction of Early Renal Allograft Injury Following Kidney Transplantation. *Journal of Clinical Medicine*. 2022;11(20):6148. doi:10.3390/jcm11206148

197. Zhou J, Wang M, Deng H, Chen J. Quantification of Peripheral White Blood Cell Subtypes and Delayed Graft Function after Kidney Transplantation: A Single Center Analysis. *Transplantation Proceedings*. 2025;57(6):1050-1057. doi:10.1016/j.transproceed.2025.06.008

198. Shimamura M, Nakagami H, Osako MK, et al. OPG/RANKL/RANK axis is a critical inflammatory signaling system in ischemic brain in mice. *Proc Natl Acad Sci U S A*. 2014;111(22):8191-8196. doi:10.1073/pnas.1400544111

199. Vries DK de, Lindeman JHN, Tsikas D, et al. Early Renal Ischemia-Reperfusion Injury in Humans Is Dominated by IL-6 Release from the Allograft. *American Journal of Transplantation*. 2009;9(7):1574-1584. doi:10.1111/j.1600-6143.2009.02675.x

200. Chang HM, Peng KY, Chan CK, et al. FGF23 ameliorates ischemia-reperfusion induced acute kidney injury via modulation of endothelial progenitor cells: targeting SDF-1/CXCR4 signaling. *Cell Death Dis*. 2021;12(5):409. doi:10.1038/s41419-021-03693-w

Printed by Media-Tryck, Lund 2026 NORDIC SWAN ECOLABEL 3041 0903

LUND UNIVERSITY

FACULTY OF MEDICINE

Department of Clinical Sciences, Malmö

Lund University, Faculty of Medicine
Doctoral Dissertation Series 2026:22
ISBN 978-91-8021-820-7
ISSN 1652-8220